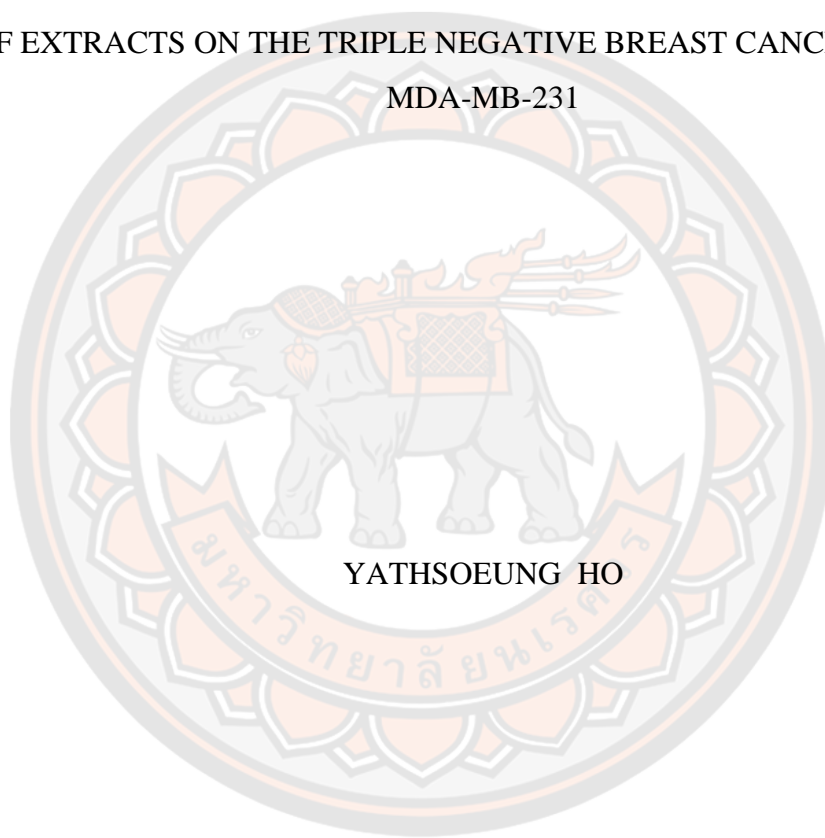




ANTICANCER EFFECT OF *CITRUS HYSTRIX*  
LEAF EXTRACTS ON THE TRIPLE NEGATIVE BREAST CANCER CELL LINE  
MDA-MB-231



A Thesis Submitted to the Graduate School of Naresuan University  
in Partial Fulfillment of the Requirements  
for the Master of Science in (Biomedical Sciences - (Type A 2))

2020

Copyright by Naresuan University

ANTICANCER EFFECT OF *CITRUS HYSTRIX*  
LEAF EXTRACTS ON THE TRIPLE NEGATIVE BREAST CANCER CELL LINE  
MDA-MB-231



A Thesis Submitted to the Graduate School of Naresuan University  
in Partial Fulfillment of the Requirements  
for the Master of Science in (Biomedical Sciences - (Type A 2))  
2020

Copyright by Naresuan University

Thesis entitled "ANTICANCER EFFECT OF *Citrus hystrix*  
LEAF EXTRACTS ON THE TRIPLE NEGATIVE BREAST CANCER CELL LINE  
MDA-MB-231"

By YATHSOEUNG HO

has been approved by the Graduate School as partial fulfillment of the requirements  
for the Master of Science in Biomedical Sciences - (Type A 2) of Naresuan University

**Oral Defense Committee**

..... Chair  
(Professor Sarawut Jitrapakdee, Ph.D.)

..... Advisor  
(Associate Professor Kanchana Usuwanthim, Ph.D.)

..... Co Advisor  
(Assistant Professor Nungruthai Suphrom, Ph.D.)

..... Internal Examiner  
(Associate Professor Kornkanok Ingkaninan, Ph.D.)

**Approved**

.....  
(Professor Paisarn Muneesawang, Ph.D.)

for Dean of the Graduate School

**Title** ANTICANCER EFFECT OF *CITRUS HYSTRIX*  
LEAF EXTRACTS ON THE TRIPLE NEGATIVE  
BREAST CANCER CELL LINE MDA-MB-231

**Author** YATHSOEUNG HO

**Advisor** Associate Professor Kanchana Usuwanthim, Ph.D.

**Co-Advisor** Assistant Professor Nungruthai Suphrom, Ph.D.

**Academic Paper** Thesis M.S. in Biomedical Sciences - (Type A 2),  
Naresuan University, 2020

**Keywords** MDA-MB-231, *Citrus hystrix*, leave extract, citronellol,  
citronellal, anticancer

### ABSTRACT

Triple-negative breast cancer is one of the most aggressive types of breast cancer due to the ability of early metastasis and chemoresistance, which accounts for almost 10-15% of invasive breast cancer. *Citrus hystrix* DC. is a tropical plant known for its high aroma. It has been used as spices, in cosmetic products and also has been reported to possess many biological activities including anticancer effects. However, the effect of *C. hystrix* against triple-negative breast cancer has yet been identified. In this study, cytotoxicity of *C. hystrix* leave extracts, and its bioactive compounds citronellal and citronellol against the triple-negative breast cancer MDA-MB-231 cell line were observed. *C. hystrix* leaves powder was sequentially extracted using maceration with hexane, ethyl acetate and ethanol. Cytotoxic effect of extracts were evaluated using MTT assay. Cell proliferation, wound scratch migration, colony formation, and apoptosis assay were used to identify the *in vitro* effect of the extracts and its active compounds against this cell line. RT-qPCR and Western blot analysis were used to understand some mechanism which may lead to the cause of cells dead. The results significantly showed that crude hexane of *C. hystrix* leaves extract, and its bioactive molecules could reduce cell proliferation, colony forming, migration of the cancer cells, and induced cell cycle arrest when compared to control. The results also indicated that crude hexane, citronellol and citronellol could induce apoptosis in MDA-MB-231 cells through the inhibition of the anti-apoptotic Bcl-2 expression and

leading to the activation of the caspase-dependent pathway through the activation of the executioner Caspase-3. This is the first demonstration of the effect of *C. hystix* and its bioactive compounds citronellol and citronellal against the triple negative breast cancer MDA-MB-231 cells. Further study should be held to help understanding more deeply on mechanism that caused by the extract and the molecules on cells.



## ACKNOWLEDGEMENTS

The author would like to show gratitude toward the Royal Scholarship under Her Royal Highness Princess Maha Chakri Sirindhorn Education Project to the Kingdom of Cambodia for providing this Master's degree scholarship, which allowed the author to acquire new knowledge and technology to fulfill the missing gaps in the career as a scientist.

The author would like to acknowledge Assoc. Prof. Kanchana Usuwanthim, Ph.D. as advisor, and Asst. Prof. Nungruthai Suphrom, Ph.D. as co-advisor for providing consultation and technical supports on the lab experiment and on results. Also, thank to Dr. Krai Daowtak who gave recommendation on the experiments.

Also, thanks to all professors from the Faculty of Allied Health Sciences who providing lectures that equipped with a considerable amount of precious knowledge that stands as the base of the research. And thanks to the Faculty of Allied Health Sciences itself, Faculty of Science, Naresuan University for providing the facility for performing labs experiment, expense, and accommodation.

Finally, the author would like to attribute special thanks to author's family for mental and financial support during this the whole study at Naresuan University.

YATHSOEUNG HO

## TABLE OF CONTENTS

	<b>Page</b>
ABSTRACT.....	C
ACKNOWLEDGEMENTS.....	E
TABLE OF CONTENTS.....	F
TABLE OF TABLES .....	K
TABLE OF FIGURES .....	L
ABBREVIATIONS .....	N
CHARPTEr I INTRODUCTION .....	1
Background.....	1
Statement of the problems .....	2
Research significant.....	2
Hypotheses of the study .....	2
Scope of the study.....	3
Key words.....	3
CHARPTEr II LITERATURE REVIEWS.....	4
Breast cancer.....	4
1. Types of breast cancer.....	4
2. Cancer development .....	5
3. Risk factors.....	5
Triple Negative Breast Cancer (TNBC) .....	7
1. Classification of TNBC subtypes .....	7
2. Treatment of TNBC.....	7
Plant-derived anticancer drugs .....	10
1. Plants that have anticancer effect on MDA-MB-231 cell lines.....	14
<i>Citrus hystrix</i> DC.....	15
1. Chemical constituents of <i>C. hystrix</i> .....	15

2.	Potential effect of <i>C. hystrix</i> .....	20
2.1.	Anticancer effect of <i>C. hystrix</i> .....	30
2.2.	Citronellal and citronellol.....	30
Apoptosis.....		31
1.	Apoptosis Pathways.....	32
1.1.	The death receptor-dependent pathway.....	32
1.2.	The mitochondrial pathway.....	33
3.	The effector caspases activation.....	36
4.	Cross linking between extrinsic and intrinsic apoptosis pathway.....	37
5.	Apoptosis analysis.....	38
Cell Cycle progression.....		38
1.	Roles of Cyclin and Cyclin Dependent Kinase (Cdk) in cell cycle regulation.....	39
1.1.	Regulation of Cyclin/Cdk in G0/G1 phase.....	40
1.2.	Regulation of Cyclin/Cdk in S phase.....	41
1.3.	Regulation of Cyclin/Cdk in G2/M phase.....	42
2.	The Cdk inhibitor.....	43
3.	Cell cycle checkpoints.....	43
3.1.	G1/S checkpoint.....	43
3.2.	Intra-S checkpoint.....	45
3.3.	G2/M checkpoint.....	45
3.4.	Spindle assembly checkpoint.....	46
4.	Cell cycle analysis.....	47
Tumor protein p53.....		48
Chromatography techniques for chemical profiles identification.....		50
1.	Thin layer chromatography.....	50
2.	Gas Chromatography – Mass Spectrometry (GC-MS).....	51
Cell cytotoxic by MTT assay.....		52
Clonogenic or colony formation assay.....		52

Wound scratch migration assay .....	53
Flowcytometry analysis on apoptosis .....	53
Hoechst staining.....	55
Assessment to the level of genes expression .....	56
1. Evaluation mRNA expression by RT-qPCR technique .....	56
2. Evaluation proteins expression by Western Blot technique .....	56
CHAPTER III METHODOLOGY.....	60
Experimental Design .....	60
Extraction of <i>C. hystrix</i> leaf powder.....	62
1. <i>C. hystrix</i> leaf powder .....	62
2. Maceration.....	62
<i>C. hystrix</i> leaf extracts preparation for experiment .....	63
β-Citronellol and citronellal.....	64
Thin Layer Chromatography .....	64
Gas Chromatography – Mass Spectrometry (GC-MS).....	64
Cells and Cell culture.....	66
1. Triple Negative Breast Cancer Cells .....	66
2. Macrophage .....	66
3. Cells Cultures .....	67
4. Cell Sub-culture.....	67
5. Cryopreservation .....	67
Monocytes Isolation .....	69
Cell Viability by MTT Assay .....	69
Preparation <i>C. hystrix</i> crude extracts, citronellol and citronellal for MTT assay .....	70
Cell Proliferation Rate .....	72
Colony Forming Assay .....	72
Scratch-Wound Assay .....	73
Apoptosis and cell cycle analysis .....	73

1. Apoptosis analysis .....	73
2. Cell cycle analysis .....	74
Hoechst 33342 staining.....	74
RT-qPCR .....	74
1. mRNA extraction protocol .....	74
2. Primer sequences .....	76
Polyacrylamide Gel Electrophoresis and Western Blot.....	77
1. Sample preparation.....	77
2. Protein extraction .....	77
3. Total protein determination .....	77
4. Polyacrylamide Gel Electrophoresis .....	78
5. Membrane transfer .....	79
6. Antibody probing .....	79
7. Immuno-detection .....	79
Statistical Analysis.....	80
Research Approval.....	80
CHAPTER IV RESULTS .....	81
Extraction yields of <i>C. hystrix</i> leaf powder .....	81
Identification of volatile components in crude hexane extract by GC-MS .....	81
Screening of crude extracts using thin layer chromatography (TLC) .....	86
MDA-MB-231 cell culture .....	89
Primary macrophage cells culture .....	90
Cytotoxicity of crude extracts, citronellol, citronellal on MDA-MB-231 cells .....	91
Crude hexane, citronellol and citronellal decreased down MDA-MB-231 cell proliferation rate .....	94
<i>C. hystrix</i> hexane extract, citronellol and citronellal reduced number of colonies forming in MDA-MB-231 cells.....	97
Crude hexane, citronellol and citronellal induced cell cycle arrest in MDA-MB-231 cells.....	99

Crude hexane, citronellol, and citronellal induced apoptosis in MDA-MB-231 cells .....	101
Crude hexane, citronellol and citronellal modulated apoptosis-related proteins gene expression in MDA-MB-231 cells .....	103
Crude hexane, citronellol and citronellal induced apoptosis and DNA fragmentation in the cells by inhibiting the anti-apoptotic Bcl-2 protein and activating caspase dependent apoptotic pathway .....	104
CHARPTER V DISCUSSIONS AND CONCLUSIONS .....	106
REFERENCES .....	112
APPENDIX.....	125

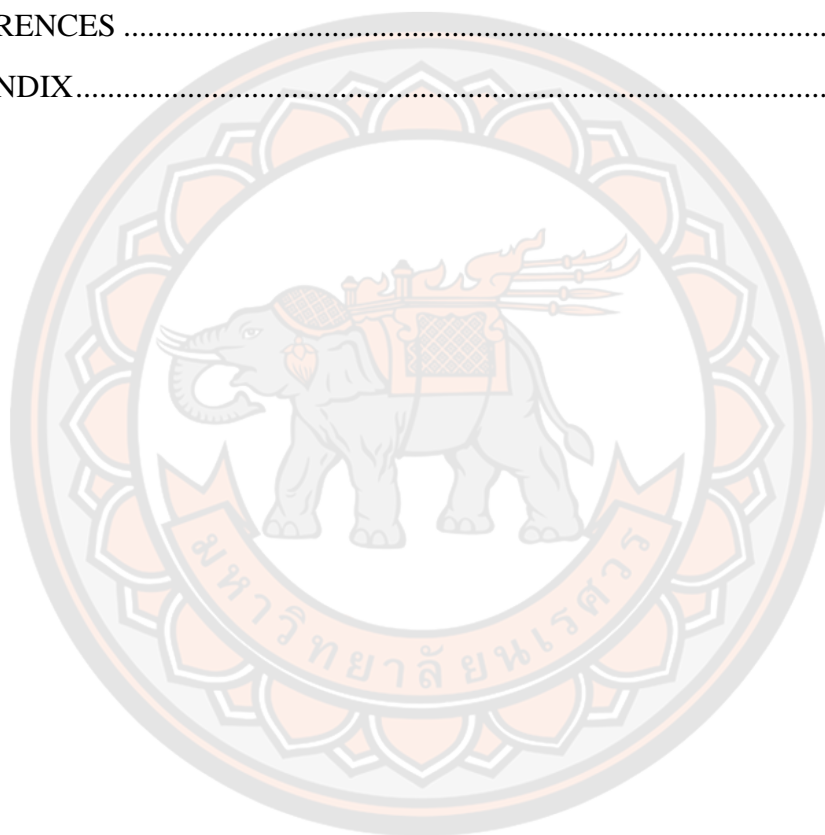


## TABLE OF TABLES

	<b>Page</b>
Table 1 Commonly used single agent chemotherapy in Triple-Negative Breast Cancer .....	9
Table 2 Plant-derived anticancer drugs.....	12
Table 3 Identified compounds of <i>C. hystrix</i> leaves and peels.....	17
Table 4 Volatile compounds identified in chloroform crude extract from <i>C. hystrix</i> leaves and their biological activities .....	21
Table 5 Volatile compounds identified in ethyl acetate crude extract from <i>C. hystrix</i> leaves and their biological activity .....	25
Table 6 Two-fold dilution of <i>C. hystrix</i> crude extracts, citronellol, citronellal and doxorubicin .....	71
Table 7 Primer sequences .....	76
Table 8 Proteins for Western Blot analysis.....	79
Table 9 The identified compounds from crude hexane by GC-MS.....	84
Table 10 $R_f$ value from TLC of crude <i>C. hystrix</i> extracts.....	87
Table 11 Cytotoxicity of <i>C. hystrix</i> crudes extract and its compounds citronellol and citronellal on MDA-MB-231 cell line .....	93
Table 12 Comparing $IC_{50}$ , $IC_{10}$ , $IC_5$ of crude hexane, citronellol and citronellal on MDA-MB-231 cell and primary macrophage.....	93
Table 13 Statistical comparison on proliferation rate of MDA-MB-231 cells.....	132
Table 14 Statistical comparison on wound migration assay.....	132
Table 15 Statistical comparison on colony formation assay .....	133

## TABLE OF FIGURES

	<b>Page</b>
Figure 1 <i>Citrus hystrix</i> (Kaffir lime) flowers, fruits and leaves .....	15
Figure 2 The death receptor signaling of apoptosis. ....	32
Figure 3 The mitochondrial pathway of apoptosis.....	34
Figure 4 DNA fragmentation induced by caspase 3. ....	37
Figure 5 Cell cycle progression .....	39
Figure 6 Cyclin/cyclin-dependent kinase (Cdk) complexes roles in each phase of cell cycle.....	40
Figure 7 Concentration of cyclin protein through cell cycle .....	42
Figure 8 G1/S cell cycle checkpoint .....	44
Figure 9 G2/M cell cycle checkpoint.....	46
Figure 10 Tumor Protein p53 pathway .....	49
Figure 11 Thin Layer Chromatography system.....	51
Figure 12 Reduction of MTT dye .....	52
Figure 13 Apoptotic cell analyzed by flowcytometry.....	54
Figure 14 Analysis of nuclear morphology by phase-contrast microscopy.....	55
Figure 15 Western Blot analysis workflow .....	59
Figure 16 Experimental Design .....	61
Figure 17 Extraction of <i>C. hystrix</i> leaf by maceration method.....	63
Figure 18 MDA-MB-231 cells under microscope .....	66
Figure 19 Neubauer Haemocytometer .....	68
Figure 20 Separation of RNA by Ribozol™ Reagent kits.....	75
Figure 21 Total ion chromatogram of volatile compounds in crude <i>C. hystrix</i> hexane extract obtained from GC-MS .....	82
Figure 22 Total ion chromatogram of standard citronellol at 13.03 min.....	82
Figure 23 Total ion chromatogram of standard citronellal at 10.88 min .....	83
Figure 24 Peaks of citronellal and citronellol were observed at retention times at 10.75 min and 12.85 min. ....	83

Figure 25 Thin layer chromatography .....	86
Figure 26 MDA-MB-231 cells growth morphology by time of incubation .....	89
Figure 27 MDA-MB-231 proliferation curve .....	90
Figure 28 Primary monocytes at day 0 and macrophage derived at day 7 .....	90
Figure 29 IC <sub>50</sub> value from treatments on MDA-MB-231 cell and primary macrophage .....	92
Figure 30 Inhibition of cell proliferation of crude hexane, citronellol, citronellal on MDA-MB-231 cells .....	94
Figure 31 Wound scratch migration assay .....	96
Figure 32 Clonogenic Assay on MDA-MB-231 cells .....	98
Figure 33 Comparing effect of crude hexane and crude ethyl acetate by screening on cells apoptosis and cell cycle .....	100
Figure 34 Flow cytometry and Hoechst33258 staining on MDA-MB-231 cells.....	102
Figure 35 Alteration apoptosis-related genes expression in treated cells .....	103
Figure 36 Crude hexane, citronellol, citronellal induced apoptosis through caspase dependent pathway by inhibiting Bcl-2 protein.....	105
Figure 37 Inhibition of Bcl-2 protein in MDA-MB-231 cells by <i>C. hystrix</i> , citronellal and citronellol leading to the activation of caspase dependent apoptotic pathway .....	111
Figure 38 Cell viability of 2.5% DMSO compared to culture medium.....	134

## ABBREVIATIONS

ALT	= Alanine transaminase
AP	= Alkaline Phosphate
APS	= Ammonium persulfate
AST	= Aspartate transaminase
ATCC	= American Type Culture Collection
Bid	= BH3 interacting-domain death agonist
BL-1 or BL-2	= Basal-like 1 or Basal-like 2
BMI	= Body mass index
BRCA	= Breast cancer gene
<i>C. hystrix</i>	= <i>Citrus hystrix</i>
CHEK	= Checkpoint kinase
Cyt C	= Cytochrome C
DDR	= DNA damage response
DED	= Death effector domain
DFF45	= DNA fragmentation factor 45
DMEM	= Dulbecco's modified eagle high glucose medium
DMSO	= Dimethyl sulfoxide
DNA	= Deoxyribose nucleic acid
Dox	= Doxorubicin
EGFR	= Epidermal growth factor receptor
ER	= Estrogen receptor
FADD	= Fas-associated protein with death domain
FBS	= Fetal bovine serum
GC-MS	= Gas chromatography - Mass spectrometry
Her-2	= Human epidermal growth factor 2
HRP	= Horseradish peroxidase
IC50	= Inhibition concentration 50%
ICAD	= Caspase-Activated DNase Inhibitor
IDC	= Invasive ductal carcinoma

**ABBREVIATIONS (CONT.)**

ILC	=	Invasive lobular carcinoma
IM	=	Immunomodulatory
Ki-67	=	Antigen Ki-67
LAR	=	luminal androgen receptor
MDM2	=	Mouse double minute 2 homolog
MDR	=	Multi drug resistance
MSL	=	Mesenchymal stem-like
MTT	=	3-(4, 5dimethylthiazolyl-2)-2,5-diphenyltetrazolium bromide
N.I.H	=	National Institute of Health
p.H	=	Power of hydrogen ion concentration
p21	=	Tumor protein 21
p53	=	Tumor protein 53
PAGE	=	Polyacrylamide gel electrophoresis
PBS	=	Phosphate buffer saline
PDVF	=	Polyvinylidene difluoride
PI	=	Propidium iodide
PR	=	Progesterone receptor
PS	=	Phosphatidylserine
RF	=	Retention factor
RI <sub>s</sub>	=	Retention indices
RNA	=	Ribose nucleic acid
ROS	=	reactive oxygen species
RT-qPCR	=	Quantitative reverse transcription polymerase chain reaction
SDS	=	Sodium dodecyl sulphate
tBid	=	Truncated Bid
TBS	=	Tris buffer saline
TBST	=	Tween-20 -base tris buffer saline
TEMED	=	N, N, N', N'-tetramethylethylenediamine

**ABBREVIATIONS (CONT.)**

TGF- $\beta$	=	Transforming growth factor beta
TLC	=	Thin layer chromatography
TNBC	=	Triple negative breast cancer
TNF- $\alpha$	=	Tumor growth factor alpha
UV	=	Ultraviolet
WHO	=	World health organization



# CHAPTER I

## INTRODUCTION

### Background

Breast Cancer is one of the most frequent cancer that usually occur in women. In 2018, World Health Organization has pointed out that around 2.1 million new cases of breast cancer incidence have been reported. The number of cancer related-death in women around the globe were estimated to be around 626,679 (6.6%) (WHO, 2018). In 2015, a review from 15 studies revealed means of very high cumulative treatment costs in breast cancer treatments by its stages. At stage I, the cost were estimated to be \$29,724, \$39,322 for stage II, \$57,827 for stage III, and \$62,108 for stage IV (Sun et al., 2018). There are many subtypes of breast cancer base on histological arrangement including luminal breast cancer, basal-like, HER-2 enriched and claudin low (Eroles et al., 2012). Triple negative breast cancer is one of the basal-like breast cancers. It is known for its less expression of estrogen receptor (ER), progesterone receptor (PR), and human epidermal growth factor receptor-2 (HER-2). This type of breast cancer was reported as an aggressive breast cancer type with early metastasis, and resistance to many kinds of chemotherapy drugs with poor prognosis in patients (Aysola et al., 2013).

For centuries, folklore medicines have been used to treat many kinds of diseases in many countries around the world. Animal parts or organs have been used as the treating drugs, but the major parts of the medicines were from plant derived. Lots of experiments have been conducted to evaluate the effect of the plants that have been used in the traditional medicine to the molecular level in order to find new active compounds that could be potential in the treatments against the diseases including cancer. *Citrus hystrix* DC. or kaffir lime is a tropical plant which is native to Southeast Asia. Kaffir lime is known for its aromatic oil, which is widely used in lots of country around the world. Its leaves have been used as spices in many cuisines for its aromatic fragrant. Furthermore, kaffir lime has also been developed into many products such as shampoo, mosquito repellent, perfume, and so on. Despite from this,

kaffir lime is used in traditional medicine for many treatments. It has been used as anti-inflammatory as an ingredient in herbal compressed (Dhippayom et al., 2015), digestive aid, treating cold (Wongpornchai, 2012). More than that, kaffir lime has been reported to possess anti-bacterial activity in many bacteria strains, (Nanasombat & Lohasupthawee, 2005; Srisukh et al., 2012). So far, many researcher has been pointed out that kaffir lime possessed anti-cancer effect in many cancer cell lines such as leukemic cell lines (Chueahongthong et al., 2011), neuroblastoma cell lines, cervical cancer cell line (Tunjung et al., 2015), melanoma cell lines , the adenocarcinoma pancreatic cell line (Sun et al., 2018), MCF-7 breast cancer cell line (MAMUR, 2019). And yet, none of these have reported its anticancer effect on the triple negative breast cancer cell line MDA-MB-231.

### **Statement of the problems**

*C. hystrix* is a tropical plant which is easy to cultivate and available at any seasons, and since there has not been any reported about the effect of *C. hystrix* on the triple negative breast cancer cell line MDA-MB-231, the *in vitro* study should be conducted to evaluate the anticancer effect of *C. hystrix* on this cell line, and either for citronellol and citronellal.

### **Research significant**

This study will provide first *in vitro* study of the anticancer effect of *C. hystrix* leaf extracts, for citronellol and citronellal against the triple negative breast cancer MDA-MB-231 and some mechanism of death trigger by the extract on the cells.

### **Hypotheses of the study**

*C. hystrix* leaf extract, for citronellol and citronellal possessed the anticancer effect against MDA-MB-231 cell line whether it could inhibit cancer cell proliferation and induce apoptosis and cell cycle arrest in MDA-MB-231.

## Scope of the study

The purpose of this study was to investigate anticancer effects of *C. hystrix* leaf extracts, citronellol and citronellal on the triple negative breast cancer cell line MDA-MB-231. *C. hystrix* leaf powder extraction processes were carried out at Department of Chemistry, Faculty of Sciences while the *in vitro* study of *C. hystrix* extracts activity on MDA-MB-231 was performed at Faculty of Allied Health Sciences, Naresuan University. *C. hystrix* leaf powder was received from Khaolaor company, Nakhon Pathom, Thailand. Crude extracts obtained from extraction process were used in the experiment to treat MDA-MB-231 cells. Then cell cytotoxic assay was used to evaluate the toxicity of the leaf extracts on human normal cells and for selection safety dose for the next experiments. Crude hexane, a high sensitivity against cancer, was selected for future experiments. Its chemical profiles were identified by using thin layer chromatography and gas chromatography-mass spectrometry. The doses receive from the cytotoxic assay were used for cell proliferation assay, wound scratch migration assay and colony formation assay. Then the selected doses were used to evaluate the ability of kaffir lime leaf extract in inducing apoptosis and cell cycle arrest to the cells. Moreover, level of genes expression and proteins expression correlate to the apoptosis and cell cycle arrest were identified using RT-qPCR and Western blot analysis.

## Key words

Triple Negative Breast Cancer, MDA-MD-231, *Citrus hystrix* DC. (kaffir lime), leaf extract, citronellol, citronellal, anti-cancer

## CHAPTER II

### LITERATURE REVIEWS

#### Breast cancer

Breast Cancer is one of the most common cancers which were reported up to 2.08 million cases around the world, and causing the cancer-related death up to 626,679 deaths by 2018 (WHO, 2018). Breast cancer is a type of cancer that caused by the uncontrollable growth of cells that could occur in many different tissues in the breast. The cancer normally starts at milk duct or at mammary gland then starting to spread to other surrounding tissues like lymph nodes and metastases to other tissues or organ especially lung and bone (American Cancer Society, 2017a).

#### 1. Types of breast cancer

According to American Cancer Society (2017b), breast cancer is divided into *in situ* carcinoma and invasive carcinoma (infiltrating cancer) based on its invasivity. The *in situ* carcinoma can be classified into sub-categorizes based on its histology. It was divided into ductal carcinoma and lobular carcinoma. Ductal carcinoma *in situ* which appeared at the milk duct and the lobular carcinoma which located at in the mammary gland. Both of these types of cancer are non-invasive or pre-invasive form of the breast cancer. The major sub-types of invasive breast carcinoma consisted of invasive lobular carcinoma (ILC) and invasive ductal carcinoma (IDC) which accounted as major class of invasive breast cancer.

In Eroles et al.(2012), breast cancer was classified into six sub-types reflected by its mRNA expressions and immunohistochemical profiles. Frequently, it is categorized base on hormonal receptors such as progesterone receptor (PR), estrogen receptor (ER), and human epidermal growth factor receptor 2 (HER-2). Luminal cancer shows intermediate prognostic for its hormonal and HER-2 receptor expression, Luminal A (ER+, HER-2-, Ki-67 low, and PR high), luminal B (ER+, HER-2-, Ki-67 low or PR low). Basal-like accounted around 10-20% of the breast

cancer with bad prognosis. This cancer type has higher rate of genes mutation which responsible for higher rate of relapse to chemotherapy, and its aggressiveness. One of this type includes the triple negative breast cancer which absent in (ER-, PR-, HER-2-) genes expression. HER-2 enriched has worse prognostic as the cancer has highly HER-2 expression. Claudin low described for its low expression of cell-cell adhesion molecules like claudin, cingulin, E-cadherin. One other type was defined as the normal breast covered nearly 5 to 10% of breast cancer. This cancer does not response to the neo-adjuvant chemotherapy and shows lack expression of ER, PR and HER-2.

## **2. Cancer development**

The American Joint Committee on Cancer anatomically classified cancer development stage into the T.N.M system which includes the primary tumor (T), the surrounding lymph nodes (N), and the distance metastasis (M). Primary tumor at T stage is define by its location and size. T stage present locally at the site of breast tissues with size not larger than 2 mm. In this stage, there is no present of tumor evading the surrounding lymph nodes or distances metastasis at the other organ. The N stage, which is the regional lymph nodes stage, present the tumor cells deposit in the surrounding lymph nodes tissues. Even the present of tumor in lymph, cancer cells still not found in the distance metastasis. The M stage is the metastasis stage. The tumor cells grow bigger at the local cancer site. Its metastases into lymph nodes and travels to the distance organ such as bone, lung. (Gabriel N. Hortobagyi & 2017).

## **3. Risk factors**

Breast cancer seems to link to many risk factors. Age is one of the risk factors usually describe in the breast cancer patient. Women age higher than 50 faces higher risk to breast cancer. A study showed the number of incidences were increased in elderly women aged over 60 (Alberg & Singh, 2001). Another result from SEER program (Surveillance, Epidemiology, and End Results) in U.S.A indicated that more than 60% of women age after 60 have been diagnosed with breast cancer (Maisonneuve, 2017). Race is also a factor that may relate to breast cancer occurrence. Data from W.H.O illustrated that number of breast cancer incidences

from both sexes tend to be higher in the Asian region, which was reported to be around 43.6% of the world population, also the mortality rate (49.6%) and prevalence (38.2%) (WHO, 2018).

Hormonal status is very important in breast cancer and has also been considered as one of the most important risk factors that may link to the treatment and prognosis of the patients. The increasing level of endogenous hormones from ovaries such as estrogen and progesterone during pregnancy stimulates the growth of mammary epithelium cells and breast tissues, which would support the growth of the cancer if the malignancy transformation is present at this state (Russo et al., 1979). Early age of menarche, and late menopause were also mentioned to increase the risk of having breast cancer. A study found that the relative risk of having breast cancer increased in patient who were having early-age menarche, and women who enter menopause late at or after 55 years old (Collaborative Group on Hormonal Factors in Breast, 2012). Women who have early menstruation below 10 years old tends to have 20% higher risk to those between 11 and 12 years old (Bodicoat et al., 2014). Another mentioned risk factor may relate to the late of having first full-term pregnancy (>30 years old or older). The risk of having lobular breast cancer was increased by 2.4 fold in women who gave first birth after 30, when compared to women who gave labor before of 20 years old in association with postmenopausal body mass index (BMI), history of having oral contraceptive, and the postmenopausal hormones replacement therapy (Newcomb et al., 2011). The heredity was also been considered as a factor that would involve with breast cancer. Women who have relatives or family history with breast cancer are highly expose to the chance of having breast cancer (Brewer et al., 2017). Some genes mutation like breast cancer (BRCA) genes, tumor protein (p53) gene, checkpoint kinase 2 (CHEK2) gene were observed, and were concluded to links to this factor (Walsh et al., 2006).

## **Triple Negative Breast Cancer (TNBC)**

### **1. Classification of TNBC subtypes**

Known for its lack of 3 important receptors expression ER, PR, and HER-2, these 3 receptors have been used to distinguish TNBC from other breast cancer types. American Society of Clinical Oncology guide line recommendation consider the negativity of ER and PR when the immunohistochemical staining (IHC) present less than 1% repartition of these receptors in the tissue (Hammond et al., 2010), and less than 10% for HER-2 receptor (Wolff et al., 2013). However, molecular analysis of gene expressions has classified TNBC into another 6 different sub-types. These 6 sub-types groups consist of basal-like (BL) which has 2 type basal-like 1 (BL-1) and basal like 2 (BL-2), an immunomodulatory (IM), a mesenchymal (M), a mesenchymal stem-like (MSL), and a luminal androgen receptor (LAR) subtype. In this research, the TNBC cell line MDA-MB-231 was categorized into the MSL subtype.

The MSL subtype is enriched for gene ontologies in cell mortality pathway (Rho pathway), cellular differentiation and growth pathways (ALK pathway, TGF- $\beta$  signaling and Wnt/ $\beta$ -catenin pathway, and growth factor signaling pathways that include inositol phosphate metabolism, EGFR, PDGF, calcium signaling, G-protein coupled receptor, and ERK1/2 signaling as well as ABC transporter and adipocytokine signaling. It shares similar features with the highly differentiated metaplastic breast cancer which is a chemoresistance cell. MSL subtype expresses low levels of proliferation genes accompanied with high expression of genes associated with stem cell (ABCA8, PROCR, ENG, ALDHA1, PER1, ABCB1, TERF2IP BCL2, BMP2, and THY1), numerous HOX genes (HOXA5, HOXA10, MEIS1, MEIS2, MEOX1, MEOX2, and MSX1), and mesenchymal stem cell-specific markers (BMP2, ENG, ITGAV, KDR, NGFR, NT5E, PDGFRB, THY1, and VCAM1) (Lehmann et al., 2011).

### **2. Treatment of TNBC**

The aggressiveness and early metastasis of TNBC leaving the patients with poor prognostic and lower survival rate. Surgery and radiotherapy are performed with the

evaluation of TNM staging of the cancer. However due to lack of hormonal targeted therapy such as anti-PR, anti-ER and anti-HER-2, the chemotherapy still be applicable for the systemic treatment of TNBC. Most commonly used chemotherapy in TNBC include the antimetabolites such as the anthracycline, microtubule modulators, the intercalating agents (Wahba & El-Hadaad, 2015) (**Table 1**).



**Table 1 Commonly used single agent chemotherapy in Triple-Negative Breast Cancer**

<b>Drug</b>	<b>Dose</b>	<b>Frequency</b>	<b>Drug Action</b>
Docetaxel	75-100 mg/m <sup>2</sup>	Day 1 of 21 day cycle	Microtubule inhibitor
Paclitaxel	80 mg/m <sup>2</sup>	Weekly	Microtubule inhibitor
Nab-paclitaxel	100-150 mg/m <sup>2</sup>	Day 1, 8, and 15 of 28 day cycle	Microtubule inhibitor
Doxorubicin	60 mg/m <sup>2</sup>	Day 1 of 21 day cycle	Anti-topoisomerase II
Epirubicin	60 mg/m <sup>2</sup> 90 mg/m <sup>2</sup>	Day 1 of 21 day cycle Day 1 of 21 day cycle	DNA intercalating agent
Pegylated liposomal doxorubicin	40-50 mg/m <sup>2</sup>	Day 1 of 28 day cycle	Anti-topoisomerase II
Cisplatin	60-75 mg/m <sup>2</sup>	Day 1 of 21 day cycle	DNA intercalating agent
Carboplatin	AUC 6 AUC 2	Day 1 of 21-28 day cycle Day 1, 8, and 15 of 21 day cycle	DNA intercalating agent Microtubule inhibitor
Capecitabine	1000-1250 mg/m <sup>2</sup>	Twice a day, day 1-14 of 21 day cycle	DNA synthetase inhibitor
Gemcitabine	800-1250 mg/m <sup>2</sup>	Day 1, 8, and 15 of 28 day cycle	DNA synthetase inhibitor
Gemcitabine	20-30 mg/m <sup>2</sup>	Day 1, 8, and 15 of 21 day cycle	DNA synthetase inhibitor
Vinorelbine	1.4 mg/m <sup>2</sup>	Day 1 and 8 of 21 day cycle	Microtubule inhibitor
Ixabepilone	40 mg/m <sup>2</sup>	Day 1 of 21 day cycle	Microtubule inhibitor
Cyclophosphamide	600 mg/m <sup>2</sup>	Day 1 of 21 day cycle	Anti-metabolite

## Plant-derived anticancer drugs

For years, herbal medicines have been developed and have been used as a therapeutic potential in modern medicine. Many active compounds have been identified and have been extracted from the medical plants and have been developed as the preferential alternative medicine in cancer treatments (**Table 2**).

Sulforaphane is an isocyanate group of organosulfur compounds. It is an anticancer compound identified in *Brassica* of cruciferous vegetables. It was reported to induce apoptosis in several types of human breast cancer cell lines including the MDA-MB-231, and also able to decrease the expression of many proliferation factors such as HER-2, EGFR, ER (Pledge-Tracy et al., 2007). Follow by this, pre-clinical and clinical study have supported that sulforaphane helps increase cytoprotective enzymes NQO1 and HO-1 in rat mammary gland and human breast tissues (Cornblatt et al., 2007). Most of anticancer drugs derived from plants are usually the microtubules modulator which they interfere with microtubules formation during mitosis. Paclitaxel is a taxane alkaloid derived from *Taxus brevifolia*. It acts as cytostatic agent which inhibit the depolymerization of microtubules during telophase of mitosis (Jauhari et al., 2009; Papich, 2016). Paclitaxel was able to induce cell cycle arrest in A549 lung cancer. A549 cells arrested at G1 phase with the accumulation of p53 proteins. This arrest has been shown to involve with the correlation between p53 protein and p21 protein in dose dependent manner in which the expression of p21 protein has been seen in the dose below 25 nM (Demidenko et al., 2008). In term of this, vinca alkaloids have also been developed as anticancer drugs by inhibiting the polymerization of microtubules. Vincristine, vinblastine, vinorelbine, vindesine and vinflunine are the anti-mitotic molecules found in *Catharanthus roseus* (Amin et al., 2009). These molecules bind to beta subunit of tubulin proteins, which prevent the polymerization of microtubules in metaphase of mitosis (Avenidaño & Menéndez, 2015). This mechanism has also been found in noscapine which is the phthalideisoquinoline alkaloid derived from *Papaver somniferum* (Chen et al., 2015). Similar action was shown by its analogue EM011 on human non-small cell lung cancer cells by inhibiting the polymerization of tubulin, and resulted in transient effect of cell arrest in M phase before undergone apoptosis (Karna et al., 2009).

Epipodophyllotoxin from *Podophyllum peltatum* L was reported to inhibit the tubulins assembly which induced cell cycle arrest at G2/M phase in human non-small cell lung cancer cells (Abad et al., 2012), and also acted as the topoisomerase II inhibitor which caused double strains DNA break leading to DNA damage and cell death (Hande, 2008).

Many other notified plant-derived anticancer drugs include pomiferin (histone deacetylase inhibitor) the isoflavonoid extracted from *Maclura pomifera* (Myzak et al., 2004; Seidel et al., 2012), Combretastatin A-4 phosphate (anti-angiogenic, tubulin modulator) found in *Combretum caffrum* (Dorr et al., 1996; M. Su et al., 2016), Roscovitine (Cdks inhibitor) from *Raphanus sativus* L (Węsierska-Gądek et al., 2011), Epigallocatechin-3-gallate derived from Green tea, which was reported for its anti-oxidant property and anti-proliferative effect (Du et al., 2012; Raza & John, 2005).

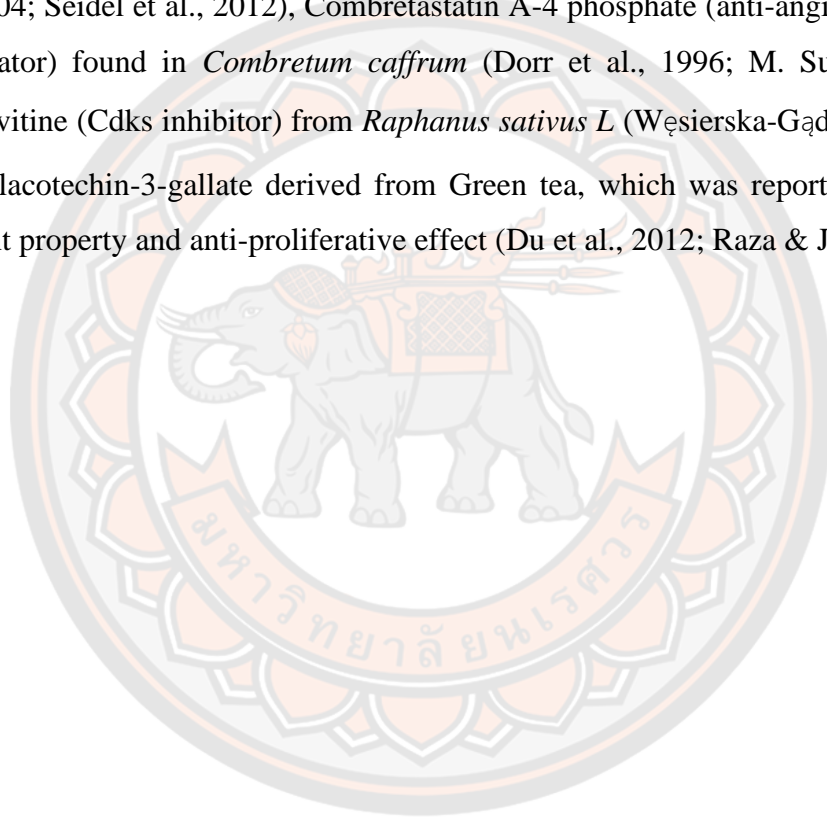


**Table 2 Plant-derived anticancer drugs**

Active Molecules	Isolated or Derived from	Actions	Cells	References
Sulforaphane	<i>Brassica</i> of cruciferous vegetables	Induce phase 2 enzymes expression, histone deacetylase inhibitor, anti-proliferative, induce apoptosis, induce cell cycle	Breast cancer cell lines	(Cornblatt et al., 2007; Pledgie-Tracy et al., 2007)
Paclitaxel	<i>Taxus brevifolia</i>	Microtubules modulator, induce cell cycle arrest	Lung cancer cell lines	(Demidenko et al., 2008; Jauhari et al., 2009; Papich, 2016)
Vincristine	<i>Catharanthus roseus</i>	Microtubules modulator	Breast cancer cell lines	(Amin et al., 2009; Avendaño & Menéndez, 2015; Blajeski et al., 2002)
Noscapine	<i>Papaver somniferum</i>	Microtubules modulator	Lung cancer cell line	(Chen et al., 2015; Karna et al., 2009)

**Table 2 (Cont.)**

Active Molecules	Isolated or Derived from	Actions	Cells	References
Epipodophyllotoxin	<i>Podophyllum peltatum</i> L	Microtubules modulator, Topoisomerase II inhibitors	Lung cancer cell line	(Abad et al., 2012; Hande, 2008)
Pomiferin	<i>Maclura pomifera</i>	Histone deacetylase inhibitor	Human embryonic kidney cell line	(Myzak et al., 2004; Seidel et al., 2012)
Combretastatin A-4 phosphate	<i>Combretum caffrum</i>	Microtubules modulator, Anti-angiogenic	Ovary cancer cell line, human umbilical vascular cells, cellsendothelial cells	(Dorr et al., 1996; M. Su et al., 2016)
Roscovitine	<i>Raphanus sativus</i> L	Cdk inhibitor	Breast cancer	(Węsierska-Gądek et al., 2011)
Epigallocatechin-3-gallate	Green tea	Anti-oxidant, Anti-proliferative	Kidney cancer	(Du et al., 2012; Raza & John, 2005)

### 1. Plants that have anticancer effect on MDA-MB-231 cell lines

Many researches have been performed in purpose to find out new therapeutic molecules that could act as a cytostatic or cytotoxic agent against the TNBC. Noscapine and papaverine, the alkaloids isolated from *Papaverine somnifrum* L. (opium), have been reported to comprise cytotoxic effect on TNBC cell lines. These two molecules could inhibit the growth of MDA-MB-231 and MCF-7 cell lines respectively with IC<sub>50</sub> value of 20.15±4.01 µM and 15.47±0.78 µM for noscapine, and 6.06±1.98 µg/ml and 6.16±0.84 µg/ml for papaverine. Both of the alkaloids could induced apoptosis in MDA-MB-231 and MCF-7 cancer stem cells with cell cycle arrest at G1 phase (Sajadian et al., 2015). Sulforaphane, a molecule belongs to isocyanate group from *Brassica* of cruciferous vegetables, as described above also shown its effect on these two cell lines. It decreased the expression of EGFR and Her-2, which these two proteins play an important role in the growth of the cancer. Moreover, it could induce the caspases cascade activation shown by Western blot. Another result of the study shown that sulforaphane could induced cell cycle arrest at G2/M with cyclin B1 inhibition-related, and was able to inhibit histone deacetylase activity preventing some genes of MDA-MB-231 cells from expressing their tumor proteins (Pledge-Tracy et al., 2007).

Beside these, many researches papers have been published that reported about plant extracts which have shown the anticancer actions against this triple negative breast cancer cell line even though those active compounds have not been identified. Many mechanisms related to cell toxic or cell death causing by the extracts have been revealed. In Ahmad et al., (2012) the methanolic extract from *Nigella sativa* was able to induce the apoptosis in MDA-MB-231 cells with an up-regulation of pro-apoptotic protein Bax and with down-regulation of Bcl-2 proteins. Another research indicated a result from black turtle bean extracts which it induced cell cycle arrest in S and G2/M phase. More than that black turtle bean extracts induced cell apoptosis by modulation of mitochondrial membrane potential, increasing of Bax protein, and decreased of Bcl-2 protein (Kumar et al., 2017).

### *Citrus hystrix* DC.

*Citrus hystrix* DC. (*C. hystrix*) or kaffir lime is a plant belong to Rutaceae family. *C. hystrix* has many names such as ក្រូចសើច, មះក្រូច, or kaffir lime. Kaffir lime is a stood-up tree up to about 6 meters high with branches and branchlets cover with spines. It has double pointy oval shape leaf with dark green in color. It has small, white and fragrant flower. The fruit is lemon yellow, with semi-rough-smooth texture, ellipsoid to sub-globose in shape (**Figure 1**). It can be found all over the world, especially in tropical area. Kaffir lime is known for its aroma and has been used as spice among Asian cuisine and all over the world for its highly aromatic and hence flavoring spice. (Ravindran, 2016). Apart of the leave, kaffir lime fruits have been used in many products such as shampoo, hair conditioner, moisturizer, mosquito repellent, and so on. Also, it has been used traditional medicine as digestive aid, treating cold, and as herbal compressed against inflammation (Wongpornchai, 2012). It also be founded in herbal compress as a combination with other herbal plants to reduce pain and inflammation (Dhippayom et al., 2015).



**Figure 1** *Citrus hystrix* (Kaffir lime) flowers, fruits and leaves

**Source:** <https://www.pinterest.co.uk/pin/523473156674546430/>

#### 1. Chemical constituents of *C. hystrix*

There are many components that has been reported in *C. hystrix* including phenolic compounds, flavonoids, terpenoids, alkaloids, coumarins, glycosides, saponins, tanins, hydrocarbons and fatty acids from the hydrodistillation extraction (**Table 3**) (Agouillal et al.,2017; Butryee et al.,2009; Dilla et al.,2017). Terpenoids was found as the most abundant compound in kaffir lime leaf. Result from GC-MS

showed the present of five major monoterpenoid compound in the leaves extract by hydrodistillation including  $\beta$ -citronellal (46.40%), L-linalool (13.11%),  $\beta$ -citronellol (11.03%), citronelyl acetate (6.76%) and sabinen (5.91%). Other minor compounds consist of  $\beta$ -pinene (1.24%),  $\beta$ -micrene (1.27%), tran- $\beta$ -ocimene (1.56%), (-)-isopulegol (1.57%), 4-terpeneol (1.52%), *cis*-Linalol oxide (1.86%), trans- $\beta$ -caryopilene (1.48%) and nerolidol (1.11%) (Warsito et al., 2017).



**Table 3 Identified compounds of *C. hystrix* leaves and peels**

Plant parts	Extraction methods	Components							
		Monoterpene Hydrocarbon	%	Oxygenated Monoterpene	%	Sesquiterpene Hydrocarbon	%	Oxygenated Sesquiterpene	%
Fresh leaves	Likens-Nikerson Extraction	Sabinene	1.6	Citronellal	61.7	$\beta$ -Elemene	tr	Nerolidol	1.2
		$\beta$ -Pinene	0.1	$\beta$ -Citronellol	13.4	$\alpha$ -Muuroolene	tr	Guaiol	0.2
		$\beta$ -Myrcene	0.7	iso-Pulegol	0.9	$\beta$ -Bisabolene	tr	Caryophyllene oxide	tr
		Limonene	5.9	Citronellyl acetate	2	$\delta$ -Cadinene	tr		
		$\beta$ -Cymene	0.1						

**Table 3 (Cont.)**

Plant parts	Extraction methods	Components							
		Monoterpene Hydrocarbon	%	Oxygenated Monoterpene	%	Sesquiterpene Hydrocarbon	%	Oxygenated Sesquiterpene	%
Fresh leaves	Likens-Nikerson Extraction	$\alpha$ -Pinene	0.1	Linalool	1.6	$\delta$ -Cadinene	tr	Elemol	tr
		Sabinene	2	Citronellal	72.5			Nerolidol	tr
		$\beta$ -Pinene	0.1	$\beta$ -Citronellol	10.3			Guaiol	tr
		$\beta$ -Myrcene	0.6	iso-Pulegol	1.2				
		Limonene	6.8	Citronellyl acetate	1.2				
		$\beta$ -Cymene	tr						

**Table 3 (Cont.)**

Plant parts	Extraction methods	Components							
		Monoterpene Hydrocarbon	%	Oxygenated Monoterpene	%	Sesquiterpene Hydrocarbon	%	Oxygenated Sesquiterpene	%
Peels	Likens-Nikerson Extraction	$\alpha$ -Pinene	1.7	Linalool	1.8	$\beta$ -Bisabolene	1.2	Elemol	tr
		Sabinene	20	Citronellal	12.6	$\delta$ -Cadinene	0.6	Nerolidol	0.2
		$\beta$ -Pinene	23.5	$\beta$ -Citronellol	3.3			Guaiol	0.1
		$\beta$ -Myrcene	1	iso-pulegol	0.5			Caryophyllene oxide	0.1
		Limonene	11.8	Citronellyl acetate	1.7				
		$\beta$ -cymene	0.3						

**Note:** tr (trace level)

**Source:** Warsito et al., 2017

## 2. Potential effect of *C. hystrix*

Many researches have been conducted to confirm the therapeutic potential of kaffir lime (**Table 4**). The extracts from kaffir lime have been reported to own the antioxidant propriety proved by its ability to inhibited free radicals (Hutadilok et al., Butryee et al., 2009; 2006). Respectively, a methanolic crude extract from kaffir lime leaf was reported to contain the hepatoprotective effect to male Sprague-Dawley (SD) rats. The experiment showed the prevention of alanine transaminase (ALT) and aspartate transaminase (AST) proteins level elevation in serum of SD rats pre-treated by kaffir lime leaf extract (200 mg/kg) and exposed to paracetamol (2g/kg) to induce liver cells damage and necrosis (Abirami et al.,2015). In Sumonrat et al.,(2008) kaffir lime leaf extract has been detailed to contain the broad spectrum anti-microbial activity against gram-positive bacteria, yeast, molds, and able to inhibit biofilm formation of (Kooltheat et al., 2016). It has also been reported for its pesticide effect against larvae of *Aedes albopictus* (Nishan et al.,2017) (mosquito larvae) , against bow flies and house flies larvae by causing by skin damage-related death (Suwannayod et al., 2018), and for its growth modulation against *Spodoptera litura* (Tobacco worm) larvae (Siew et al.,2011).

**Table 4 Volatile compounds identified in chloroform crude extract from *C. hystrix* leaves and their biological activities**

Peak Area (%)	Compound Name	Groups	Biological Activity	Cancer cells
17.24	9,12,15-octadecatrien-1-ol	Fatty alcohol	Antioxidant	
9.77	Citronellyl propionate	Terpenoids	Cytotoxicity and antioxidant	Leukemia (HL-60, NB-4)
8.32	Palmitic acid	Fatty acid	Cytotoxicity, anti-inflammatory, antibacterial and antifungal	Leukemia (MOLT-4)
6.18	1,5,9-decatriene,2,3,5,8-tetramethyl	Alkene hydrocarbon		
4.76	Heneicosane	Long chain alkane	Cytotoxicity, antibacterial	Cervical (Hela), Breast (MCF-7)
3.20	Neophytadiene	Alkene hydrocarbon	Antioxidant, analgesic, antipuretic, anti-inflammatory and antimicrobial	
2.75	14- $\beta$ -pregnane	Sterol lipid		
2.06	Squalene	Terpenoids	Antioxidant, antitumor against skin carcinogens, skin hydration, antibacterial	
2.02	Isophytol	Terpenoids	Antibacterial	

**Table 4 (Cont.)**

Peak Area (%)	Compound Name	Groups	Biological Activity	Cancer cells
1.98	9-tricosene	Alkene hydrocarbon		
1.83	citronellyl acetate	Terpenoids	Cytotoxicity, antioxidant, antiproliferative	Colorectal (Caco-2)
1.64	tetradecanoic acid /myristic acid	Fatty acids	Anti-inflammatory, antioxidant, antibacteria	
1.25	9-octadecanoic acid/ Oleic acid	Fatty acid	Reduce Her-2/NEU overexpression in breast cancer, antibacterial	Breast (MCF-7, MDA-MB-231), Prostate (PC-3), Cervical (Hela), Colorectal (HT-29), Lung (A549)
2.18	Phytol	Fatty alcohol	Cytotoxicity, anti-inflammatory, anti-neoceptive, antioxidant	
0.87	Cyclooctacosane	Alicyclic hydrocarbon		

**Table 4 (Cont.)**

Peak Area (%)	Compound Name	Groups	Biological Activity	Cancer cells
0.81	3-eicosene	Alkene hydrocarbon	Cytotoxicity, antibacterial	Cervical (Hela), Breast (MCF-7)
0.76	Citronella	Terpenoids	Cytotoxicity, antibacterial, Analgesic-like activity on mouse	
0.75	6-octen-1-ol	Alcohols		
0.74	Phenol,3,5-bis(1,1-dimethylethyl)-	Phenolic		
0.52	1-eicosanol	Fatty alcohols		
0.48	Benzene,1-methoxy-2-[(4-methoxyphenyl)methyl]	Aromatic hydrocarbon		
0.46	Spathulenol	Terpenoids	Cytotoxicity, anti-inflammatory, antioxidant	
0.38	trans-linalool oxide	Terpenoids	antioxidant and antibacterial, Anxiolytic-like effect	
0.37	hexanedioic acid/Adipic acid	Dicarboxylic acid		

**Table 4 (Cont.)**

Peak Area (%)	Compound Name	Groups	Biological Activity	Cancer cells
0.36	Phytene	Diterpenoid alkene		
0.34	1,2-benzenedicarboxylic acid,bis(2-ethylhexyl)ester	Aromatic ester	Antioxidant	
0.24	Styrene	Aromatic hydrocarbon		
0.23	Eicosane	Long chain alkane	Cytotoxicity, antibacterial	

**Source:** Tunjung, & Dertyasasa, 2017

**Table 5 Volatile compounds identified in ethyl acetate crude extract from *C. hystrix* leaves and their biological activity**

Peak Area (%)	Compounds Name	Groups	Biological Activity	Cancer cells
10.13	Palmitic acid	Fatty acids	Cytotoxicity, anti-inflammatory, antibacterial and antifungal	Leukemia (MOLT-4)
6.67	Caryophyllene oxide	Terpenoids	Cytotoxicity, analgesic-like activity on mouse, antimicrobial	Colon (HT-29, T84)
6.67	Citronellal	Terpenoids	Cytotoxicity, antibacterial, Analgesic-like activity on mouse	
9.59	Citronellyl acetate	Terpenoids	Cytotoxicity, antioxidant, anti-proliferative	
3.96	Oleic acid	Fatty acids	Reduce Her-2/NEU overexpression in breast cancer, antibacterial	
3.85	Tetratetracontane	Long chain alkanes		
4.1	Phytol	Fatty alcohol	Cytotoxicity, anti-inflammatory, anti-neoceptive, antioxidant	Breast (MCF-7, MDA-MB-231), Prostate (PC-3), Cervical (Hela), Colon (HT-29)
4.59	Citronellyl formate	Terpenoids		
3.3	Hexatriacontane	Long chain alkanes		
3.52	Farnesol	Fatty alcohol	Cytotoxicity, antioxidant,	Colorectal (Caco-2)

**Table 5 (Cont.)**

Peak Area (%)	Compounds Name	Groups	Biological Activity	Cancer cells
3.58	1,7-Nonadiene, 4,8-dimethyl-	Alkene hydrocarbon	antimicrobial	
2.58	Palmitaldehyde	Fatty aldehyde		
2.23	Nerolidol	Terpenoids	Cytotoxicity, antibacterial	
2.4	Germacrene	Terpenoids	Cytotoxicity	
2.17	Stearyl aldehyde	Fatty aldehyde		
1.62	Stearyl vinyl ether			
1.33	Longipinenepoxide	Terpenoids		
1.31	1,4-Heptadiene, 3,3,6-trimethyl	Alkene hydrocarbon		
1.19	2-Sitosterol	Sterol lipid	Cytotoxicity, antibacterial, anti-hypercholesterolemia	Breast (MCF-7), Lymphoma (SW-480)
1.86	Citronellol	Terpenoids	Cytotoxicity, antioxidant and antibacterial	
1.07	1-Hexacosanal	Fatty aldehyde		
1.07	Globulol	Terpenoids		
1.02	$\alpha$ -Tocopherol	Vitamine	Cytotoxicity, antibacterial, antioxidant, neuroprotective effect	Prostate (PC-3)

**Table 5 (Cont.)**

Peak Area (%)	Compounds Name	Groups	Biological Activity	Cancer cells
1.54	Linalool-oxide	Terpenoids		
0.91	Limonene-oxide	Terpenoids	Analgesic-like activity on mouse	
0.91	Octacosane	Long chain alkanes	Cytotoxic against melanoma B16F10-Nex2 cancer cell line	Melanoma (B16F-10)
0.88	Patchulane	Hydrocarbon		
1.17	1,6-Octadiene, 2,5-dimethyl	Alkane hydrocarbon		
0.84	2-Dodecanol	Fatty alcohol		
0.79	Dichlorobenzene	Aromatic hydrocarbon		
0.71	Squalene	Terpenoids	Antioxidant, antitumor against skin carcinogens, skin hydration, antibacterial	
0.66	9-Eicosyne	Alkyne hydrocarbon		
0.65	Dihydromyrcenol	Fatty alcohol	Antibacterial, antifungal, cytotoxicity against colorectal, hepatic and breast cells	Breast (MCF-7), Colon (HCT-116), Liver (HUH-7), Lung (A-549)
0.54	Myrcenol	Fatty alcohol		
0.47	Dihydrobrassicasterol	Sterol lipid		

**Table 5 (Cont.)**

<b>Peak Area (%)</b>	<b>Compounds Name</b>	<b>Groups</b>	<b>Biological Activity</b>	<b>Cancer cells</b>
0.66	9-Eicosyne	Alkyne hydrocarbon		
0.41	Melonal	Fatty aldehyde		
0.39	Eicosane	Long chain alkanes	Cytotoxicity, antibacterial	
0.37	Geraniol	Terpenoids		
0.32	1-octadecyne	Alkyne hydrocarbon		
0.28	$\alpha$ -Cubene	Terpenoids		
0.27	$\beta$ -Pinene	Terpenoids	Cytotoxicity, analgesic-like activity on mouse and rat	
0.27	Geranyl Butyrate			
0.24	Calarene			
0.24	$\alpha$ -Cedrane	Terpenoids		

**Table 5 (Cont.)**

Peak Area (%)	Compounds Name	Groups	Biological Activity	Cancer cells
0.23	Cyclohexane	Alicyclic hydrocarbon		
0.22	$\alpha$ -Thujene	Terpenoids		
0.2	2-Dodecanal	Fatty aldehyde		
0.19	$\alpha$ -Calacorene	Sesquiterpene		
0.18	1,5,9-Decatriene,2,3,5,8-tetramethyl	Alkane hydrocarbon		

**Source:** Tunjung & Dertyasasa, 2017

### 2.1. Anticancer effect of *C. hystrix*

Beside many others potential biological activity. *C. hystrix* also has anti-cancer effect too. Crude extractions from *C. hystrix* have been exerting cytotoxic effect on four different types of leukemic cell lines (K562, U937, Molt4, and HL60). Among 4 of crude extract receiving from the consequential maceration method, crudes from hexane and ethyl acetate showing lower IC<sub>50</sub> value in inhibiting these cells compared to other solvents (Chueahongthong et al., 2011). In another experiment, crude ethyl acetate and crude chloroform from kaffir lime leaf reduced cellular dehydrogenases enzyme indicating its cytotoxicity on neuroblastoma cell lines (UKF-NB3 and SK-N-AS ) and cervical cancer cell line (Hela) in micromolar concentrations (Tunjung et al., 2015). *In vitro* study of Borusiewicz (2017), essential oil of kaffir lime peel from hydrodistillation process demonstrated cytotoxic and cytostatic effects to the both of melanoma cell lines (WM793 and A375). The toxicity of this essential oil was accessed by LDH cytotoxic assay and trypan blue assay. Bergamottin, a compound isolated from kaffir lime fruit, could suppress the migration of human pancreatic cancer cell line (PANC-1). Also, it was able to induce cell shrinkage, and led to total death within 24h (Sun et al.,2018).  $\beta$ -citronellol, a major compound in kaffir lime was reported to reduce cell viability of MCF-7 breast cancer cells (MAMUR, 2019). In another point of view, kaffir lime leaf extract also has its inhibitory effect on cell cycle progression. Result from Utthawang W. et al.,(2017) indicated fraction 9 from crude hexane of kaffir lime leaf extract was able to increase the expression of p53 protein level, and alter cell cycle regulatory proteins expression (cyclin A, cyclin B, and cdc2) leading leukemic Molt-4 cells to arrest at G2/M phases.

### 2.2. Citronellal and citronellol

Monoterpenoid is the most abundant compound found *C. hystrix*. Citronellol and citronellal are the two monoterpenoids which have been identified in *C. hystrix*, and have been reported to exert many biological actions (Sato et al., 1990). Citronellal has been reported to contain the anti-inflammatory effect and redox-protective activity in the inflammation-induced in the animal model (Melo et al., 2011). Anti-inflammatory activity of citronellol has been shown in RAW264.7 macrophage by

reduced the level of prostaglandin E2 and the LPS-induced NO production (Su et al., 2010). Furthermore, citronellal reduced the proliferation of Huh7 hepatocellular carcinoma cell line by mediated the phosphorylation of p38 MAPK (Maßberg et al., 2015). Also there are other report action that both citronellal and citronellol inhibited the action of P-glycoprotein, which could ameliorate the efficacy of drug treatment (Yoshida et al., 2006). Citronellal also exhibited cytotoxicity against the estrogen positive breast cancer MCF-7 cell lines with IC<sub>50</sub> of 0.091 mM (Stone et al., 2013). Citronellol induced necroptosis of NCI-H1299 cells by up-regulated TNF- $\alpha$ , RIP1/RIP3 activities, and induced ROS accumulation (Yu et al., 2019a). Citronellol also exhibited anticancer effect against A-549 non-small cell lung cancer cells by increased the ROS generation and decreased mitochondrial membrane potential leading to DNA laddering and chromatin condensation (Song et al., 2015). Besides, there were also reported about the anti-microbial effect of citronellal and citronellol against *Escherichia coli* and *Staphylococcus aureus* (Romero et al., 2015), anti-fungal against *Candida albicans* (Saibabu et al., 2017), larvicidal (Barros et al., 2009), anti-diabetic in mouse model (Srinivasan & Muruganathan, 2016).

### **Apoptosis**

Apoptosis or program cell death is a phenomenon which appears at the end of cells' life span. It also can be triggered by the miss-regulation of cell cycles checkpoints or DNA mutations, or sometimes in response to toxic substances. The improper regulation of apoptosis contributes to disorders such as cancer, viral infection, autoimmune diseases, neurodegenerative disorders (Favaloro et al., 2012). Two major pathways have been described in the process of triggering the activation of apoptosis include the cell death receptor pathways or the extrinsic pathway which is triggered by the extracellular signals and the mitochondrial pathway or the intrinsic pathway which initiate from mitochondria triggered by from DNA damage signal.

## 1. Apoptosis Pathways

### 1.1. The death receptor-dependent pathway

Death receptors are transmembrane receptor which trigger the death signal in response to the death receptor ligands (**Figure 2**). There are many types of death receptor like CD95 (or Fas), TRAILR, TNFR, DR. When CD95L (or FasL) bind to its receptor, it provokes the trimerization of Fas followed by the recruitment of adaptor molecule Fas-associated death domain (FADD). FADD containing the dead effector domain (DED) which trigger the autoproteolytic of pro-caspase 8 and pro-caspase 10 resulting in the active form of caspase 8 and caspase 10. These active caspases activate the common pathway caspase 3/6/7 then trigger the death of cell (Lavrik et al., 2005).

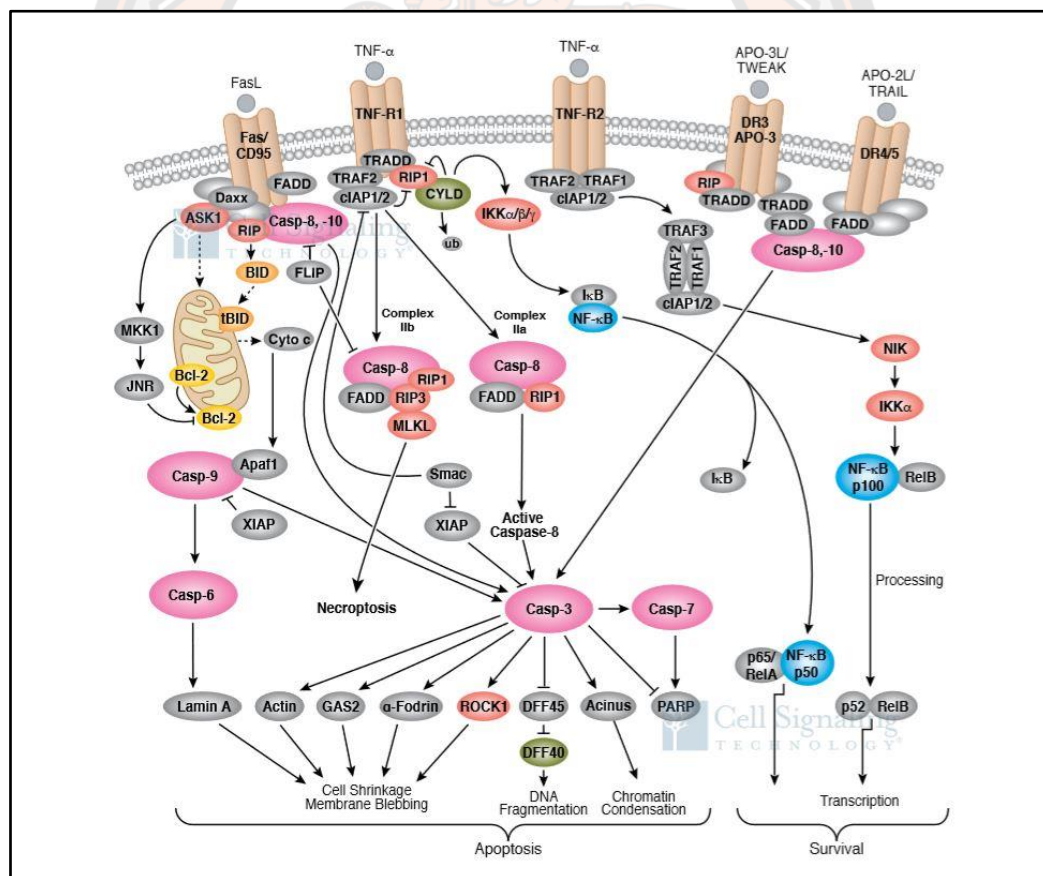


**Figure 2** The death receptor signaling of apoptosis.

**Source:** <https://www.cellsignal.com/contents/science-cst-pathways-cell-death/death-receptor-signaling/pathways-apoptosis-death>

Apoptosis can be induced through the activation of death receptors including Fas, TNF $\alpha$ R, DR3, DR4, and DR5 by their respective ligands. Death receptor ligands characteristically initiate signaling via receptor oligomerization, which in turn results in the recruitment of specialized adaptor proteins and activation of caspase cascades. Binding of FasL induces Fas trimerization, which recruits initiator caspase-8 via the adaptor protein FADD. Caspase-8 then oligomerizes and is activated via autocatalysis. Activated caspase-8 stimulates apoptosis via two parallel cascades: it can directly cleave and activate caspase-3, or alternatively, it can cleave Bid, a pro-apoptotic Bcl-2 family protein. Truncated Bid (tBid) translocate to mitochondria, inducing cytochrome c release, which sequentially activates caspase-9 which then activate caspase-3.

## 1.2. The mitochondrial pathway

In response to DNA damage, cells express p53 protein, then activate its downstream pathways (**Figure 3**). In intrinsic or mitochondrial pathway of apoptosis, p53 increases Bax/Bak proteins activity (Bcl-2 family protein) which mediate the pore formation complex at the outer membrane of mitochondria, and consequentially triggers the release of Cytochrome C (Cyt C) into cytoplasm. When release to cytoplasm, Cyt C bind to apoptotic protease activating factor 1 (Apaf-1) in the present of ATPs to form the apoptosome which activate the cascade activation of caspases. The apoptosome cleave pro-caspase 9 into caspase 9. With this active form, caspase 9 activate the common apoptosis caspase 3/6/7, and therefore inducing the death in damage cell (Loane et al., 2015; L.-T. J. a. A.-G. Yang, 2012).

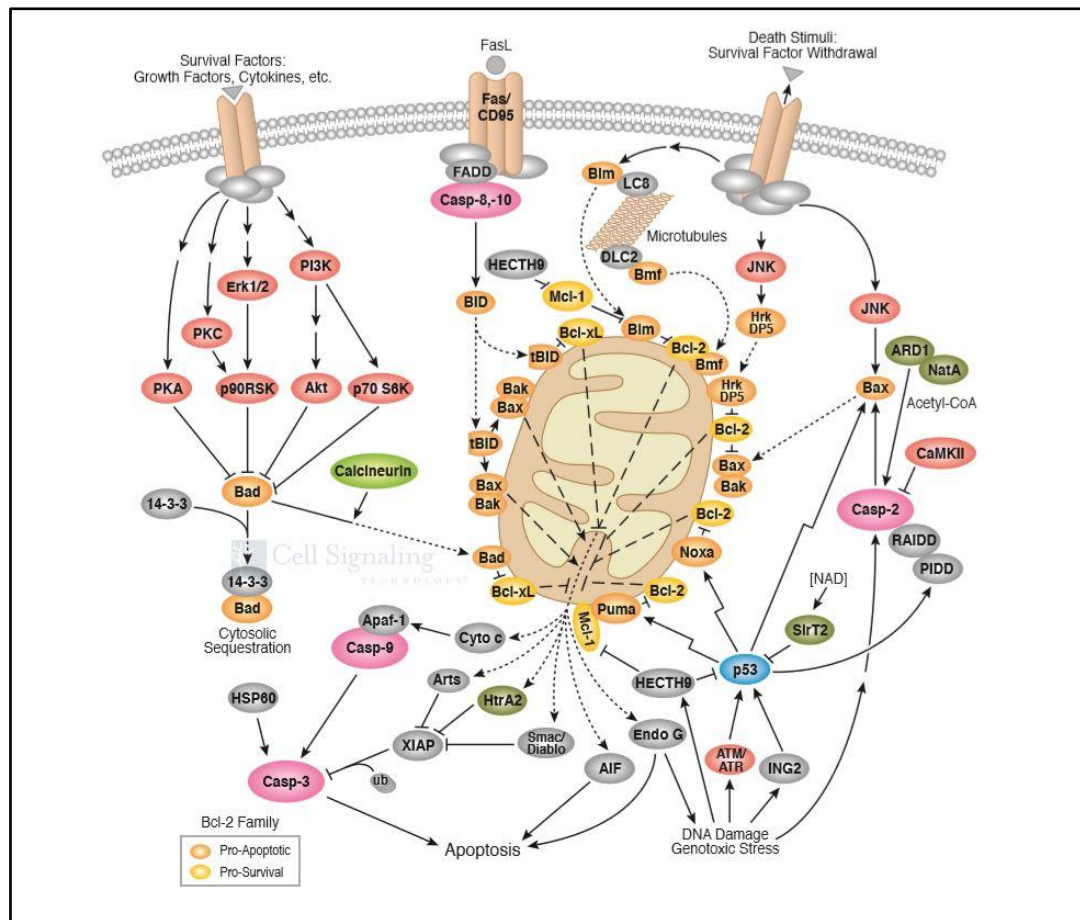


**Figure 3 The mitochondrial pathway of apoptosis.**

**Source:** Cell Signaling Technology, <https://www.cellsignal.com>

The Bcl-2 family proteins regulate apoptosis by controlling mitochondrial permeability. The anti-apoptotic proteins Bcl-2 and Bcl-xL reside in the outer mitochondrial membrane and inhibit cytochrome c release. The pro-apoptotic Bcl-2 proteins Bad, Bid, Bax, and Bim may reside in the cytosol, but could translocate to mitochondria following death signaling, where they promote the release of cytochrome c. Bad translocates to mitochondria and forms a pro-apoptotic complex with Bcl-xL. This translocation is inhibited by survival factors that induce the phosphorylation of Bad, leading to its cytosolic sequestration. Cytosolic Bid is cleaved by caspase-8 following signaling through Fas; its active fragment (tBid) translocates to mitochondria. Bax and Bim translocate to mitochondria in response to

death stimuli, including survival factor withdrawal. Activated following DNA damage, p53 induces the transcription of Bax, Noxa, and Puma. Upon release from mitochondria, cytochrome c binds to Apaf-1 and forms an activation complex with caspase-9

## 2. Bcl-2 protein family

Bcl-2 protein family is a group of protein that involve in a major part responsible to the activation of apoptosis pathway (**Figure 3**). Bcl-2 is an anti-apoptotic protein in Bcl-2 protein family. It functions as a pro-survival protein by constraining the activation of Bad/Bak proteins in the mitochondrial apoptosis pathway (Adams & Cory, 2007). A study evaluate the apoptosis-inducing effect of antrocin on MDA-MB-231 cell line showed increasing expression level of pro-apoptotic protein Bax, and the release of Cyt C increased while the anti-apoptotic Bcl-2 protein decreased in response to the increasing dose of antrocin (Rao et al., 2011). The same level of these gene expression have been identified in MDA-MB-231 cells treated with methanolic extract of *Nigella sativa*. The extract caused cell apoptosis and cell cycle arrest at G0/G1 with the reported of increasing level of Bax, Caspase 3 genes expression and lower expression of Bcl-2 gene (Ahmad et al., 2012).

On the other point of view, Bcl-2 gene expression has been reported to relate to multidrug resistance (MDR) in cancer chemotherapy (Dai et al., 2013; Krishna & Mayer, 2000). One of the mechanism is due to the over expression of Bcl-2 gene induced by p53 in response to the DNA targeted anti-cancer drugs such as doxorubicin (Dox), taxol, cisplatin (Shitashige et al., 2001). An survival analysis from 64 female patients with TNBC indicated that patients with high expression of Bcl-2 gene tend to have lower overall survival rate, and has been counted as a remarkable marker of the invasivity of TNBC (Ozretic et al., 2017).

### 3. The effector caspases activation

Caspase 3/6/7 are known as the downstream effector caspases in the apoptotic pathway. Activated by the effector caspases, caspase 3 consequently cleaves ICAD (Caspase-Activated DNase Inhibitor) or DFF45 (DNA fragmentation factor 45) and inactivates its CAD-inhibitory function (Sakahira et al., 1998). DFF (DNA fragmentation factor) contained two heterodimers subunits, the DFF45 (ICAD) and DFF40 (CAD). These proteins had been originally purified from a cytoplasmic fraction of HeLa cells (Liu et al., 1997) suggested that these proteins are translated in the cytoplasm and then translocated into nucleus by the nucleus transporter proteins (Neimanis et al., 2008). In live cells, DFF40 or CAD is inhibited by its inhibitory subunit DFF45 or ICAD. DFF45 contains two Caspase 3 binding sites at aspartate residues 117 and 224 (Widlak, 2000). But during apoptosis, cells undergo the cascade activation of caspases, which leads to the activation of the effector caspase 3. Caspase 3 then binds to the inhibitory subunit of DFF, and consequently causes the activation of CAD or the DFF40 subunit inside nucleus. It has been reported that DFF40 interacts with the histone-1 proteins and HGM (High Mobility Group, proteins which modulate chromatin structure and cellular phenotype) proteins leading to cleavage of linker DNA of the nucleosomes and consequently causing DNA fragmentation (Liu et al., 1999; Toh et al., 1998). Also, in the experiments which evaluated the effect of DFF40 on chromatin condensation, either DFF40 alone or the DFF complex activated by Caspase 3 show the formation of chromatin condensation in nuclei of the cell (Liu et al., 1998) (**Figure 4**).

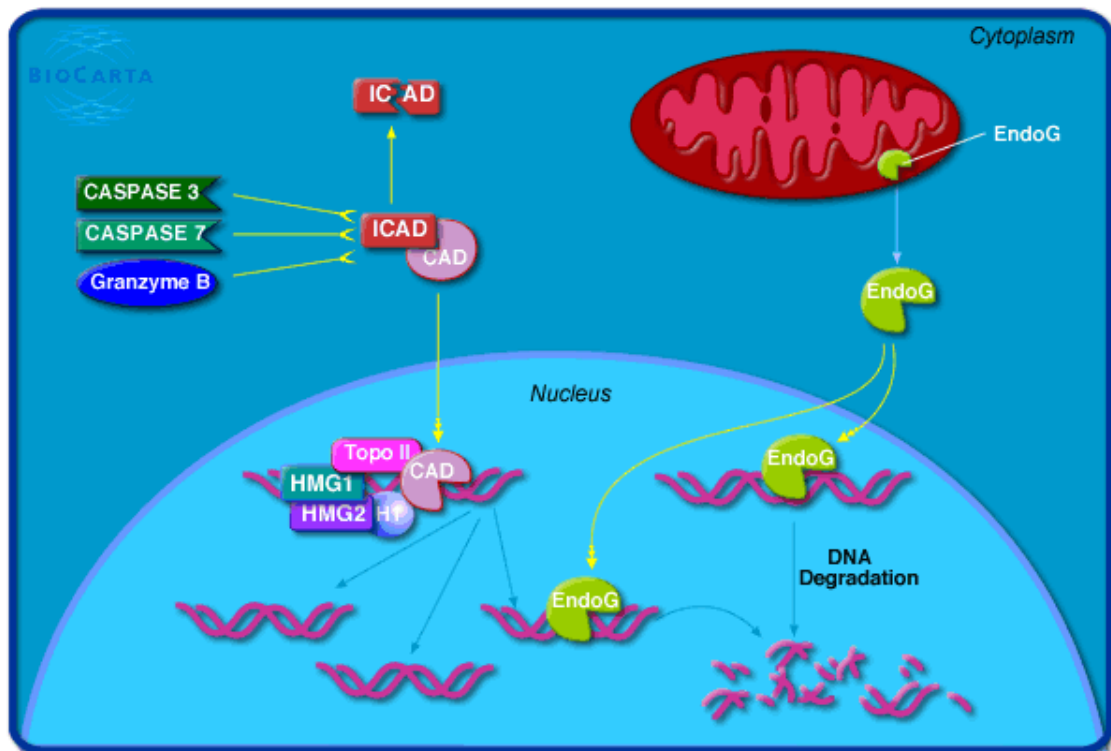


**Figure 4 DNA fragmentation induced by caspase 3.**

**Source :** <http://worldofbiochemistry.blogspot.com/>

Caspase 3 cleaves and activates CAD. CAD then interact with H1 protein and HMG complex causing the structure change of chromatin and leading to DNA cleavage by endonuclease.

#### **4. Cross linking between extrinsic and intrinsic apoptosis pathway**

In some certain cells, cell exhibit the cross-talk between the extrinsic and the intrinsic apoptosis pathway by the activation from the initiators caspase 8 and 10 via the BH3 interacting-domain death agonist (BID) (Roy & Nicholson, 2000; Wachmann et al., 2010). BID is a pro-apoptotic protein serves its function as the death ligand. It has the ability to inactivated Bcl-2 protein or activate Bak, which indeed inducing the permeability of Cyt C from mitochondria. The initiator caspases 8 and 10 were reported to be able to cleave the BID into its active form the truncated Bid (tBid). tBid then translocates into the outer membrane of mitochondria, and

induces the conformational change and oligomerization of Bak resulting in the releasing of Cyt C (Korsmeyer et al., 2000).

## 5. Apoptosis analysis

Apoptosis, or programmed cell death, is an important and active regulatory pathway of cell growth and proliferation. Cells respond to specific induction signals by initiating intracellular processes that result in characteristic physiological changes. Among these are externalization of phosphatidylserine (PS) to the cell surface, cleavage and degradation of specific cellular proteins, compaction and fragmentation of nuclear chromatin, and loss of membrane integrity (in late stages). Annexin V is a calcium-dependent phospholipid-binding protein with a high affinity for PS, a membrane component normally localized to the internal face of the cell membrane. Early in the apoptotic pathway, molecules of PS are translocated to the outer surface of the cell membrane where Annexin V can readily bind them.

### Cell Cycle progression

Cell cycle is a process where a cell undergoes self-division into two daughter cells. This process happens during the development of our body, the replacement of dead cells, or sometime in diseases like cancer. In common eukaryotic cell, cell cycle is divided into 2 separating states the interphase and the division phase or mitosis (**Figure 5**). G1 phase (gap 1), which corresponds to the interval (gap) between mitosis and initiation of DNA replication. During G1 the cell is metabolically active and continuously grows but does not replicate its DNA. G1 is followed by S phase (synthesis) during which DNA replication takes place. The completion of DNA synthesis is followed by the G2 phase (gap 2) during which cell growth continues and proteins are synthesized in preparation for mitosis. The M phase of the cycle corresponds to mitosis, which is usually followed by cytokinesis. The interphase is the phase where cells rests, undergo its metabolic activity, functions, or prepare for mitosis. In interphase the cells pass through three different phases which are G1 phase, S phase, G2 phase and several check points between each phase to ensure the correct multiplication of DNA. In some case cell ceases the cell cycle to enter the

resting G0 phase which prevent cell from division in response to DNA damage or toxic factors (Cooper & Hausman., 2007).

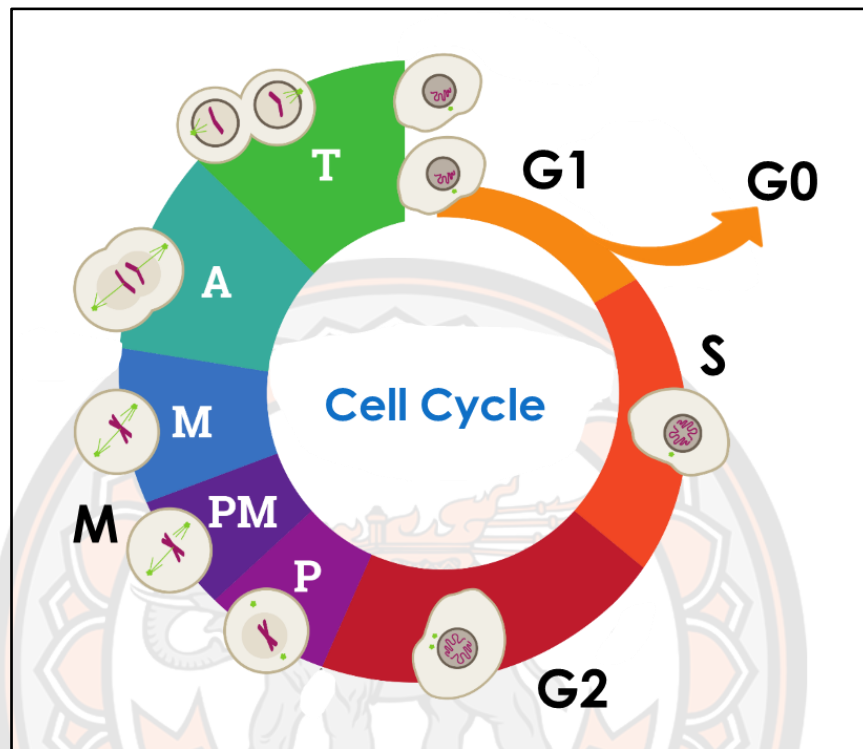


**Figure 5 Cell cycle progression**

### **1. Roles of Cyclin and Cyclin Dependent Kinase (Cdk) in cell cycle regulation**

Through the whole phases of cell cycle cyclin and cyclin dependent kinase (Cdk) play very important role in regulation of each phase of cell cycles. Four classes of cyclin with their cyclin dependent kinases have been classified due to its functions through each phase of the cycle including Cyclin D- Cdk 4/6, Cyclin E- Cdk 2, Cyclin A- Cdk 2 and Cyclin B- Cdk 1 (**Figure 6**).

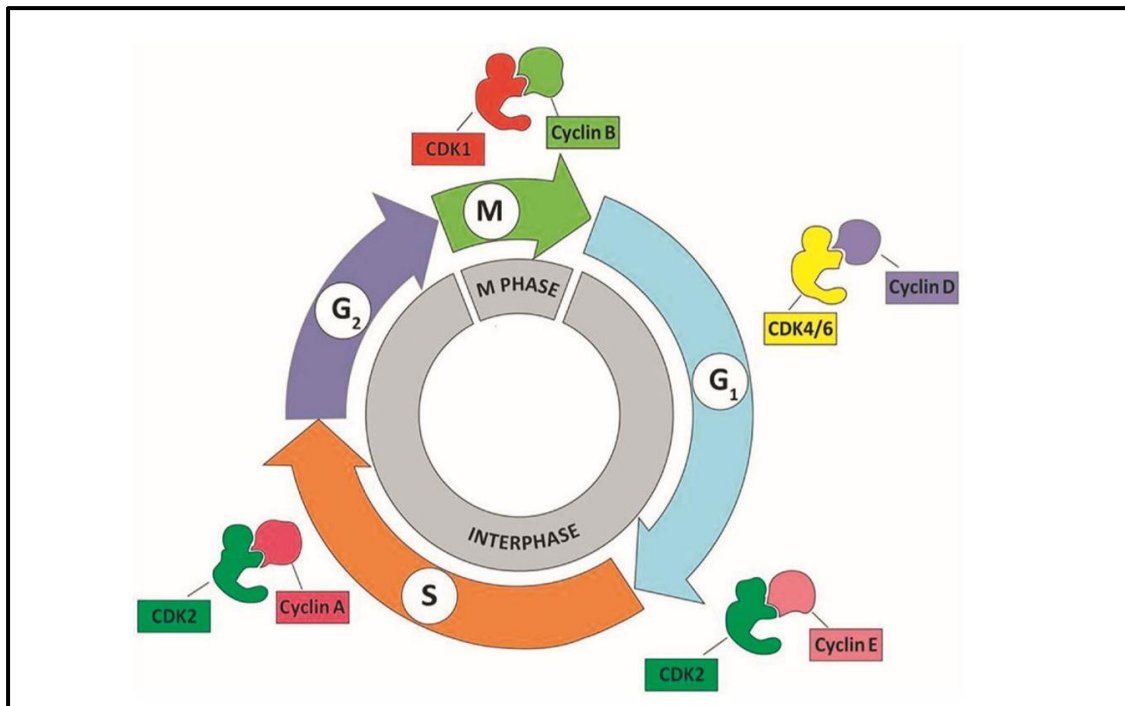


**Figure 6** Cyclin/cyclin-dependent kinase (Cdk) complexes roles in each phase of cell cycle.

### 1.1. Regulation of Cyclin/Cdk in G<sub>0</sub>/G<sub>1</sub> phase

In the early G<sub>1</sub> phase, cyclin D regulates cell cycle before letting the cells enter the S phase. Cyclin D with its kinase Cdk 4/6 act as an important regulator to the retinoblastoma (RB) protein (Connell et al., 1997). In the absence of mitogenic stimuli, RB binds and inhibits the activity of the transcription factor E2F in its hypophosphorylated form. E2F present in the promoters of many genes required for cell cycle progression (Bracken et al., 2004). Cyclin D- Cdk 4/6 phosphorylate the RB protein and inactivates its binding to E2F. At its hyperphosphorylated form the complex RB-E2F prevent the cell cycle progression from G<sub>1</sub> phase to the next S phase. The levels of G<sub>1</sub> cyclin are low in the G<sub>0</sub> phase (**Figure 7**) and increase progressively upon addition of growth factors or mitogens to the cells (Yang et al., 2006). The transcription of cyclin D is regulated depend on the Ras/Raf/mitogen-activated kinase (MEK)/ extracellular signal-regulated kinase (ERK) signaling pathway (Talarmin et al., 1999). At the post-translation level, cyclin D protein has

shorter life which is degraded by proteasome. Stabilization of cyclin D protein dependent on phosphorylation of cyclin D1 by glycogen synthase kinase-3 $\beta$  (GSK-3 $\beta$ ). Growth factors prevent cyclin D1 degradation by inhibiting GSK-3 $\beta$ -dependent phosphorylation of cyclin D1 through the Ras/phosphatidylinositol3-OH kinase (PI3K)/AKT pathway (Talarmin et al., 1999). In Razeai et al., (2012), methanolic extract from *Pistacia atlantica* sub *kurdica* down-regulated the expression of cyclin D level of human breast cancer cell line T47D leading to cell cycle arrest at G1 phase.

At the late G1 phase, the complex cyclin E- Cdk 2 is needed to complete the hyperphosphorylation of RB protein. Cyclin E- Cdk 2 phosphorylates RB on different sites from cyclin D- Cdk 4/6, and progressively block RB functions making cells passes from G1 to S phase. The amounts of cyclin E protein and its associated kinase (Cdk 2) activity are maximal in late G1 and early S phases (**Figure 7**) (Ohtsubo et al., 1995).

## **1.2. Regulation of Cyclin/Cdk in S phase**

Transcription of the cyclin E gene is regulated by E2F, which as described earlier, is activated due to cyclin D- Cdk 4/6-stimulated phosphorylation of RB. In early S phase, cyclin E- Cdk 2 activity abruptly ceases as a consequence of cyclin E degradation. The stabilization of cyclin E protein is mediated by inhibition of GSK-3 $\beta$  through PI3K/AKT signaling pathway. Similar to cyclin D, the degradation of cyclin E is mediated by phosphorylation of cyclin E protein by both GSK-3 $\beta$  and Cdk 2, which leading to the degradation of cyclin E by proteasome in S phase (Morris et al., 2000). In S phase, another cyclin E involves in the process preparing cell to enter the S phase. Cyclin A- Cdk 2 level increases during the S phase until the late G2 phase (R. Yang et al., 1999). Cyclin A and its partner, Cdk 2, phosphorylate substrates that commence DNA replication from preformed replication initiation complexes. Cyclin A- Cdk 2 is also required to coordinate the end of S phase with activation of cyclin B at the M phase (Mitra & Enders, 2004).

### 1.3. Regulation of Cyclin/Cdk in G2/M phase

At the late G<sub>2</sub> phase the concentration of cyclin A increases to its peak and then start to degrade down when cell enter M phase. There are increasing concentration of cyclin B through the process of cell cycle in M phase. Cyclin B is activated by M-phase inducer phosphatase 3 or Cdc25 by dephosphorylation on complex cyclin B-Cdk 1 on threonine and tyrosine residues (Timofeev et al., 2010). Once the complex cyclin B-Cdk 1 is activated, it leads to many series of event that proceeding in the cell division including separation of centrosomes, condensation of chromosomes, breakdown of the nuclear lamina, and disassembly of the Golgi apparatus (V. W. Yang, 2018). At the end of M phase, the inactivation of cyclin B-Cdk 1 must be held to end the mitosis. Inactivation of these complex is achieved by the degradation of B-type cyclins by ubiquitin-mediated proteolysis that is regulated by the anaphase promoting complex/cyclosome (APC/C) (Yamamoto et al., 2005).

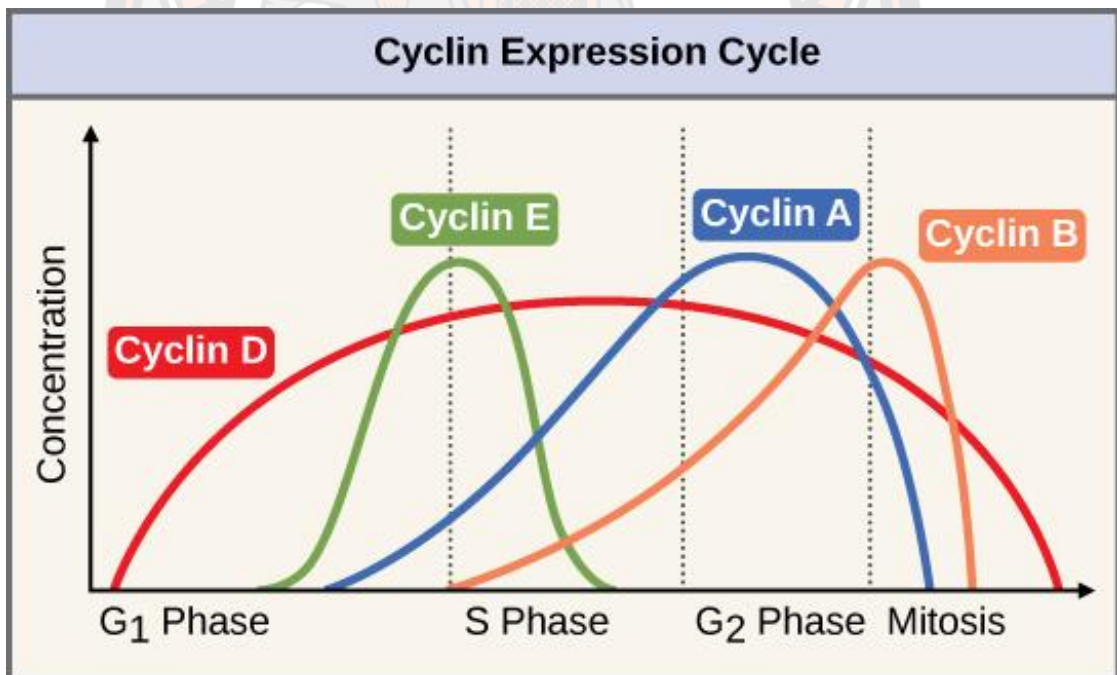


**Figure 7** Concentration of cyclin protein through cell cycle

**Source:** <https://courses.lumenlearning.com/suny-biology1/chapter/control-of-the-cell-cycle/>

Dash line represent the restriction point.

## 2. The Cdk inhibitor

There are two type of the Cdk inhibitor family the inhibitors of 4 (INK4) proteins which include p16INK4a, p15INK4b, p18INK4c, and p19INK4d, all of which bind to Cdk 4 and Cdk 6 and inhibit their kinase activities by interfering with their association with cyclin D (Sherr & Roberts, 1999). The other family is the Cdk-interacting protein (Cip/Kip) family which include p21<sup>Cip1</sup> p27<sup>Kip1</sup> and p57<sup>Kip2</sup>. The Cip/Kip family bind to both cyclin and Cdk subunits and can modulate the activities of cyclin D-, E-, A-, and B- Cdk complexes (Besson et al., 2008). p21<sup>Cip1</sup> protein express in response to DNA damage signal mediated by the ATM/ATR pathway through activation of p53 protein and induces cell cycle arrest at G1 and G2 phase (El-Deiry et al., 1993). In Kaur et al., (2008), grape seeds extract induced cell cycle arrest at G1 phase on colon cancer cell lines (HT29 and LoVo) and cell cycle arrest at S and/or G2/M arrest in SW480 colon cancer cell line with an association of elevating level of p21 protein expression. The association of elevation of p27 protein expression with cell cycle arrest at S phase can be seen in breast cancer cell (MDA-MB-231) treated by crude methanol from *Echinophora platyloba*, in which its concentration increased to 2.2 folds (Birjandian et al., 2018).

## 3. Cell cycle checkpoints

Throughout cell cycle, there are several checkpoints between each phase of cell cycle to ensure the correctness of cell cycle progression. Four major checkpoints in cell cycle are the G1/S phase checkpoint, intra-S phase check point, G2/M phase checkpoint and spindle assembly checkpoint.

### 3.1. G1/S checkpoint

The G1/S checkpoint is activated upon detection of DNA damage (**Figure 8**). In response to DNA damage, signals initiated by the sensors rapidly transduce to the ataxia telangiectasia, mutated (ATM) and ataxia telangiectasia and Rad3-related (ATR) kinases (Maréchal & Zou, 2013), there are many substrate of the ATM/ATR, but two of them are the checkpoint serine/threonine kinases, checkpoint kinase 1 (Chk1) and checkpoint kinase 2 (Chk2). Chk1 and Chk2 act as a regulator of the cell

cycle by phosphorylate the cell cycle regulatory phosphatase Cdc25A, leading to its inactivation by ubiquitin-mediated proteolysis. Since Cdc25A acts as the activator by phosphorylation of cyclin E-Cdk 2 in the late G1 phase, its inactivation prevent the cell transition from G1 to S phase (Donzelli & Draetta, 2003). Also, the Chk1 and Chk2 phosphorylate and activate p53 proteins, which in consequence increase the expression of p21 protein which act as the inhibitor of cyclin E-Cdk 2 and prevent cell to enter S phase.

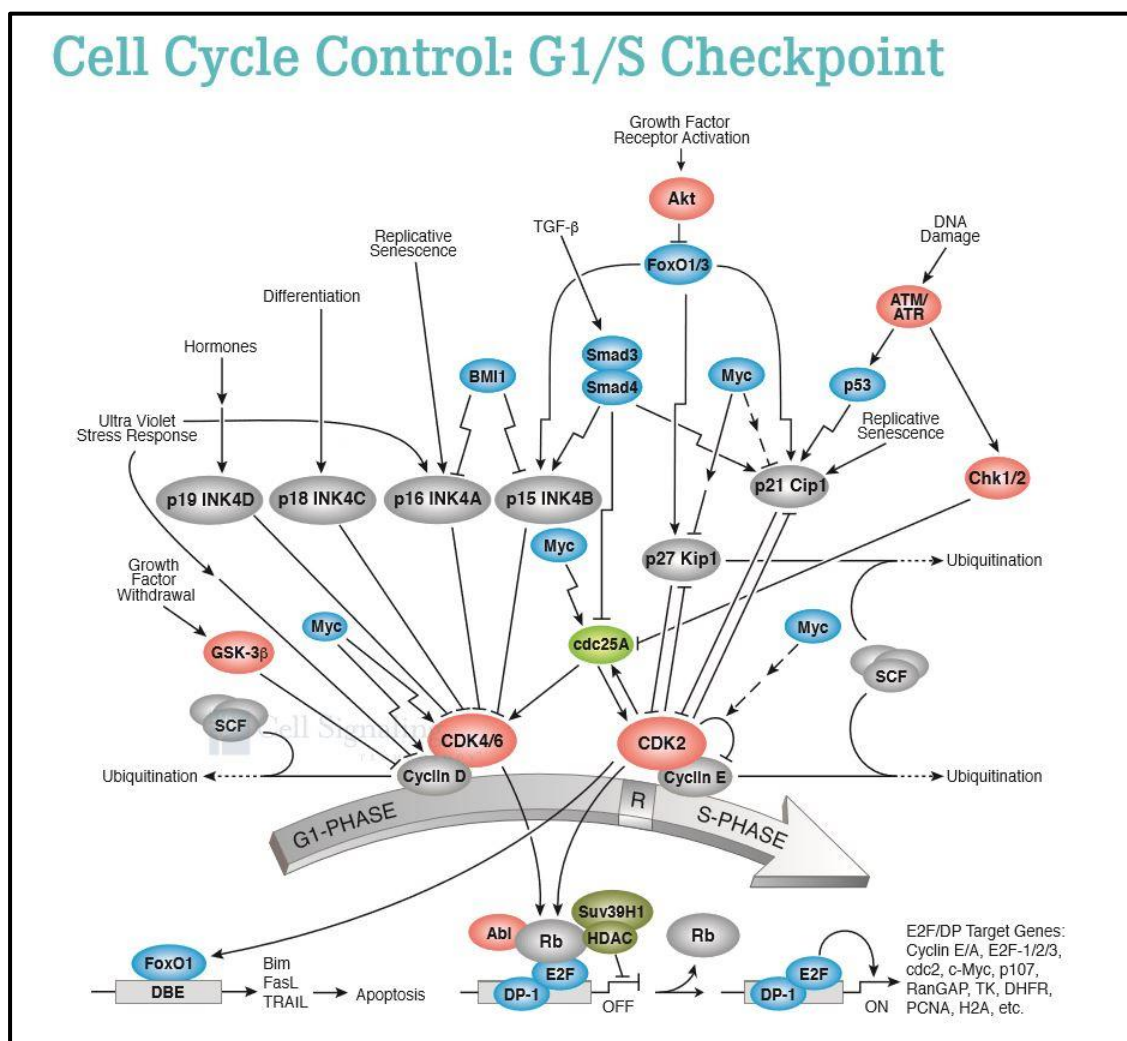


**Figure 8 G1/S cell cycle checkpoint**

**Source:** <https://www.cellsignal.com/contents/science-cst-pathways-cell-cycle-regulation/g1-s-checkpoint/pathways-cc-g1s>

### 3.2. Intra-S checkpoint

Since S phase is the phase where DNA begin its replication, the restriction point in S phase is held to prevent the nucleotides disorder during DNA synthesis. The activation of intra-S checkpoint is by the signal of double-strand DNA break, which activate the ATM/ATR pathway as describe above, the cascade activation of ATM/ATR pathway will result in inhibition of cyclin E-Cdk2 and arrest cell in S phase (Pauty et al., 2016).

### 3.3. G2/M checkpoint

When cells finish their DNA synthesis, they will enter the G2 phase. But if the process is miss regulated, unrepaired DNA sustained during the previous S or G1 phase, or when they possess incompletely replicated DNA from S phase, the G2 checkpoint will arrest the cell at G2 before letting it to enter M phase (Xu et al., 2002). Similar to the other checkpoint, the G2 check point (**Figure 9**) is mediated by activation of p53 protein through the ATM/ATR pathway. The p53 protein mediates the expression of the Cdk inhibitor such as p21<sup>Cip1</sup>, growth arrest and DNA damage-inducible 45 (GADD45) which cooperatively inhibit cyclin B-Cdk 1 activity by directly binding to cyclin B- Cdk 1). The dissociation of Cdk 1 from cyclin B, and sequestering Cdk 1 in the cytoplasm resulting in G2 arrest (Taylor & Stark, 2001).

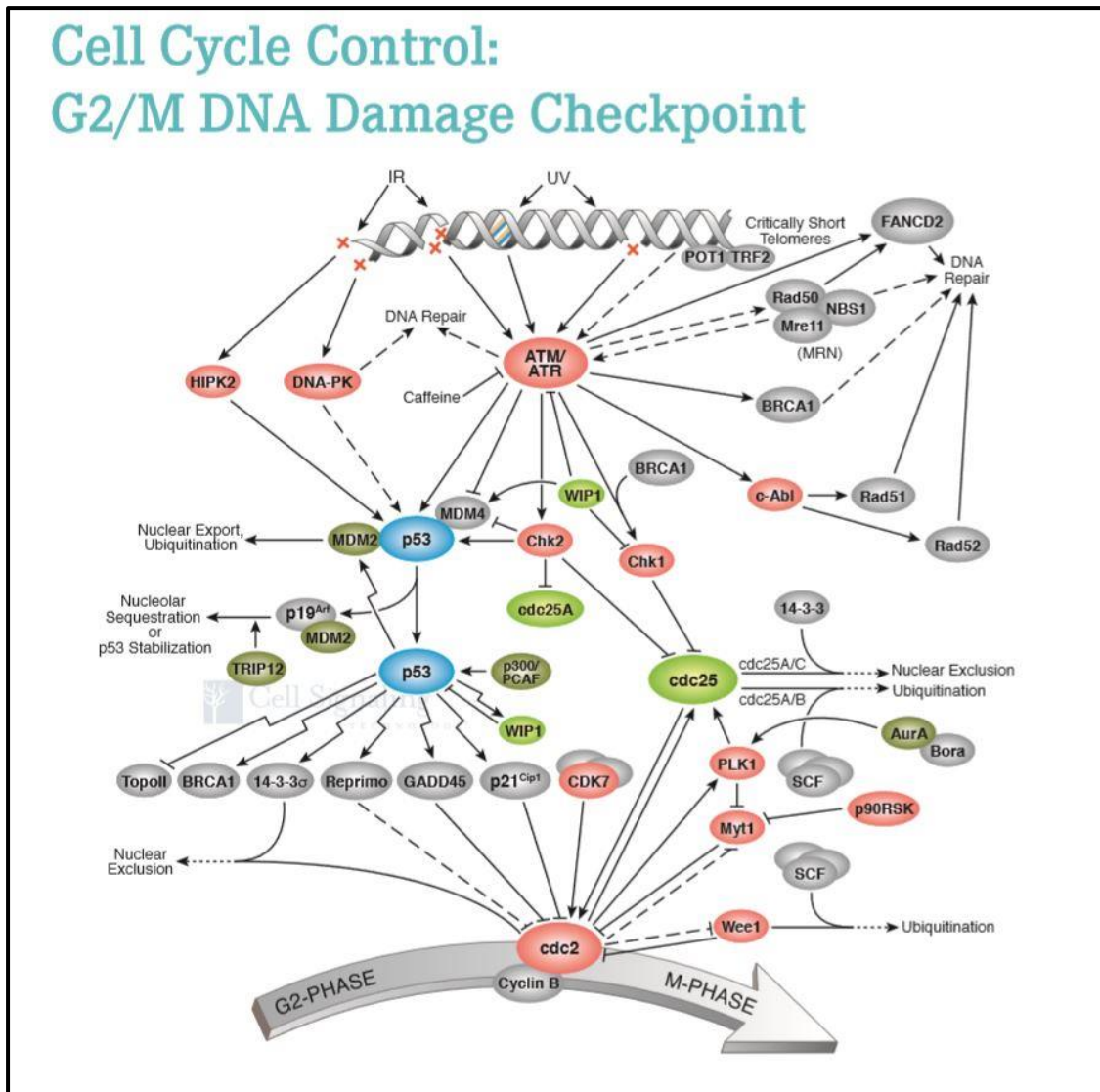


**Figure 9 G2/M cell cycle checkpoint**

**Source:** <https://www.cellsignal.com/contents/science-cst-pathways-cell-cycle-regulation/g2m-dna-damage-checkpoint/pathways-cc-g2m>

### 3.4. Spindle assembly checkpoint

There are four sub-sequential phases in mitosis, the prophase where chromosomes start to condense with the formation of mitotic spindle, metaphase where there are attachment of the microtubules on the kinetochores on the chromosome with the two centrosomes begin pulling the chromosomes towards opposite ends of the cell, anaphase the two identical daughter chromosomes begin to

form with cell elongation, and telophase the nuclear envelopes begin to form and cytokinesis takes place to separate the two daughter cells (McIntosh, 2016).

Before entering the anaphase, the alignment of chromosomes on the mitotic spindle is assured by the spindle assembly checkpoint (SAC). SAC ensures the stabilization of the kinetochore binding on the microtubules. When sister kinetochores are properly attached to opposite spindle poles, forces in the mitotic spindle generate tension at the kinetochores. But if the kinetochore attaches only at one side of the mitotic spindle, the chromosomal passenger complex Aurora-B/Ipl1 kinase act as the tensions sensor in improper kinetochore attachments. AuroraB/Ipl1 will consequently activates the assembly of the mitotic complex checkpoint (MCC) proteins complex (Krenn & Musacchio, 2015). This complex will then inhibit the complex APC/C-Cdc20. Normally at the end of mitosis, the degradation of cyclin B mediated by 26S proteasome is needed for cell to exit from M phase. But the ubiquitination of cyclin B by APC/C preventing its degradation by the 26S proteasome. The non-degraded cyclin B will then induces cell cycle arrest and prevent the transition from metaphase to anaphase (Chang et al., 2003).

#### **4. Cell cycle analysis**

The cell cycle represents one of the most significant and fundamental processes in eukaryotic cells, resulting in cell growth and division into two daughter cells. The regulation of the cell cycle is critical to cell survival, as it governs the repair of genetic damage and the prevention of uncontrolled cell division. Defects in cell cycle regulation are a characteristic feature of tumor cells, and mutations in the genes involved in controlling the cell cycle are extremely common in cancer. Cell cycle analysis has become increasingly important in understanding the action of anti-cancer compounds or studying mechanisms of cell division. Propidium iodide (PI) is a nuclear DNA intercalating stain. PI discriminates cells at different stages of the cell cycle, based on differential DNA content in the presence of RNase to increase the specificity of DNA staining. Resting cells (G<sub>0</sub>/G<sub>1</sub>) contain two copies of each chromosome. As cells begin cycling, they synthesize chromosomal DNA (S phase). Fluorescence intensity from PI increases until all chromosomal DNA has doubled

(G2/M phase). At this stage, the G2/ M cells fluoresce with twice the intensity of the G0/G1 population. The G2/M cells eventually divide into two cells. The assay utilizes PI-based staining of DNA content to discriminate and measure the percentage of cells in each cell cycle phase (G0/G1, S, and G2/M).

### **Tumor protein p53**

Tumor protein p53 is a protein encoded by the tumor suppressor gene p53 located on the short arm of chromosome 17 (McBride et al., 1986). It has been defined as the guardian of the genome (Lane, 1992). p53 inhibits cell growth, induces cell cycle arrest or causes apoptosis in response to DNA damage or to toxic substances (Vousden, 2000). In normal growing phase of the cells, the level of p53 expression is low accompanied with fast degradation by the protease, which is initiated by a regulator protein called MDM2 (Mouse double minute 2 homolog). MDM2 plays a role in stabilizing the functions of p53 by being involved in post-transcriptional modification of p53. It functions as a ligase enzyme that adds ubiquitin to p53 protein, which facilitates the recognition and degradation of p53 protein by the 26S proteasome. (Shi & Gu, 2012). But in cancer cells, the function of p53 protein in controlling cell proliferation is decreased, causing the uncontrollable proliferation of the cells leading to tumor formation. Cytotoxic stresses, such as ionizing radiation and hypoxia, can cause single- or double-strand breaks to cellular DNA. The DNA damage response (DDR) is an important cellular mechanism that prevents the cell from replicating before the damage is repaired or the cell containing damaged DNA is eliminated. The p53 tumor suppressor protein is a transcriptional regulator that plays a major role in DDR. DNA damage induces phosphorylation of p53 at multiple sites by a number of upstream kinases including ATM, ATR, DNA-PK, and Chk2 (**Figure 10**). Phosphorylation of p53 at Ser15 and Ser20 leads to a reduced interaction between p53 and its negative regulator, the oncoprotein MDM2. MDM2 inhibits p53 accumulation by targeting it for ubiquitination and proteasomal degradation. Activated p53 binds to target genes to induce a number of effector pathways including cell cycle arrest, DNA repair, senescence, or apoptosis. Studies have shown p53 to promote apoptosis through upregulation of the pro-apoptotic factors Puma and Noxa.

Loss-of-function mutations in p53 or other elements of the DDR can result in cancer. (Stegh, 2012).

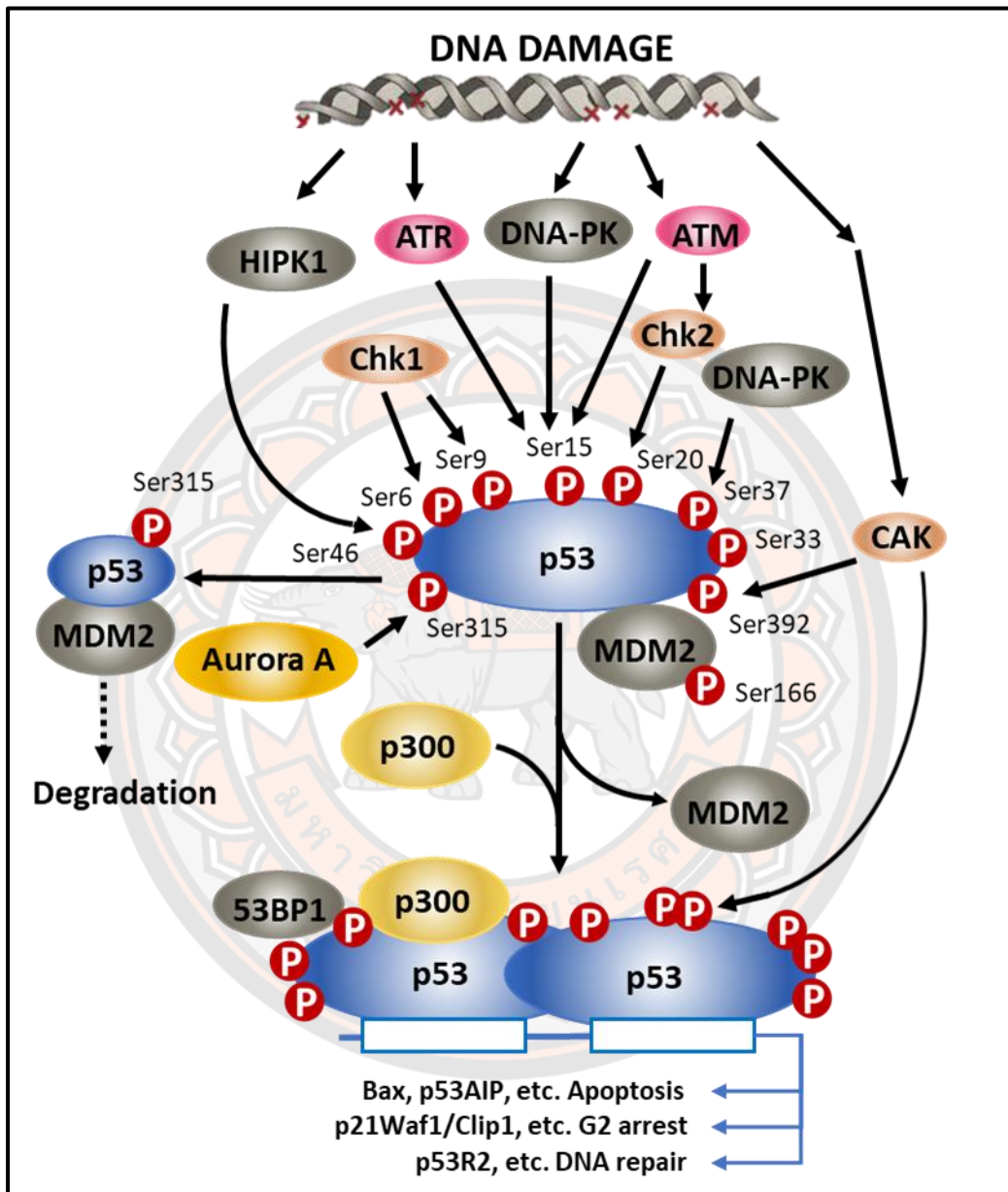


**Figure 10 Tumor Protein p53 pathway**

Source: <https://www.tocris.com/pathways/p53-signaling-pathway>

## **Chromatography techniques for chemical profiles identification**

### **1. Thin layer chromatography**

Thin layer chromatography or TLC is one of the chromatography methods used for separating compounds on a membrane. It has been usually used as a profile screening method to identify the presence of the compounds or give a brief detail on types or groups of the compounds. It involves in using of a thin, even sorbent layer, usually about 0.10 to 0.25 mm thick, applied to a firm backing of silica, cellulose, glass, aluminium or plastic sheet to act as a support. The sample is dissolved in an appropriate solvent and applied as spots or bands along one side of the sorbent layer approximately 1 cm from the edge. An eluent (single solvent or solvent mixture) is allowed to flow by capillary action through the sorbent starting at a point just below the applied samples. Commonly, this is achieved by using a glass rectangular tank in which the eluent is poured to give a depth of about 5mm. The plate is placed in the tank or chromatographic chamber and the whole covered with a lid (**Figure 11**). As the eluent front migrates through the sorbent, the components of the sample also migrate, but at different rates, resulting in separation. When the solvent front has reached a point near the top of the sorbent layer, the plate or sheet is removed and dried. The spots or bands on the developed layer are visualised if required, by exposing under UV light or by chemical treatment or derivatisation. For quantitative determinations, zones can be removed or eluted from the layer, or the plate can be scanned at pre-determined wavelengths without disturbing the layer surface. The modern use of TLC has seen a strong move in the direction of plate scanning and video imaging as a means of providing sensitive and reliably accurate results and a more permanent record of the chromatogram (Wall, 2005).

#### **Calculation of retention factor (R<sub>f</sub>)**

$$R_f = \frac{\text{Distance travel by sample}}{\text{Distance travel by solvent}}$$

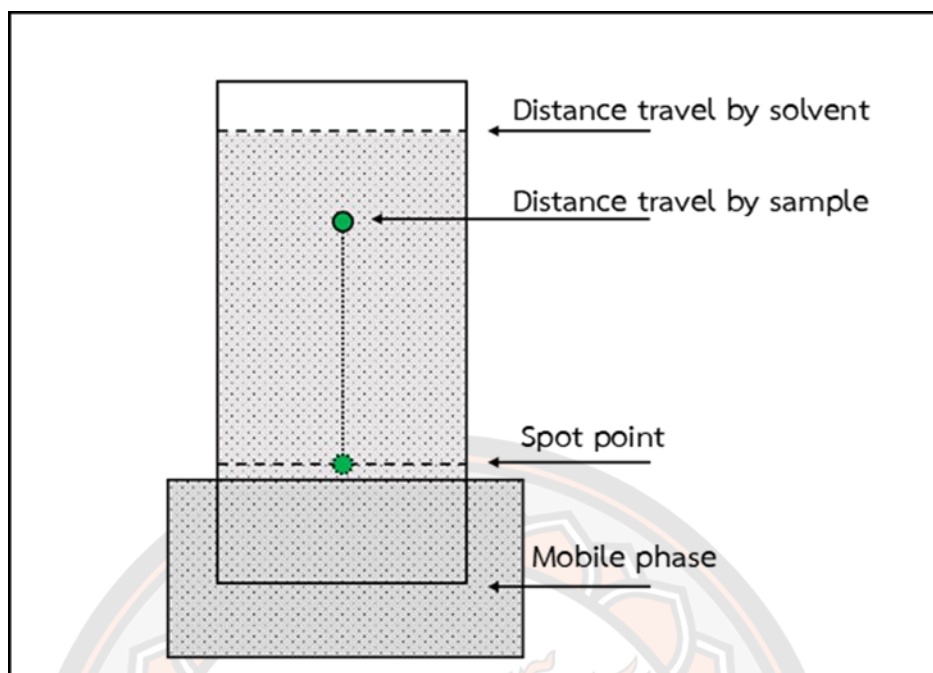


**Figure 11 Thin Layer Chromatography system**

## 2. Gas Chromatography – Mass Spectrometry (GC-MS)

Gas Chromatography – Mass Spectrometry or GC-MS is an analytical method consist of combining two analytical identification methods together, the gas chromatography and mass spectrometry. The principle of gas chromatography is based on separate the molecules inside the sample which can be vaporized into gas and carry by inert gas into the column. The different boiling point, polarity and affinity to the stationary phase will result with different elution time which gives its different retention time. The separated molecules will then directly pass into the mass spectrometer. Inside mass spectrometer, the bombardment of the molecules by beam of electrons create the positively charge ions fragment of the molecule. These positive ions then accelerated and deflected into a curve by magnetic fields. The detector then detects the mass of each ions corresponding to the variation of electric field of the arrival ions (mass-to-charge ratio  $m/z$ ) (McMASTER, 2008). Identification of volatile components was performed by computer matching their recorded mass spectra fragmentation patterns with those stored on the MS spectral library. Further identification was made by comparison of their mass spectra and their RIs relative to  $n$ -alkanes with those of the National Institute of Standards and Technology (NIST)

Chemistry WebBook (Babushok et al., 2007; Linstrom & Mallard, 2001) or with previously published data.

### Cell cytotoxic by MTT assay

MTT assay is a colorimetric assay based on assessing the cell metabolic activity. The biochemical basis behind the MTT assay involves with NAD(P)H-dependent cellular oxidoreductase enzyme that converts the yellow tetrazolium MTT [3-(4, 5dimethylthiazolyl-2)-2,5-diphenyltetrazolium bromide] into insoluble (E,Z)-5-(4,5-dimethylthiazol-2-yl)1,3-diphenylformazan (formazan) (**Figure 12**). The formed formazan can be dissolved with dimethyl sulfoxide (DMSO), and produces a purple color which can be measured by ELISA reader (Khor Goot Heah, 2017).

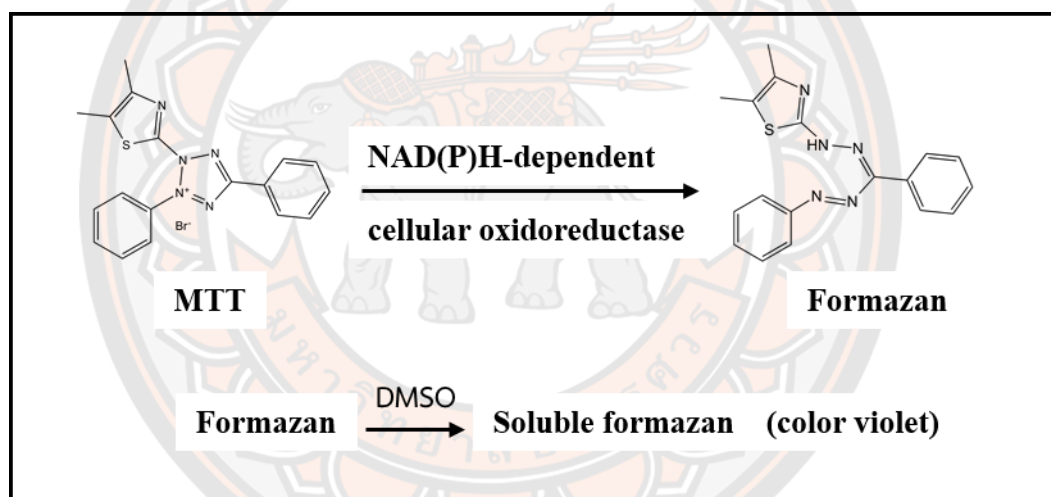


**Figure 12 Reduction of MTT dye**

The enzyme NADPH-dependent cellular oxidoreductase will change MTT into the insoluble crystal formazan in cell. This insoluble formazan then be dissolved by DMSO giving violet color which can be detect under ultraviolet light.

### Clonogenic or colony formation assay

Clonogenic assay or colony formation assay is an *in vitro* cell survival assay based on the ability of a single cell to grow into a colony. The colony is defined to consist of at least 50 cells. The assay essentially tests every cell in the population for

its ability to undergo “unlimited” division, which able us to compare the character and aggressivity between cancer cells base on the ability of cells to survive under rough conditions. Clonogenic assay is the method of choice to determine cell reproductive death after treatment with ionizing radiation but can also be used to determine the effectiveness of other cytotoxic agents (Franken et al., 2006).

### **Wound scratch migration assay**

The scratch-wound assay is a simple, reproducible assay commonly used to measure basic cell migration parameters such as speed, persistence, and polarity. Cells are grown to confluence and a thin "wound" introduced by scratching with a pipette tip or cell scratcher. Cells at the wound edge polarize and migrate into the wound space. Advantages of this assay are that it does not require the use of specific chemo-attractants or gradient chambers and it generates a strong directional migratory response, even in cell types that do not show robust responses in "single cell" migration assays. It is most reliably analyzed when performed using time-lapse imaging, which can also yield valuable cell morphology/protein localization information (Jonkman et al., 2014).

### **Flowcytometry analysis on apoptosis**

Apoptosis is a highly regulated process of cell death that occurs as a normal part of development. Deregulation of apoptosis is implicated in disease states, such as Alzheimer's disease and cancer. Apoptosis is distinguished from necrosis, or accidental cell death, by characteristic morphological and biochemical changes, including compaction and fragmentation of the nuclear chromatin, shrinkage of the cytoplasm, and loss of membrane asymmetry.<sup>1-5</sup> In normal live cells, phosphatidylserine (PS) is located on the cytoplasmic surface of the cell membrane. However, in apoptotic cells, PS is translocated from the inner to the outer leaflet of the plasma membrane, thus exposing PS to the external cellular environment. The human anticoagulant, annexin V, is a 35–36 kDa Ca<sup>2+</sup>-dependent phospholipid-binding protein that has a high affinity for PS. Annexin V labeled with a fluorophore or biotin can identify apoptotic cells by binding to PS exposed on the outer leaflet.

The red-fluorescent propidium iodide (PI) is a nucleic acid binding dye. PI is impermeant to live cells and apoptotic cells, but stains dead cells with red fluorescence, binding tightly to the nucleic acids in the cell. The staining of FITC Annexin V and PI apply to flow cytometry provides a rapid and convenient assay for apoptosis. After staining a cell population with FITC annexin V and PI in the provided binding buffer, apoptotic cells show green fluorescence, dead cells show red and green fluorescence, and live cells show little or no fluorescence. These populations can easily be distinguished using a flow cytometer with the 488 nm line of an argon-ion laser for excitation (Wlodkowic et al., 2009). Apoptotic cells can be identified by gated on Annexin V-FITC positive cells and P.I positive cells (see **Figure 13**).

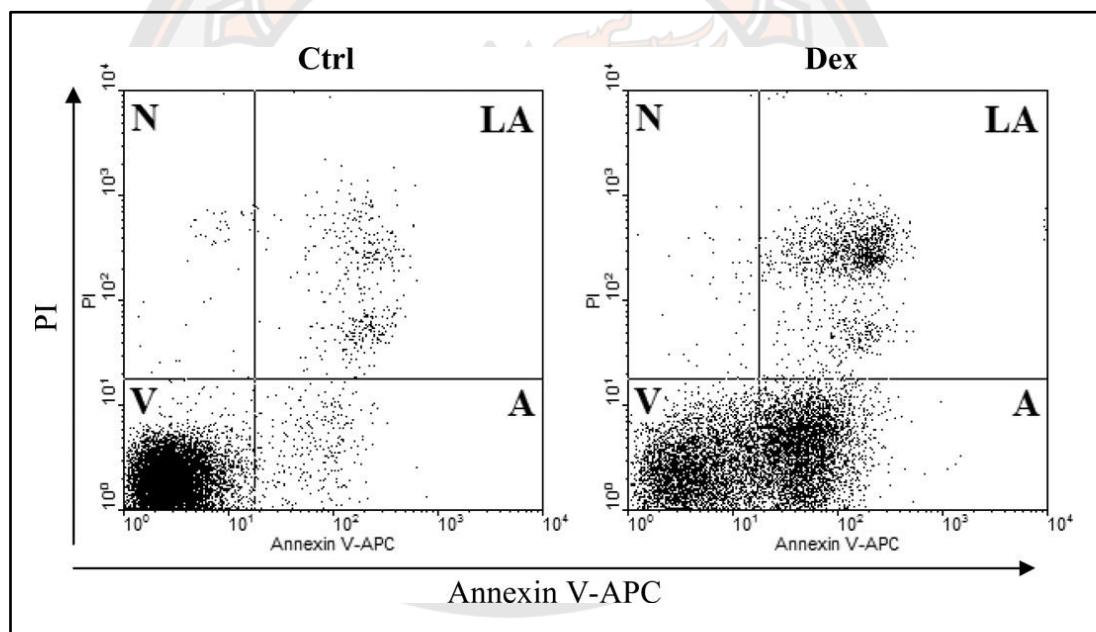


**Figure 13** Apoptotic cell analyzed by flowcytometry

**Source:** (Wlodkowic et al., 2009)

Apoptotic changes in plasma membrane. Detection of apoptosis by concurrent staining with annexin V–APC and PI. Human B-cell lymphoma cells were untreated (left panel) or treated with dexamethasone (right panel). Cells were subsequently stained with annexin V – APC conjugate and PI and their far-red and red fluorescence was measured by flow cytometry. Live cells (V) are both annexin V and PI negative.

At early stage of apoptosis (A) the cells bind annexin V while still excluding PI. At late stage of apoptosis (LA) they bind annexin V-FITC and stain brightly with PI (**Figure 13**).

### Hoechst staining

During apoptosis, DNA fragmentation and chromatin condensation occurred during the late phase of apoptosis. This phenomenon could be detected by using fluorescent DNA-binding dyes such as Hoechst33342 or propidium iodide (PI). The dyes can be excited with a UV laser or the xenon or mercury lamp of a fluorescence microscope and emits blue fluorescence. Cells stained in this way can then be visualized under a UV or fluorescence microscope, with apoptotic nuclei displaying characteristic hyper condensation and fragmentation into distinct globules. Alternatively, Hoechst33342 can be used to stain cells directly in the culture dish (Hollville & Martin, 2016).

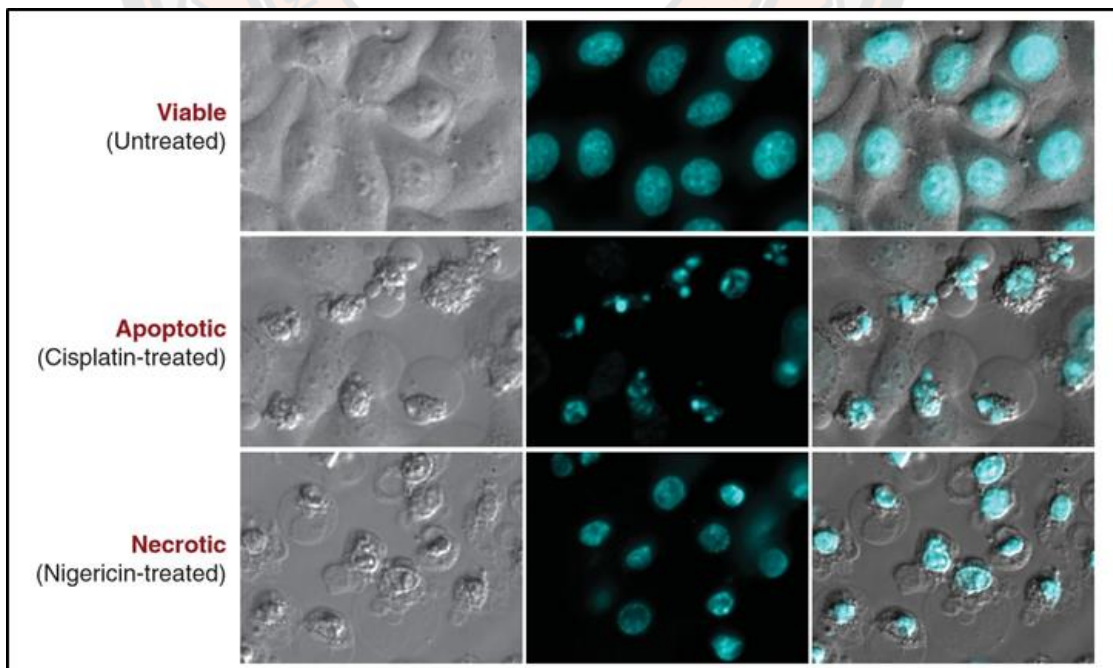


**Figure 14** Analysis of nuclear morphology by phase-contrast microscopy

HeLa cells were left untreated (top panel), treated with cisplatin (50  $\mu$ M, 24 hr) to induce apoptosis (middle panels), or treated with Nigericin (10  $\mu$ M, 20 hr) to induce necrosis (bottom panel). Cells in culture were stained with Hoechst33258 (4  $\mu$ g/ml, 10 min). Images of cell culture were taken with the 40 $\times$  lens of an inverted microscope (Olympus IX71) equipped with a digital camera (QIClick, QImaging). Phase contrast (left column), fluorescence (middle column), and merged (right column) images are shown.

## **Assessment to the level of genes expression**

### **1. Evaluation mRNA expression by RT-qPCR technique**

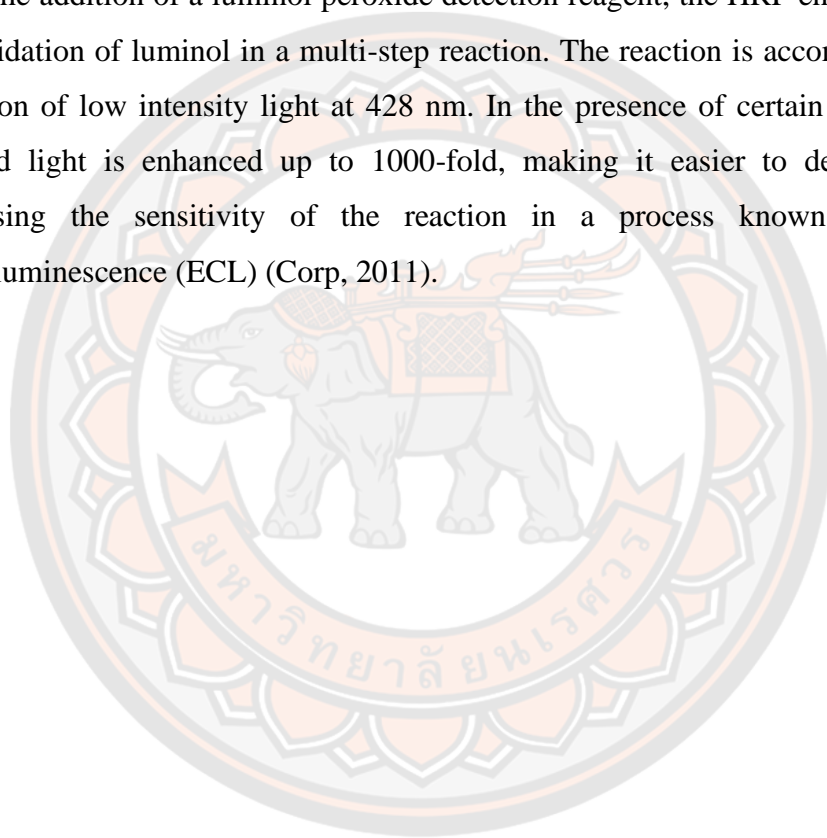
RT-qPCR is a PCR based method consisting of combining the quantitative PCR method and the real time PCR method together. Reverse transcription PCR, or RT-PCR, allows the use of RNA as a template. An additional step allows the detection and amplification of RNA. The RNA is reverse transcribed into complementary DNA (cDNA), using reverse transcriptase enzyme with the help of specific primer sequence correspondent to the specific protein of interest. The quality and purity of the RNA template is essential for the success of RT-PCR. The first step of RT-PCR is the synthesis of a DNA/RNA hybrid. Reverse transcriptase also has an RNase H function, which degrades the RNA portion of the hybrid. The single stranded DNA molecule is then completed by the DNA-dependent DNA polymerase activity of the reverse transcriptase into cDNA. Then qPCR is used to amplify the cDNA sequences receive from the RT-PCR process. cDNAs are bind to dsDNA binding dye (SYBR Green) before the PCR process is started. During each cycle, the fluorescence is measured. The fluorescence signal increases proportionally to the amount of replicated DNA and hence the DNA is quantified in “real time” (Neidler, 2017).

### **2. Evaluation proteins expression by Western Blot technique**

The Western Blot analysis of protein detection separates into five important parts the proteins sample preparation, electrophoresis of proteins, membrane transfer,

antibody probing and the immuno-detection. Each part play an important role in the result of the Western Blot analysis (**Figure 15**). Sample preparation is the first process in Western Blot analysis which involves in extracting the whole proteins from the cell lysate. Many possible lysate reagents like detergent, lysate enzyme or mechanical process like ultrasonication, osmotic shock can be used to lyse the cells. Electrophoresis is a commonly used method for separating proteins based on size, shape and/or charge. It is normally carried out by loading a sample containing the molecules of interest into a well in a porous matrix to which a voltage is then applied. Differently sized, shaped and charged molecules in the sample move through the matrix at different velocities. At the end of the separation, the molecules are detected as bands at different positions in the matrix. The matrix can be composed of a number of different materials, including paper, cellulose acetate, or gels made of polyacrylamide, agarose, or starch. In acrylamide and agarose gels, the matrix can also act as a size-selective sieve in the separation. In our experiment, polyacrylamide gel will be used as the matrix for running the proteins. Gels will be load into the running buffer with the variable time and current recommend by protocol of reagents. The separated proteins in the gel will be transferred to transfer membrane for later use in antibody probing. On completion of the separation of proteins by polyacrylamide gel electrophoresis (PAGE), the next step is to transfer the proteins from the gel to a solid support membrane, usually made of a chemically inert substance, such as nitrocellulose or polyvinylidene difluoride (PVDF). Blotting makes it possible to detect the proteins on the membrane using specific antibodies. The proteins transferred from the gels are immobilized at their respective relative migration positions at the time point when the electric current of the gel run is stopped. In our experiment, wet transfer will be performed by making the sandwich of transfer membrane and the polyacrylamide gel then submerge into transfer buffer under electrical current. The proteins will then be transferred into the PVDF membrane from the anode (-) to the cathode (+). Antibody probing is the process where the antibodies bind to its target protein which later can be detected by the intensity of the emitted fluorescence probe on the secondary antibodies. The transferred membranes will be blocked in the blocking buffer. Blocking the membrane allowed the proteins to fix on the membrane which prevent the proteins from dropping out of the membrane during

the washing process. The most commonly used enzymatic detection system is chemiluminescence, based on antibodies conjugated to horseradish peroxidase (HRP) that catalyze the oxidation of luminol in presence of peroxide, and results in light emission. HRP has several advantages over other enzymes such as alkaline phosphatase (AP). HRP can be easily conjugated to antibodies or streptavidin (which binds with extraordinarily high affinity to biotin, a commonly used tag) and can be used with different chemiluminescent reagents. The target protein on the membrane. After the addition of a luminol peroxide detection reagent, the HRP enzyme catalyses the oxidation of luminol in a multi-step reaction. The reaction is accompanied by the emission of low intensity light at 428 nm. In the presence of certain chemicals, the emitted light is enhanced up to 1000-fold, making it easier to detect, and thus increasing the sensitivity of the reaction in a process known as enhanced chemiluminescence (ECL) (Corp, 2011).



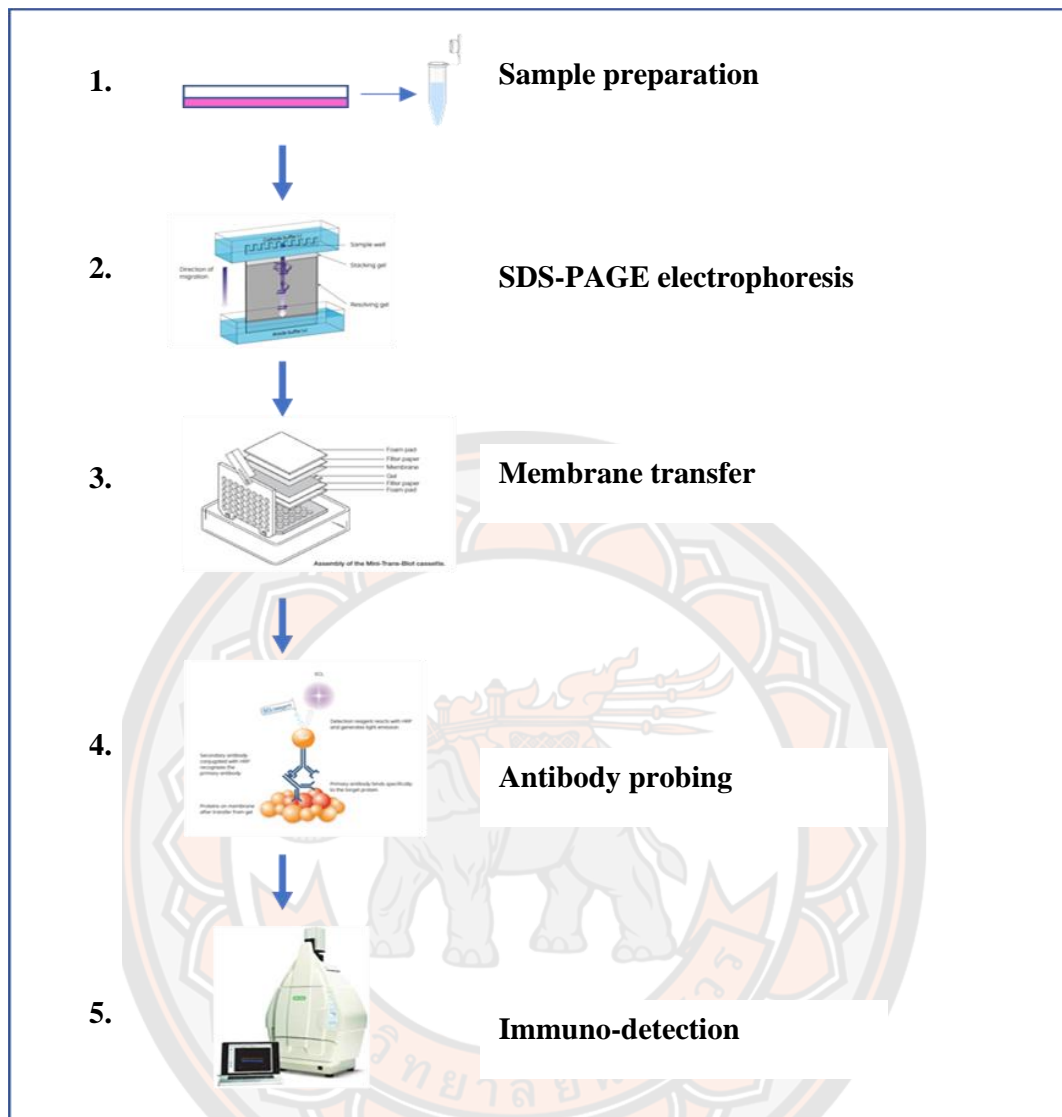


Figure 15 Western Blot analysis workflow

## CHAPTER III

### METHODOLOGY

#### Experimental Design

The experiment was divided into 2-main part follow by the experiments inside those part. The first part of the experiment was related to the phytochemistry part, which involves with the extraction of *C. hystrix* leaf powder by maceration methods. (**Figure 16.1**). After the leaf extraction process, the brief chemical profiles of *C. hystrix* or was accessed by thin layer chromatography (TLC) and followed by the gas chromatography-mass spectroscopy (GC-MS) (**Figure 16.2**). The second part of the experiment was the *in vitro* study to evaluate the anticancer effect of *C. hystrix* leaf extracts, citronellol and citronellal on MDA-MB-231 cell line. The first experiment come up with the screening of cytotoxicity of the leaf extract, citronellol, citronellal against both cancer cells line and normal primary cells by the cytotoxic MTT assay (**Figure 16.3**) followed by the selected doses from MTT assay, evaluation of the effect on crude extracts, citronellol and citronellal on cells proliferation inhibition was performed compared to untreated cells. Then the *in vitro* wound-scratch migration assay was used to evaluate the ability of *C. hystrix* leaf extracts, citronellol, citronellal on inhibiting the 2D migration of the cancer cells. The colony forming assay was used to validate the effect of colony forming inhibition of cancer cells by *C. hystrix* leaf extracts, citronellol and citronellal (**Figure 16.4**). Flowcytometry was used to identify the ability to induce cell cycle arrest and apoptosis of *C. hystrix* leaf extract, citronellol and citronellal on MDA-MB-231 cell line, and Hoechst staining was used to confirm the DNA fragmentation or chromatins condensation that happen during apoptosis (**Figure 16.5**). Then RT-qPCR was used to identify the level of genes expression related to cell death accompany with the protein analysis by western blotting (**Figure 16.6**).

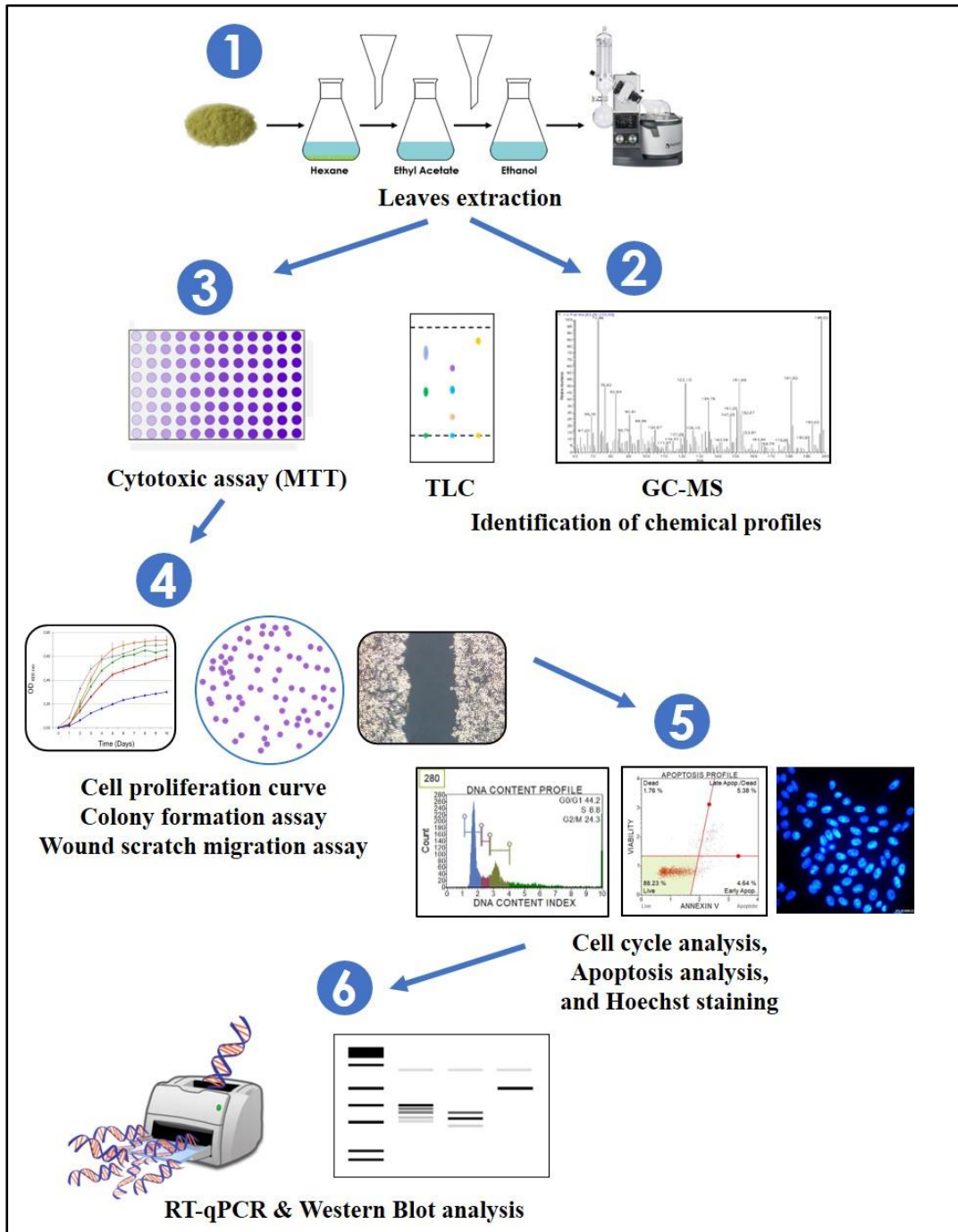


Figure 16 Experimental Design

## Extraction of *C. hystrix* leaf powder

### 1. *C. hystrix* leaf powder

Dry fine powder of *C. hystrix* leaf powder was taken from KHAOLAOR Laboratories Co., Ltd. From the central part of Thailand, Nakhon Pathom. The powder is kept at room temperature protected from light.

### 2. Maceration

Maceration is an extractive method use to isolate chemical components from the medical plants. The process is taken by totally submerge the desired part of the medical plant into the desired solvents.

In the experiment, 500 g of *C. hystrix* leaf fine powder were soaked with 1000 ml of pure hexane at room temperature covered by aluminum fold to prevent solvent evaporation with constant stir using magnetic bar for 3 days. The processes were undertaken 3 times, and each time the separated filtrate was taken to evaporate with rotary evaporator until the solvent evaporated from the crude extract. Crude extract obtained from hexane was stored at 4°C for further use. Marc remained from the process was taken for subsequent maceration with ethyl acetate and then with 95% ethanol with the same process as described below (**Figure 17**).

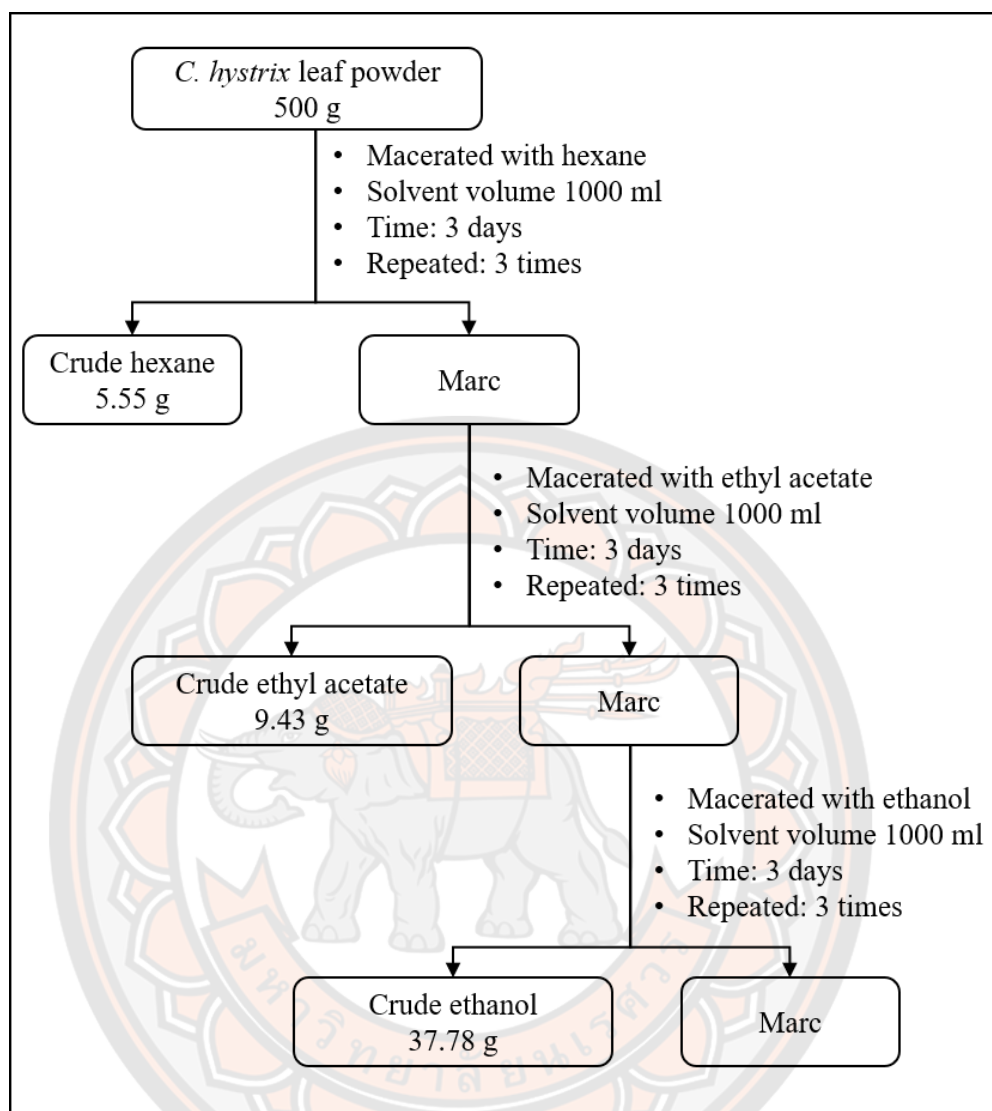


**Figure 17** Extraction of *C. hystrix* leaf by maceration method.

### ***C. hystrix* leaf extracts preparation for experiment**

Crude extracts received from the maceration process were dissolved in 100% DMSO at concentration of 100 mg/ml DMSO as stock solution and stored at  $-20^{\circ}\text{C}$ . Citronellol and citronellal were prepared at concentration of 100 nM with DMSO as stock solution and stored at  $4^{\circ}\text{C}$ . Doxorubicin was prepared as stock solution at concentration of 100  $\mu\text{M}$  with sterile deionized water and stored at  $-20^{\circ}\text{C}$ . Complete Dulbecco's modified eagle high glucose medium (DMEM; Gibco<sup>TM</sup>; Thermo Fisher

Scientific, Inc., Waltham, MA, USA) was used to dilute the extracts into desired concentrations used in the experiments.

### **$\beta$ -Citronellol and citronellal**

Two standard compounds, ( $\pm$ )- $\beta$ -citronellol and ( $\pm$ )-citronellal, were purchased from Sigma Aldrich company at analytical standard grade. For ( $\pm$ )- $\beta$ -citronellol lot number BCBT1132, and for ( $\pm$ )-citronellal lot number BCBZ3808.

### **Thin Layer Chromatography**

Thin layer chromatography is a chromatographic technique involved in coating the stationary phase on a planar plate of glass, aluminum or plastic, and using the solvents as mobile phase to separate analytes present in the sample based on its chemical and physical property.

In the experiment, 100% chloroform was used as mobile phase. 100% chloroform was placed into the chamber for 5 minutes to allow the solvent saturated in the chamber. Samples were spotted on the silica gel coated onto aluminum and were left to dry. TLC plate were then placed into the developed chamber, and allowed the solvent to migrate until solvent front (Ministry of Public Health, 2017). The spotted TLC paper was exposed to ultraviolet light at 254 nm and at 364 nm and then was sprayed by anisaldehyde at 100°C for 5 mins. Retention factor (R<sub>f</sub>) value was used to identify the compounds.

### **Gas Chromatography – Mass Spectrometry (GC-MS)**

The analysis of volatile compounds in crude hexane extract from *C. hystrix* leaf powder was performed using a Hewlett Packard Gas Chromatograph model 6890 (Agilent Technologies, Palo Alto, CA, USA) equipped with a mass selective detector. Crude hexane extract (50 mg/ml) was prepared by dissolving in hexane and was then injected into GC-MS system. Volatile compounds in sample were separated using silica capillary Hewlett Packard HP-5 (5% phenyl methyl siloxane) column (30 m x 0.25 mm i.d., 0.25  $\mu$ m film thickness). High purity helium was used as carrier gas with constant flow rate at 13.7 ml/min. The initial injector temperature was set at

250°C with split ratio mode at ratio 10:1 and with injector volume of 1 µl. The oven temperature started at 70°C for 3 mins then increased up to 280°C (5°C/min) and held for 20 mins. Transfer temperature was set at 280°C, and the mass detection ranges was set from 50 to 700 amu in full scan. Volatiles compounds were separated using silica capillary Hewlett Packard HP-5 (5% phenyl methyl siloxane) column (30 m x 0.25 mm i.d., 0.25 µm film thickness). The analysis was performed using Hewlett Packard (Agilent Technologies, Palo Alto, CA, USA) model 6890 gas chromatographs equipped with a mass selective detector. Retention indices (RIs) were determined by analyzing a solution containing the homologous series of *n*-alkanes (C<sub>8</sub>–C<sub>32</sub>) under the same chromatographic conditions and then calculated as described by (van Den Dool & Dec. Kratz, 1963). Identification of volatile components was performed by computer matching their recorded mass spectra fragmentation patterns with those stored on the Wiley7n MS spectral library. Further identification was made by comparison of their mass spectra and their RIs relative to *n*-alkanes with those of the National Institute of Standards and Technology (NIST) Chemistry WebBook (Babushok et al., 2007; Linstrom & Mallard, 2001) or with previously published data. The present of citronellol and citronellal in extract were also confirmed by analyzing authentic standards under the same chromatographic conditions. The relative contents of each component in the sample were also calculated based on the normalization of peak areas as the percentage of total detected volatile components.

#### Calculation of retention indices from GC-MS

$$\text{R.I} = 100n + \frac{100(t_x - t_n)}{(t_{n+1} - t_n)}$$

$n$  : number reference *n*-alkane hydrocarbons eluting immediately before compound “X”

$t_n$  : retention times of the reference *n*-alkane hydrocarbons eluting immediately before compound “X”

$t_{n+1}$  : retention times of the reference *n*-alkane hydrocarbons eluting immediately after chemical compound “X”

$t_x$  : is the retention time of compound “X”.

## Cells and Cell culture

### 1. Triple Negative Breast Cancer Cells

MDA-MB-231(ATCC® CRM-HTB-26™) is a triple negative human breast cancer cells derived from pleural effusion of a 51-year old female breast adenocarcinoma patient. MDA-MB-231 are the adherent cells with duplication time around 48 h. The cells were culture in Dulbecco's Modified Eagle Medium (DMEM; Gibco™; Thermo Fisher Scientific, Inc., Waltham, MA, USA) (**Figure 18**). Progesterone receptor, estrogen receptor, and human epidermal growth factor receptor are lack of their expression in this cell. MDA-MB-231 cell line was purchased from the American Type Culture Collection (ATCC).

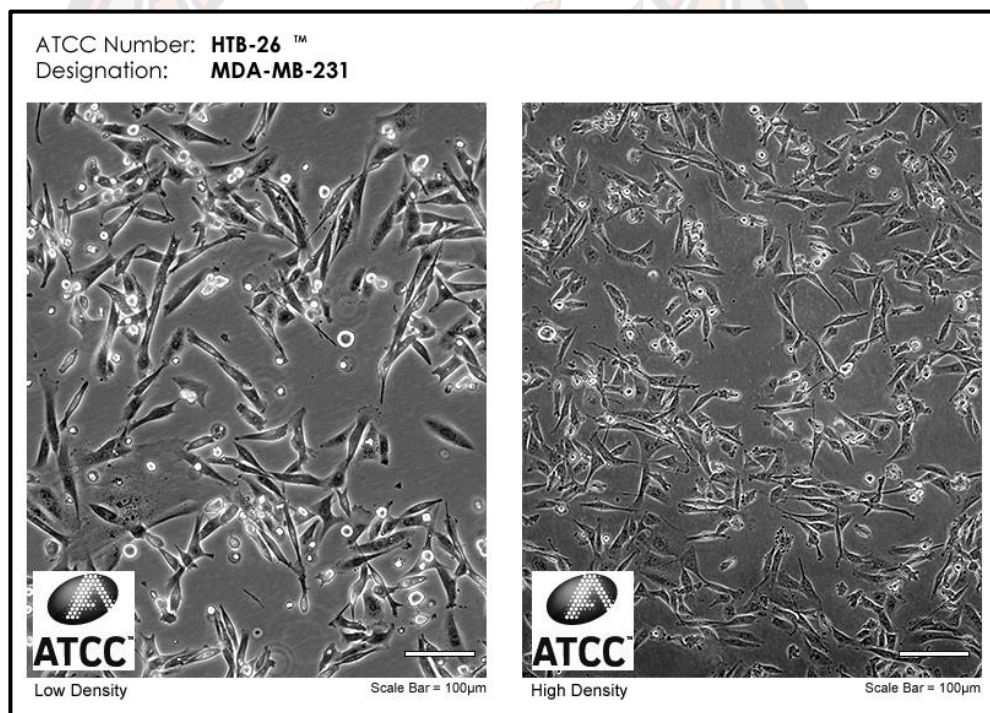


**Figure 18 MDA-MB-231 cells under microscope**

**Source:** <https://www.atcc.org/~media/Attachments/Micrographs/Cell/HTB-26.ashx>

### 2. Macrophage

Primary macrophage cells were received from the maturation of the isolated monocytes by incubated 7 days in complete RPMI medium containing 10% Fetal

Bovine Serum (FBS; Gibco™; Thermo Fisher Scientific, Inc., Waltham, MA, USA) and 1% of anti-anti (amphotericin B, penicillin, streptomycin) (Gibco™; Thermo Fisher Scientific, Inc., Waltham, MA, USA) in incubator at 37°C, CO<sub>2</sub> 5%.

### 3. Cells Cultures

MDA-MB-231 cells were seeded at density of 10<sup>6</sup> cells in T-75 cell culture flask with fresh Dulbecco's modified eagle high glucose medium (DMEM; Gibco™; Thermo Fisher Scientific, Inc., Waltham, MA, USA), 10% Fetal Bovine Serum (FBS; Gibco™; Thermo Fisher Scientific, Inc., Waltham, MA, USA) and 1% of anti-anti (amphotericin B, penicillin, streptomycin) (Gibco™; Thermo Fisher Scientific, Inc., Waltham, MA, USA) in incubator at 37°C, CO<sub>2</sub> 5%.

### 4. Cell Sub-culture

MDA-MB-231 cells were cultured until reached 80% confluence as shown in **Figure 18**. Old culture medium was removed, and cells were washed by 5 ml Ca<sup>2+</sup> and Mg<sup>2+</sup> free phosphate buffer saline (PBS). 5ml of 0.25% (w/v) Trypsin-0.53 mM-EDTA was used to detach the cells by incubated at 37°C with 5% CO<sub>2</sub> for 3-5 minutes then 5 ml of fresh DMEM was added to stop its reaction. The cells mixture was centrifuged at 1500 rpm for 5 minutes. After removing the supernatant, the cells were resuspended with fresh complete DMEM (Gibco™; Thermo Fisher Scientific, Inc., Waltham, MA, USA), and were adjusted to the desire cell concentration for various experiments as described in methodology.

### 5. Cryopreservation

After aseptically remove the medium from the flask, cells were washed with Ca<sup>2+</sup> and Mg<sup>2+</sup> free PBS. 5ml of 0.25% (w/v) Trypsin-0.53mM EDTA was used to detach the cells by incubated at 37°C with 5% CO<sub>2</sub> for 3 minutes. Fresh complete DMEM medium (Gibco™; Thermo Fisher Scientific, Inc., Waltham, MA, USA) was added to stop Trypsin-EDTA reaction. The cells mixture was centrifuged at 1500 rpm for 5 minutes. Then cells were resuspended with complete DMEM (Gibco™; Thermo Fisher Scientific, Inc., Waltham, MA, USA) and live cells were counted by using Trypan Blue assay. Cells were adjusted to 10<sup>6</sup> cells/ml/vial into cryovials and were

placed into Mr. Frosty container filled with 250 ml of isopropanol stored at 4°C one day before preservation days. Cryovials were transferred into a -80°C freezer for 24 h followed by transferring into the vapor phase of liquid nitrogen freezer. Cells Counting using Trypan Blue exclusion assay

The fresh mixture of MDA-MB-231 cells suspension were counted by using Trypan Blue dye exclusion assay. Cells were dyed with Trypan Blue dye then counted for the number of live cells by using Neubauer Hemocytometer (**Figure 19**).

$$\text{Number of viable cell} = \frac{\text{Total cells counted} \times \text{dilution factor} \times 10^3}{\text{Total counted chamber} \times 0.1 \text{ mm}^3} \quad (\text{cells/ml})$$

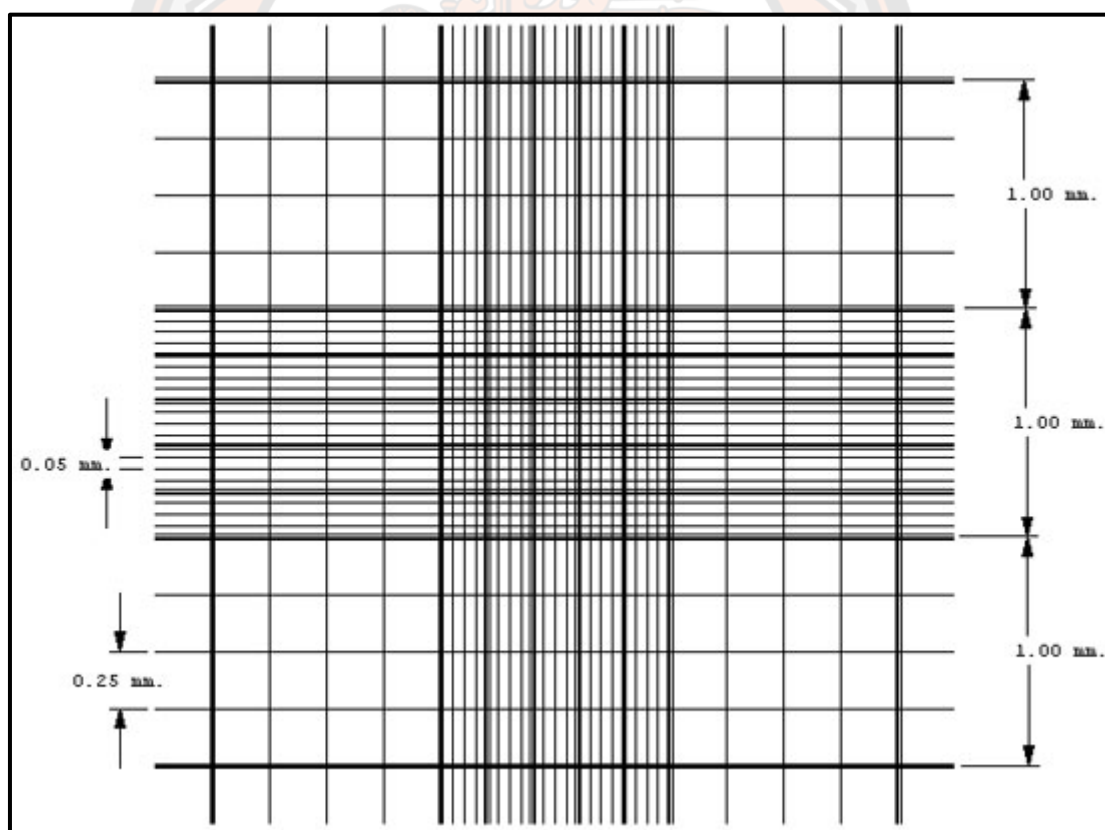


**Figure 19** Neubauer Haemocytometer

**Source:** <https://www.emsdiasum.com/microscopy/technical/datasheet/63511.asp>

## Monocytes Isolation

Human monocyte derived macrophages were isolated from fresh buffy coat received from Naresuan hospital. Human leukocytes were isolated from buffy coat centrifugation at 3000 rpm for 30 mins. Then Ficoll-Paque™ (Sigma-Aldrich, Inc., Missouri, USA) was used to isolate human peripheral blood monocytes by using the density gradient centrifugation force at 3000 rpm for 30 mins. Then 46% Percoll was used to isolate monocytes by using the density gradient centrifugation force at 3000 rpm for 30 mins. After that monocytes were washed with PBS-EDTA. After washing process, monocytes were culture with RPMI-1640 (Gibco™; Thermo Fisher Scientific, Inc., Waltham, MA, USA) with 10% FBS; Gibco™; Thermo Fisher Scientific, Inc., Waltham, MA, USA) and 1% anti-anti (amphotericin B, penicillin, streptomycin; Gibco™; Thermo Fisher Scientific, Inc., Waltham, MA, USA) in incubator at 37 °C, CO<sub>2</sub> 5% for one week for monocytes to derive into macrophages before performing the experiments.

## Cell Viability by MTT Assay

MTT assay is a colorimetric assay based on assessing the cell metabolic activity. The biochemical mechanism behind the MTT assay involves NAD(P)H-dependent cellular oxidoreductase enzyme that converts the yellow tetrazolium MTT [3-(4, 5dimethylthiazolyl-2)-2,5-diphenyltetrazolium bromide] into insoluble (E,Z)-5-(4,5-dimethylthiazol-2-yl)1,3-diphenylformazan (formazan). The formed formazan can be dissolved with dimethyl sulfoxide (DMSO) to give a purple color which can be measured by ELISA reader.

MDA-MB-231 cells were seeded in 96 wells plate at the density 10<sup>4</sup> cells/well and 5x10<sup>4</sup> cells/wells for primary macrophage for 24 h for cells to adhere. Cells were treated with 50 µl of hexane crude of *C. hystrix* leaf extracts, citronellol and citronellal (with various true flow dilution concentration) and were incubated for another 24 hours. Cells were then washed by 100 µl PBS followed by adding 50 µl/well of 0.5 mg/ml of MTT solution, incubated undisturbed for another 3 hours in dark at 37°C, CO<sub>2</sub> 5%. The supernatants were then removed, and the insoluble crystal

formazan formed inside the cells were solubilized by 100 µl of 100% DMSO in each well and were left in dark at room temperature for another 10 minutes with constant shaking. The absorbance of the soluble formazan was analyzed by ELISA microplate reader at 570nm. The results were then analyzed by Graph-Pad Prism 7 software using dose-response curved inhibition to identify the inhibition concentration of the *C. hystrix* leaf extracts, citronellol and citronellal on MDA-MB-231 cells. Cells treated with DMEM only were use as vehicle control, 2.5% DMSO were used to evaluate the toxicity of DMSO remained in the highest concentration of crude hexane used in the experiment.

#### Calculation of % cell viability

$$\% \text{ Cell viability} = \frac{\text{Absorbance of treated cells} - \text{Absorbance blank}}{\text{Absorbance of control cells} - \text{Absorbance blank}} \times 100$$

#### Preparation *C. hystrix* crude extracts, citronellol and citronellal for MTT assay

*C. hystrix* crude extracts were diluted from concentration of 5000 µg/ml to 2.44 µg/ml with complete culture (DMEM or RPMI) medium using two-fold dilution method. Citronellol and citronellal were diluted from concentration of 10 nM to 0.005 nM with complete culture medium (DMEM or RPMI) using two-fold dilution method, and 100 µM for doxorubicin (See Table 7).

**Table 6 Two-fold dilution of *C. hystrix* crude extracts, citronellol, citronellal and doxorubicin**

Treatments	Number of dilutions											
	1	2	3	4	5	6	7	8	9	10	11	12
Crude hexane ( $\mu\text{g/ml}$ )	2.44	4.88	9.77	19.53	39.06	78.13	156.25	312.50	625	1250	2500	5000
Crude ethyl acetate ( $\mu\text{g/ml}$ )	2.44	4.88	9.77	19.53	39.06	78.13	156.25	312.50	625	1250	2500	5000
Crude ethanol ( $\mu\text{g/ml}$ )	2.44	4.88	9.77	19.53	39.06	78.13	156.25	312.50	625	1250	2500	5000
Citronellol (nM)	0.005	0.01	0.02	0.04	0.08	0.16	0.31	0.63	1.25	2.50	5	10
Citronellal (nM)	0.005	0.01	0.02	0.04	0.08	0.16	0.31	0.63	1.25	2.50	5	10
Doxorubicin ( $\mu\text{M}$ )	0.05	0.10	0.20	0.39	0.78	1.56	3.13	6.25	12.50	25	50	100

### **Cell Proliferation Rate**

MDA-MB-231 cells were seeded at density of  $2 \times 10^4$  cells/well in 24 wells plate, and incubate pre-24 hours at  $37^{\circ}\text{C}$ ,  $\text{CO}_2$  5% to allow cells to attach to the wells. Cells were treated with 500  $\mu\text{l}$  of various molecules and compared with the non-treated cells. At between 24 hours of incubation, cell viability was accessed by using MTT assay. 300  $\mu\text{l}$  of MTT colour was added to cell and was allowed to incubate 3 hours in dark. 500  $\mu\text{l}$  of 100% DMSO was used to dissolve the insoluble formazan. 100  $\mu\text{l}$  of the soluble formazan was transferred to 96 wells plated and measured by using the ELISA reader. The increasing absorbance value of soluble formazan colour was representing the increasing in number of cells from each day.

### **Colony Forming Assay**

MDA-MB-231 cells were seeded at density of 500 cells/well into 6 wells plate, and were incubate for 24 hours at  $37^{\circ}\text{C}$ , 5%  $\text{CO}_2$  to allow cells to attach to the wells. Cells were gently washed by PBS and were treated with 1ml of hexane crude extracts at concentration 50  $\mu\text{g}/\text{ml}$ , 100  $\mu\text{g}/\text{ml}$ , 150  $\mu\text{g}/\text{ml}$ ,  $\beta$ -citronellol 0.5 nM or 1 nM, citronellal 0.5 nM or 1 nM, and doxorubicin as positive control at 0.5  $\mu\text{M}$ . After 24 hours of incubation, cells were washed and refresh with 2ml of completed DMEM media. Cells were incubated for 10 days with medium replacement between each 3 days.

After 10 days of incubation cells were fixed by using 2ml of neutral buffered formalin solution for 30 minutes. Then cells were stained with 2ml of 0.5% crystal violet for 1 hours. The staining dyed were removed, and number of colonies of cells were counted.

The pictures of colonies were captured by using a Canon macro lens 50 mm/f1.8 STM, then were converted to 8-bit greyscale images. Number of colonies of MDA-MB-231 cells were counted using Colony Area plugin by using ImageJ 1.52a software provided by National Institute of Health, USA. Threshold was adjusted to zero the noise of image background, number of colonies were counted by using the analyse particles tool by set the image pixel from 1 to infinity. Number of colonies

were reported as mean  $\pm$  SEM. One-way ANOVA was used to analyse the statistical different between control and treatments groups, *P* value  $<$  0.05 considered significant.

### **Scratch-Wound Assay**

MDA-MB-231 cells were seed at density of  $1 \times 10^6$  cells/well in 6 wells plate, and incubate at  $37^{\circ}\text{C}$ ,  $\text{CO}_2$  5% until cells to reach confluence. Then cells were washed twice with PBS. Cell scrappers (SPLScar<sup>TM</sup>, SPL life Sciences, Korea) were used to create wound areas by scratching on the well bottom. Cell debris and the dead cells were washed twice with PBS. Cells were treated with crude extracts,  $\beta$ -citronellol and citronellal compared to the non-treated cells and cells treated with doxorubicin. The migration of the cells was shown by wound closer areas. Photos of wound were taken at 0 hour, 12 hours and 24 hours by using inverted microscope (Carl Zeiss Microscopy GmbH, Germany) with objective 10X in bright field mode. The wound closer areas were analysed by wound healing tool plugin from ImageJ 1.52a software provided by National Institute of Health, USA. The reducing of wound areas represented the migration of the cells into the wound areas. Results were present as mean  $\pm$  SEM. Two-way ANOVA with post-hoc of Turkey's test were used to analyze the statistical different between control and treatment groups. *P* value  $<$  0.05 consider significant.

### **Apoptosis and cell cycle analysis**

#### **1. Apoptosis analysis**

Crude hexane, citronellol, citronellal or doxorubicin were used to induced apoptosis on MDA-MB-231 cells. Cells were harvested and transferred into 1.5 ml microtube. Cells were washed twice in cold PBS. And then were resuspended in 1% BSA. Then 100  $\mu\text{l}$  of Muse<sup>TM</sup> Annexin V and dead cell reagent (Merck, Darmstadt, Germany) was added to 100  $\mu\text{l}$  of cells suspension ( $5 \times 10^5$  cells/ml) and was allowed to incubate in dark for 20 min at room temperature. The apoptotic cells were analyzed using of Muse<sup>TM</sup> cell analyzer (Merck, Darmstadt, Germany) gated on Annexin V-FITC positive cells and 7-AAD positive cells.

## 2. Cell cycle analysis

Crude hexane, citronellol, citronellal or doxorubicin were used to induced cell cycle arrest on MDA-MB-231 cells. Cells were harvested and transferred into 1.5 ml microtube. Cells were washed twice in cold PBS. Cells were then fixed with 1 ml of 70% ethanol for 5 h. 200  $\mu$ l of cells suspension ( $10^6$  cells/ml) were washed with 250  $\mu$ l of PBS. 200  $\mu$ l of Muse™ cell cycle reagent and were incubated in dark for 20 min at room temperature. The apoptotic cells were analyzed using of Muse™ cell analyzer (Merck, Darmstadt, Germany) for 30 min.

### Hoechst 33342 staining

Cells were cultured on cover slide for 24 h. Cells were treated with crude hexane, citronellol, citronellal or doxorubicin for 24 h. Cells were washed twice with PBS and were then fixed with 4% formaldehyde for 15 min at room temperature. Cells were then washed twice with PBS and were permeabilize cells with 0.15% Triton-X 100 for 15 mins at room temperature followed by twice washed with PBS. 4  $\mu$ g/ml of Hoechst 33342 solution was used to stain cells for 10 min in dark at room temperature. Then 70% glycerol was used as anti-fade solution. Cover slides were then mount on slide and were sealed with nail polisher. DNA fragmented, or chromatin condense cells were observed under fluorescence microscope (Carl Zeiss Microscopy GmbH, Germany) with objective 40X.

### RT-qPCR

#### 1. mRNA extraction protocol

MDA-MB-231 cells were seeded at density of  $1 \times 10^6$  cells/well in 6 wells plate, and incubated for 24 hours at 37°C, CO<sub>2</sub> 5% to allow cells to attach to the wells. After incubation, culture medium was removed and replaced by treatment of crude hexane 200  $\mu$ g/ml, citronellol 1nM, citronellal 1 nM and doxorubicin 0.5  $\mu$ M. All treatments were removed, and total RNA was extracted from MDA-MB-231 cells using Ribozol™ RNA extraction reagent kits (AMRESCO, VWR Life Science, USA) from both treated and untreated cells at volume of 200  $\mu$ l per well and vortex for 10 mins at room temperature. Lysates were transferred into sterile 1.5 ml microtubes. 40

$\mu$ l of chloroform was added into each tube with constant shaking for 3 mins. Whole mixture then was centrifuge at 12000 G for 15 mins at 4°C. After centrifugation, the whole mixture separated into 3 phases (**Figure 20**). The aqueous phase which contain mRNA was transferred into new sterile 1.5 ml microtubes. Then 100  $\mu$ l of isopropanol was added into the aqueous phase and kept at room temperature for 10 min.

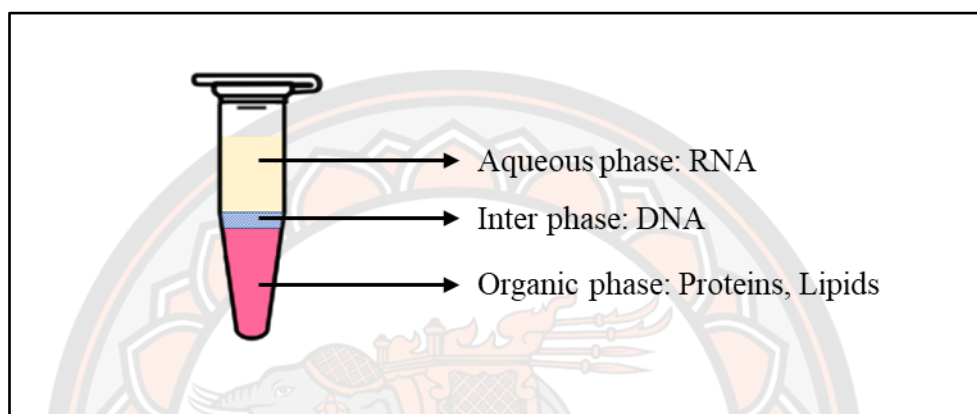


**Figure 20 Separation of RNA by Ribozol™ Reagent kits.**

**Source:** [https://blast.ncbi.nlm.nih.gov/Blast.cgi?PAGE\\_TYPE=BlastSearch](https://blast.ncbi.nlm.nih.gov/Blast.cgi?PAGE_TYPE=BlastSearch)

Briefly, cDNA synthesis was performed using the Tetro cDNA synthesis kit (Bioline Reagents Limited, UK). Real time PCR was carried out using SensiFAST™ SYBR No-ROX kits (Bioline Reagents Limited, UK). Sample preparation for PCR was acquired by mixing cDNA 3  $\mu$ l then 2  $\mu$ l of primer mix containing 1:1 ratio of forward and reverse primers, and finally with 5  $\mu$ l of SYBER green dye (Bioline Reagents Limited, UK). The initial denaturing temperature started from 95°C at 1 min following by 45 cycles of 15 sec denaturation followed by 30 sec of annealing and elongation at 60°C following protocol described in (Razak et al., 2019). The whole reaction was performed in CFX96 Touch Real-Time PCR Detection System (Bio-Rad Laboratories, USA). Primer sequences of  *$\beta$ -actin*, *Bcl-2* and *Bax* were obtained from previous studies and were checked by BLAST tool from National Institutes of Health (N.I.H) (**See Table 7**). All samples were performed in triplicate, and levels of gene expression was normalized to the level of  $\beta$ -actin as reference gene. The relative amount of target genes expression was calculated using  $2^{-\Delta\Delta CT}$ .

## 2. Primer sequences

**Table 7 Primer sequences**

Genes	Primer sequences	References
<i>β-actin</i>	Fw: 5'- AGAAAATCTGGCACCACACC -3' Rw: 5'- CCATCTCTTGCTCGAAGTCC -3'	(Khan et al., 2014)
<i>Bcl-2</i>	Fw: 5'- GATGTGATGCCTCTGCGAAG-3' Rw: 5'- CATGCTGATGTCTCTGGAATCT -3'	(Eimani et al., 2014)
<i>Bax</i>	Fw: 5'- GGTTGTCGCCCTTTTCTA -3' Rw: 5'- CGGAGGAAGTCCAATGTC -3'	(Golestani Eimani et al., 2014)

## **Polyacrylamide Gel Electrophoresis and Western Blot**

The Western Blot analysis of protein detection separates into five important parts the proteins sample preparation, electrophoresis of proteins, membrane transfer, antibody probing and the immuno-detection. Each part play an important role in the result of the Western Blot analysis. In our experiment, the operation protocol and other factors used in the experiments were optimized according to the reagents used in the experiments. We identified all proteins in **Table 8**,  $\beta$ -actin was used as internal control protein.

### **1. Sample preparation**

MDA-MB-231 cells were seeded at density of  $1 \times 10^6$  cells per well in 6 wells plate, and were left for 24 h at 37°C, 5% CO<sub>2</sub> for cells attachment. Cells were then treated by crude hexane, citronellol, citronellal and doxorubicin. Non-treated cells were used as normal control. After treatment, cells were washed by ice-cold 1X tris buffer saline (TBS) prior to proteins extraction process.

### **2. Protein extraction**

The radioimmunoprecipitation assay buffer (RIPA; Sigma-Aldrich, USA) was used as lysis buffer for whole protein extraction from MDA-MB-231 cells following by constant shaking for 30 min at 4°C. 1% of protease and phosphatase inhibitor cocktail (Sigma-Aldrich, USA) protease inhibitor was added to RIPA buffer protect the sample proteins from enzymes degradation. The extraction process is performed under temperature around 4°C. Whole cell lysates were transferred to 1.5 ml Ependorf tube followed by centrifugation at 16,000 rpm at 4°C for 30 mins. Supernatant containing total proteins was collected and stored at -20°C prior for the Western Blot analysis.

### **3. Total protein determination**

Coomassie (Bradford) protein assay kit (Thermo Fisher Scientific, Inc., New York, USA) was used to measure the amount of proteins received from the protein

isolation process following the products instruction leaflet. Bovine serum albumin was used as solution to access standard curve for total proteins measurement.

5  $\mu$ l of protein sample and 250  $\mu$ l of Coomassie reagent dye were added into each well of 96-well plate and then were left at room temperature for 10 mins covered in dark. After that, the mixture was taken for measurement of absorbent of total protein using ELISA microplate reader (PerkinElmer, Inc., Massachusetts, MA, USA) at wavelength of 595 nm. De-ionized water was used as blank. The concentration of total proteins was calculated using the formula  $y=ax+b$  generated by the standard curved, which  $y$  represented the concentration of proteins and  $x$  represented the absorbance of proteins measured by ELISA reader. Coefficient of calculation ( $R^2 < 0.98$ ) was used to represent the efficiency of the standard curve.

#### **4. Polyacrylamide Gel Electrophoresis**

12% of sodium dodecyl sulfate (SDS)–polyacrylamide gel based was used to separate the extracted proteins using Bio-rad gel electrophoresis sets. 12% of acrylamide gel containing 30% acrylamide, 1.5 M Tris-HCl (pH 8.8), 10% SDS, 10% ammonium persulfate (APS), N,N,N',N'-tetramethylethylenediamine (TEMED), TGX Stain-Free™ FastCast™ Acrylamide Solutions (Bio-Rad Laboratories, CA, USA). TGX Stain-Free™ FastCast™ Acrylamide Solutions allowed the detection of separated proteins in the gel using Bio-Rad's ImageLab™ software and stain-free enabled imagers. Gel mixture solution was poured into the assembled gel cast and allowed gel to polymerize for 15 mins. After that, 5% of acrylamide gel containing the constituents described above was overlaid on the resolving gel with comb inserted on its and left to polymerize for 15 mins. Total protein was mixed with equal volume to 2X Laemmli loading buffer (Bio-rad Laboratories, CA, USA) and undergone denaturing process for 5 min at 95°C. 30  $\mu$ g of total proteins in Laemmli loading buffer was introduced into each well of pre-cased gel in the electrophoresis chamber. The electrophoresis process was undertaken using Tris-Glycine running buffer with starting electric current of 100 mV for 15 min followed by constant current of 150 mV for around 1 hour. After separation, gels were disassembled from gel cassette and

were taken to the proteins separation detection by using Bio-Rad's ImageLab™ software and stain-free enabled imagers, and ready for transferring process.

## 5. Membrane transfer

The separated proteins on the gel were transferred to polyvinylidene fluoride (PVDF) membrane under constant electric current of 100 mV for 1 h 30 mins in transfer buffer at 4°C.

## 6. Antibody probing

After transferred, PDVF membranes were blocked using 5% skim milk powder in tween-20 -base tris buffer saline (TBST) for 1 hour at room temperature with constant shaking. Then membranes were washed 3 times 5 mins each with TBST washing buffered. Primary antibodies in TBST containing 1% BSA (1:1000 dilution ratio) was used to probe on the target proteins for overnight with constant shaking at 4°C. After that membranes were washed 3 times with TBST prior for secondary antibody probing for 1 hour at room temperature with constant shaking (1:10000 dilution in TBST containing 1% BSA) followed by 3 times washed by TBST.

## 7. Immuno-detection

Substrate was added to the membrane which allow the peroxidase enzyme that bind to the secondary antibody to degrade that substrate and produce the luminescence light which can be detect by the imaging system.

**Table 8 Proteins for Western Blot analysis**

Proteins	Functions
β-actin	Internal control
Bcl-2	Anti-apoptotic protein
Bax	Pro-apoptotic protein

### **Statistical Analysis**

All the experiments were performed in triplicate and data were expressed as the means  $\pm$  SEM, n=3. One-way ANOVA with Dunnett's multiple comparisons test was used to analyze the different between control and treatment groups (n=3), P value  $< 0.05$  consider significant.

### **Research Approval**

Research ethical was approved by Human Ethics Committee of Naresuan University (IRB No. 0945/62).



## CHAPTER IV

### RESULTS

#### Extraction yields of *C. hystrix* leaf powder

Crude extract by maceration with hexane solvent had resulting in sticky dark green extract with yield of 1.1% (w/w dried powder) from *C. hystrix* dry powder. The following sub-sequential extractions resulted in the similar consistency of extracts with yield of 1.8% obtained using ethyl acetate and 7.6% using ethanol.

#### Identification of volatile components in crude hexane extract by GC-MS

From GC-MS analysis, 45 volatile compounds from crude hexane were identified. The relative amount (%) of the identified compounds was 51.44%, which was calculated by peak-area normalization. As listed in **Table 9**, the majority of identified compounds of crude *C. hystrix* hexane extract belong to the terpenoids, which presented almost 19.84% of the identified compound. Crude hexane extract contained oxygenated monoterpenes (3.99%), hydrocarbon monoterpene (2.19%), oxygenated sesquiterpenes (7.67%), hydrocarbon sesquiterpenes (5.99%) presented as major compounds. Other compounds including hydrocarbons, fatty acids, fatty alcohols, vitamin, and other terpenes. The presented of two oxygenated monoterpenes; citronellal and citronellol, were observed at 10.75 min and 12.85 min, respectively (**Figure 24**), while the standard citronellal showed its peak at retention time of 10.88 min (**Figure 23**) and 13.03 min for citronellol (**Figure 22**). Other constituents contain such as long chain hydrocarbons, phytosterols, fatty acids, fatty alcohols, and vitamin.

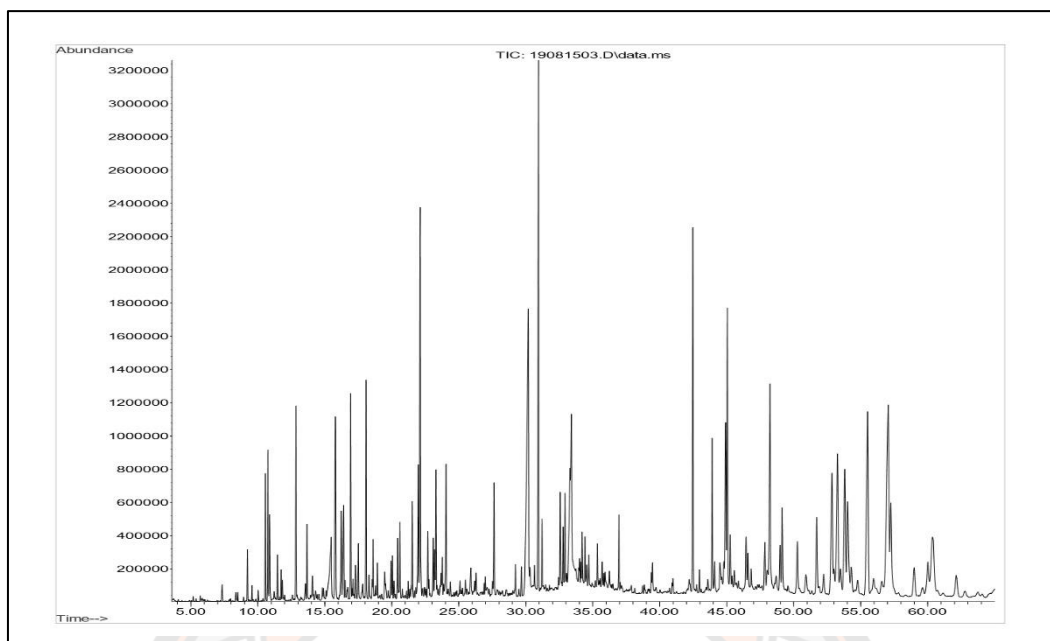


**Figure 21** Total ion chromatogram of volatile compounds in crude *C. hystrix* hexane extract obtained from GC-MS

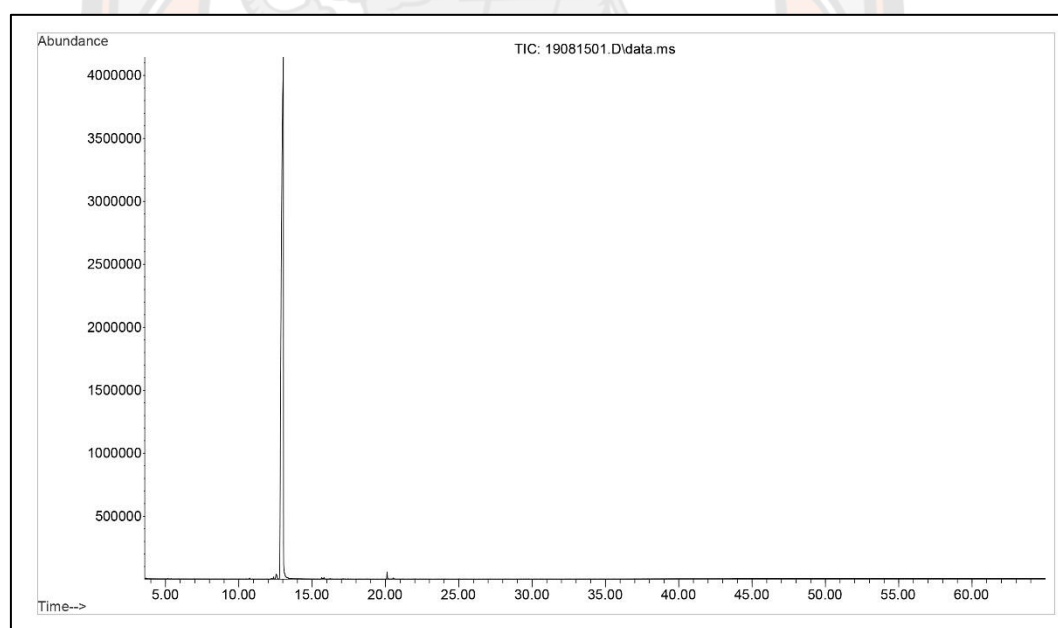


**Figure 22** Total ion chromatogram of standard citronellol at 13.03 min

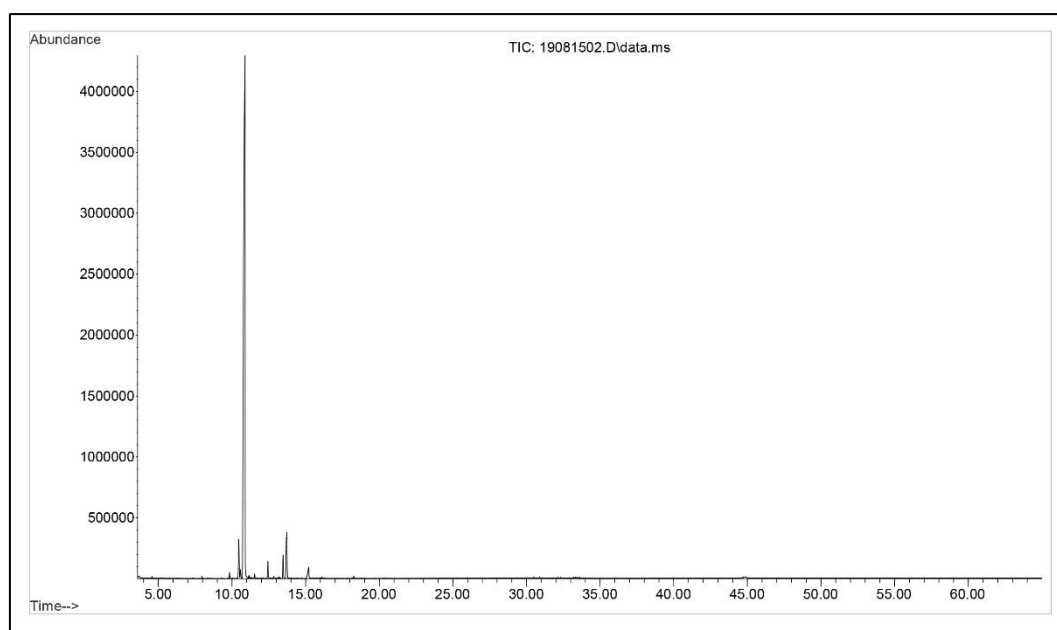


**Figure 23 Total ion chromatogram of standard citronellal at 10.88 min**

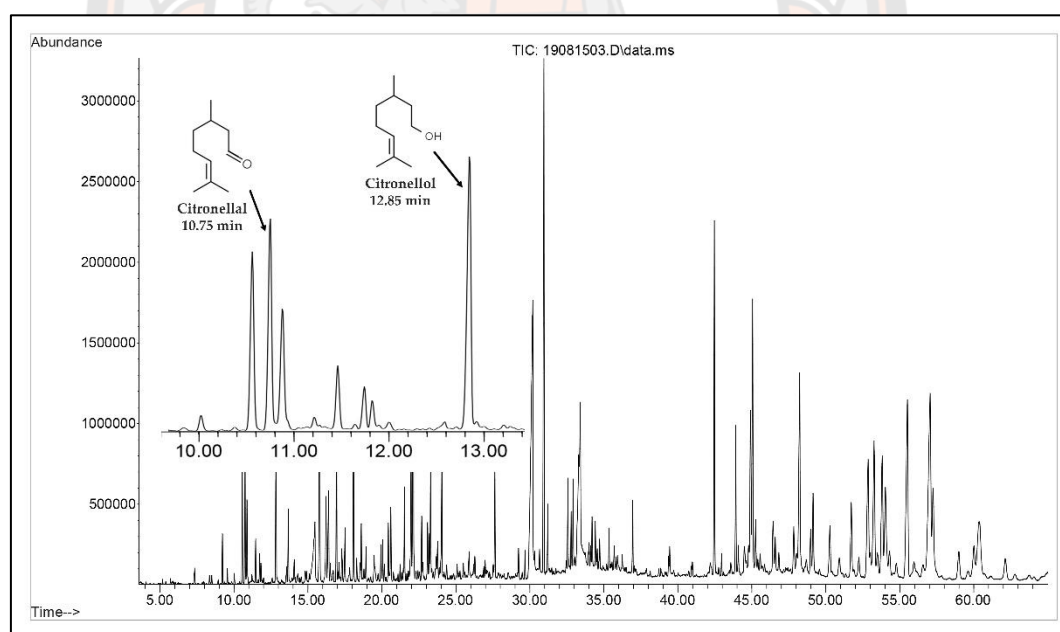


**Figure 24 Peaks of citronellal and citronellol were observed at retention times at 10.75 min and 12.85 min.**

**Table 9** The identified compounds from crude hexane by GC-MS

No.	RT (min)	R.I <sup>1</sup>	Identified compounds	Classification	R.A <sup>2</sup> (%)
1	9.23	1100	Linalool	Monoterpene <sup>a</sup>	0.34
2	10.56	1146	Isopulegol	Monoterpene <sup>a</sup>	1.01
3	10.75	1154	Citronellal	Monoterpene <sup>a</sup>	0.67
4	11.46	1179	Terpinen-4-ol	Monoterpene <sup>a</sup>	0.29
5	11.83	1193	$\alpha$ -Terpineol	Monoterpene <sup>a</sup>	0.11
6	12.85	1229	Citronellol	Monoterpene <sup>a</sup>	1.42
7	14.08	1354	3,7-dimethyloct-1,7-dien-3,6-diol	Monoterpene <sup>a</sup>	0.15
8	16.23	1354	$\alpha$ -Cubebene	Sesquiterpene <sup>b</sup>	0.94
9	16.94	1381	$\alpha$ -Copaene	Sesquiterpene <sup>b</sup>	1.44
10	17.29	1395	$\beta$ -Cubebene	Sesquiterpene <sup>b</sup>	0.34
11	18.08	1426	Caryophyllene	Sesquiterpene <sup>b</sup>	1.59
12	18.30	1435	Bicyclosequiphellandrene	Sesquiterpene <sup>b</sup>	0.20
13	18.93	1460	$\alpha$ -Humulene	Sesquiterpene <sup>b</sup>	0.23
14	19.47	1482	$\gamma$ -Muurolene	Sesquiterpene <sup>b</sup>	0.12
15	20.05	1505	$\alpha$ -Muurolene	Sesquiterpene <sup>b</sup>	0.31
16	20.61	1529	$\delta$ -Cadinene	Sesquiterpene <sup>b</sup>	0.62
17	21.23	1555	Elemol	Sesquiterpene <sup>a</sup>	0.13
18	21.53	1568	Nerolidol	Sesquiterpene <sup>a</sup>	0.71
19	21.98	1586	Spathulenol	Sesquiterpene <sup>a</sup>	1.34
20	22.12	1592	Caryophyllene oxide	Sesquiterpene <sup>a</sup>	3.74
21	23.21	1641	Caryophylladienol	Sesquiterpene <sup>a</sup>	0.39
22	23.67	1661	Viridiflorene	Sesquiterpene <sup>b</sup>	0.20
23	24.05	1678	Caryophyllenol	Sesquiterpene <sup>a</sup>	1.14
24	25.90	1764	Tetradecanoic acid	Fatty Acid <sup>a</sup>	0.34
25	26.29	1785	Alloaromadendrene oxide	Sesquiterpene <sup>a</sup>	0.22
26	27.63	18467	Hexahydrofarnesyl acetone	Sesquiterpene derivative	0.81
27	29.24	1927	Methyl palmitate	Fatty Acid <sup>a</sup>	0.30
28	30.19	1976	Palmitic acid	Fatty Acid <sup>a</sup>	6.82
29	32.79	2015	Phytol	Diterpene	0.40
30	33.30	2144	Linoleic acid	Fatty Acid <sup>a</sup>	1.89

**Table 9 Cont.**

No.	RT (min)	R.I <sup>1</sup>	Identified compounds	Classification	R.A <sup>2</sup>
31	33.40	2149	(6Z),(9Z)-Pentadecadien-1-ol	Fatty Acid <sup>a</sup>	2.39
32	44.09	2833	Supraene	Triterpene	0.31
33	44.92	2893	<i>cis</i> -2,6-Dimethyl-2,6-octadiene	Monoterpene <sup>b</sup>	2.19
34	48.24	3103	Tetracosane	Hydrocarbon	3.21
35	48.98	3139	$\alpha$ -Tocopherol	Vitamin	0.56
36	49.15	3147	Pentacosane	Hydrocarbon	1.03
37	50.92	3227	Campesterol	Phytosterol	0.46
38	51.73	3260	Stigmasterol	Phytosterol	1.07
39	52.86	3309	Heneicosane	Hydrocarbon	2.57
40	53.00	3350	1-Eicosanol	Fatty alcohol	0.37
41	53.27	3317	$\gamma$ -Sitosterol	Phytosterol	2.90
42	53.81	3335	Lanosterol	Triterpene	2.45
43	58.99	34845	Lupenyl acetate	Triterpene	0.68
44	60.02	3510	17-Pentriacontene	Hydrocarbon	2.23
45	62.13	3556	Neophytadiene	Diterpene <sup>b</sup>	0.61
<b>Total R.A of identified compounds</b>					<b>51.24 %</b>

Oxygenated monoterpenes	3.99 %
Hydrocarbon monoterpene	2.19 %
Oxygenated sesquiterpenes	7.67 %
Hydrocarbon sesquiterpenes	5.99 %
Hydrocarbons	9.04 %
Fatty acids and fatty alcohols	12.11 %
Other	10.25 %

<sup>1</sup>Retention indices were calculated using a homologous series of *n*-alkanes (C<sub>8</sub>–C<sub>32</sub>)

<sup>2</sup>Relative amounts (%) were obtained by peak areas normalization

<sup>a</sup>Oxygenated form

<sup>b</sup>Hydrocarbon form

**Note** R.A: relative amount (%), R.I: retention indice, RT: retention time (min)

### Screening of crude extracts using thin layer chromatography (TLC)

Thin layer chromatography was used to show chemical profiles of crude *C. hystrix* hexane extract, ethyl acetate extract, ethanolic extract, and two standard compounds citronellol and citronellal (**Figure 25**). From TLC chromatogram, crude hexane showed much more spots compare to crude ethyl acetate and crude ethanol when detected under UV light at 254 nm and 364 nm, and with sprayed by anisaldehyde. Moreover, standard citronellol and citronellal showed their spot when spray with anisaldehyde as violet color with  $R_f$  value of 0.43 and 0.9 (**See Table 10**).

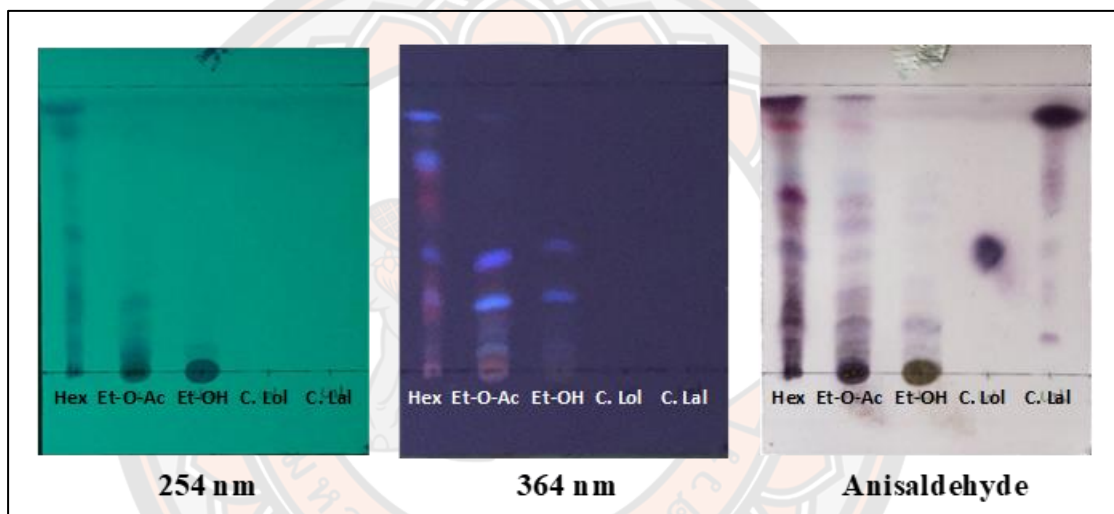


**Figure 25 Thin layer chromatography**

From left to right, each initial spot represented crude *C. hystrix* hexane extract, ethyl acetate extract, ethanolic extract, and two standard compounds citronellol and citronellal. TLC membrane were exposed to UV light at 254 nm (left), 364 nm (middle), and were sprayed by sulfuric acid reagent (right). Hex (crude hexane), Et-O-Ac (crude ethyl acetate), Et-OH (crude ethanol), C.Lol (citronellol) and C. Lal (citronellal).

**Table 10**  $R_f$  value from TLC of crude *C. hystrix* extracts

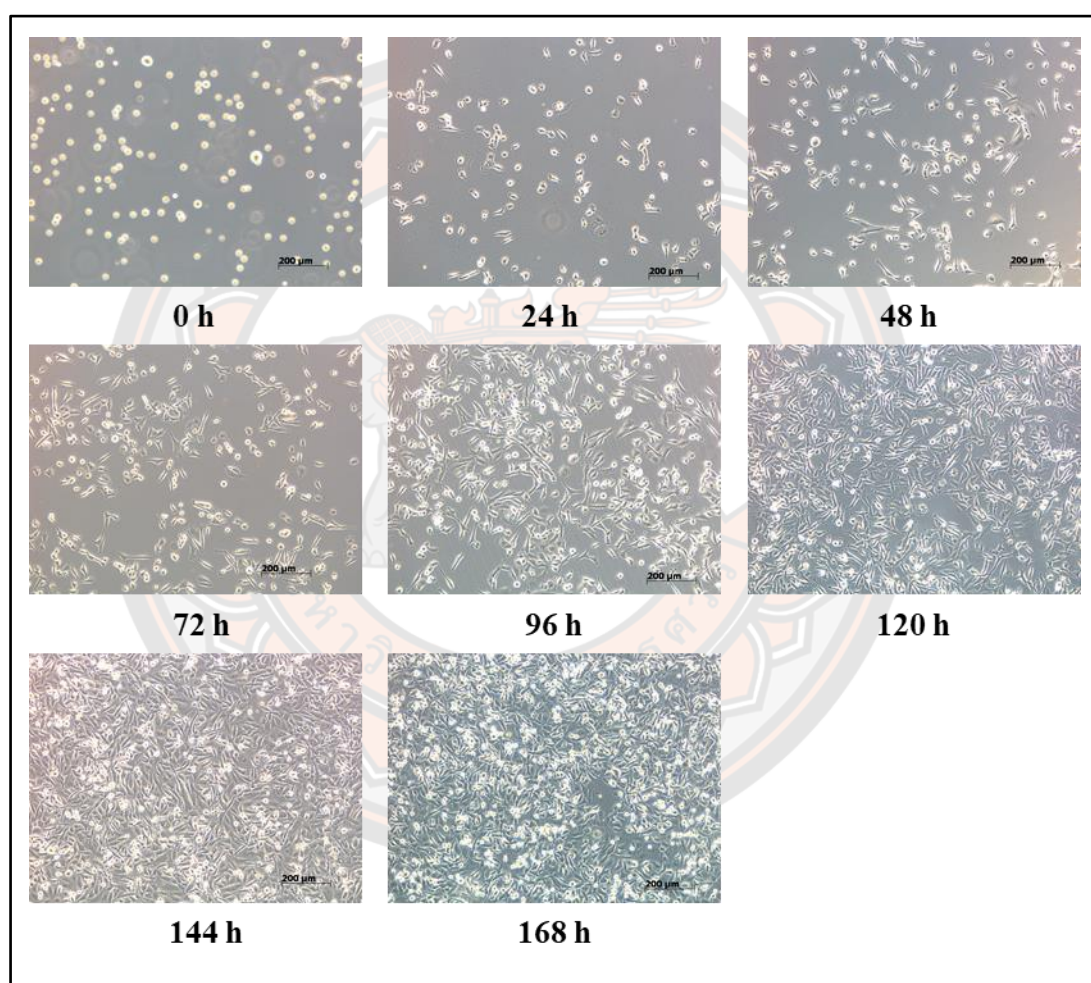
Extract	$R_f$	UV 254 nm	UV 366 nm	Anisaldehyde
Crude hexane	0.03	quenching	pale pink	dark green
	0.08	quenching	bluish violet	bluish violet
	0.15	-	-	bluish violet
	0.22	quenching	bluish violet	-
	0.25	-	red	bluish violet
	0.30	-	pale violet	-
	0.33	quenching	-	bluish violet
	0.42	quenching	-	-
	0.45	-	-	violet
	0.49	-	blue	-
	0.58	quenching	-	-
	0.60	-	dark blue	-
	0.63	-	-	violet
	0.70	-	red	-
	0.73	-	-	blue
	0.76	-	pale violet	-
	0.77	quenching	-	-
	0.80	quenching	Pale violet	-
	0.84	-	-	pink
	0.89	-	bluish violet	-
0.91	quenching	-	-	
0.94	-	-	violet	

Table 10 Cont.

Extract	R <sub>f</sub>	UV 254 nm	UV 366 nm	Anisaldehyde
Crude Et-O-Ac	0.03	quenching	orange	brown
	0.05	-	red	-
	0.10	quenching	-	brown
	0.17	quenching	pale violet	-
	0.19	-	-	bluish violet
	0.27	quenching	light blue	-
	0.30	-	-	bluish violet
	0.33	-	violet	-
	0.45	-	-	bluish violet
	0.46	-	blue	-
	0.57	-	-	bluish violet
	0.63	-	-	violet
	0.65	-	pale violet	-
	0.68	-	-	blue
0.84	-	-	pink	
0.94	-	-	violet	
Crude Et-OH	0.03	quenching	pink	brown
	0.08	quenching	-	-
	0.10	-	pale blue	bluish violet
	0.19	-	-	blue
	0.27	-	blue	-
	0.31	-	-	violet
	0.46	quenching	blue	-
	0.60	-	-	violet
0.94	-	-	violet	
Standard citronellal	0.90	-	-	violet
Standard citronellol	0.43	-	-	violet

### MDA-MB-231 cell culture

MDA-MB-231 cells are adherent cell. MDA-MB-231 cells were seeded in 12-well plates at density of  $2 \times 10^4$  cells per well and left cells to attached on plate for 24 h. Between 24 h, cells viability was measured using the MTT assay. MDA-MB-231 cells grew with good health and had stretching morphology on culture plate (**Figure 26**) and cells duplicated between each 48 h (**Figure 27**).



**Figure 26** MDA-MB-231 cells growth morphology by time of incubation

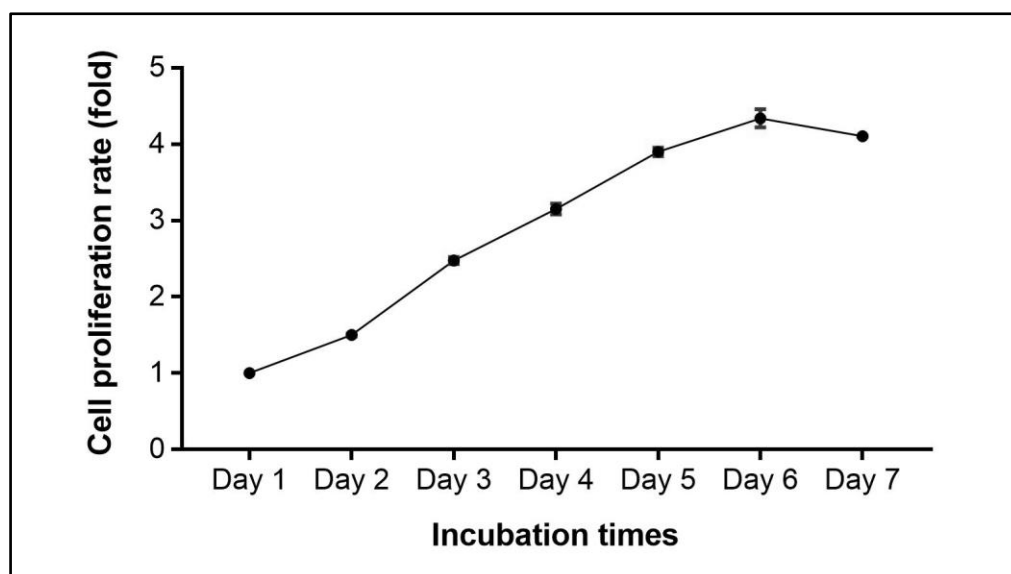


**Figure 27 MDA-MB-231 proliferation curve**

### **Primary macrophage cells culture**

Primary macrophages were derived from monocytes that were isolated from buffy coated, the cells were left for around a week for cells to attach and derive into macrophage with medium being replace in every 3 days. The derived macrophages were used after one week of cultures for determined the toxicity of crude extract and the pure compound (**Figure 28**).

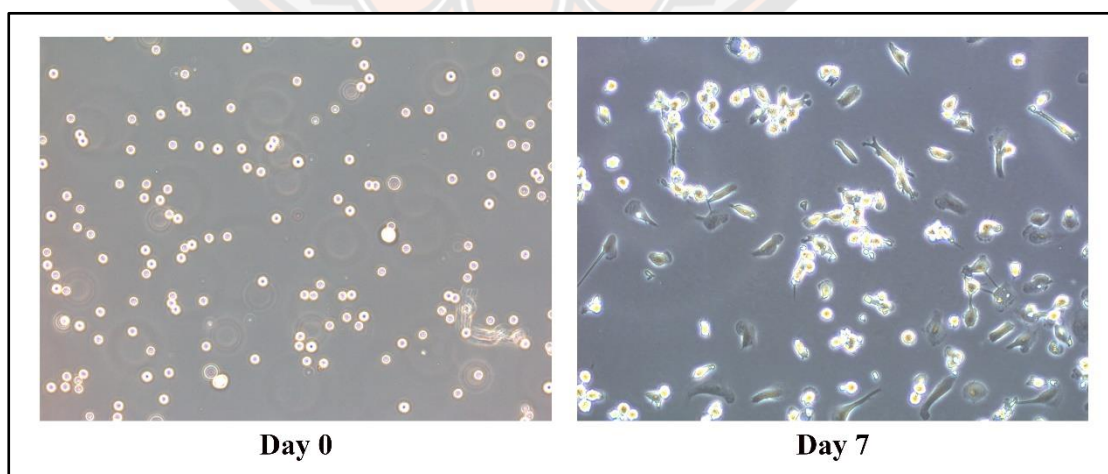


**Figure 28 Primary monocytes at day 0 and macrophage derived at day 7**

### Cytotoxicity of crude extracts, citronellol, citronellal on MDA-MB-231 cells

The cytotoxic effect of *C. hystrix* crude extracts and its bioactive molecules citronellol and citronellal, was analyzed using the *in vitro* cytotoxicity based on MTT assay. Cytotoxicity of extracts and active compounds was obtained from dose-response inhibition curve generated from GraphPad Prism application. After 24 h of treatment, *C. hystrix* crude extracts, citronellol and citronellal reduced cell viability of MDA-MB-231 cells with  $IC_{50}$  of  $317.63 \pm 2.00 \mu\text{g/ml}$  for crude hexane (**Figure 29 A**),  $547.10 \pm 0.90 \mu\text{g/ml}$  for crude ethyl acetate (**Figure 30 B**), and  $IC_{50} > 1000 \mu\text{g/ml}$  for crude ethanol (**Figure 29 C**). For citronellol  $IC_{50} = 1.16 \pm 0.10 \text{ nM}$  (**Figure 29 D**) and  $1.41 \pm 0.03 \text{ nM}$  for citronellal (**Figure 29 E**) while doxorubicin induced cell toxicity with  $IC_{50} = 1.18 \pm 0.06 \mu\text{M}$  (**Figure 29 F**). To identify the effect of crude hexane, citronellol and citronellal on normal cells, primary macrophage derived from monocyte were used as model for the experiment. The  $IC_{50}$  value of treatments on primary macrophage were crude hexane  $IC_{50} = 451.66 \pm 35.11 \mu\text{g/ml}$  (**Figure 29 G**), citronellol  $IC_{50} = 1.96 \pm 0.02 \text{ nM}$  (**Figure 29 H**) and citronellal  $IC_{50} = 1.81 \pm 0.01 \text{ nM}$  (**Figure 29 I**).  $IC_{50}$ ,  $IC_{10}$ ,  $IC_5$  value of crude hexane, citronellol and citronellal on MDA-MB-231 cells and primary macrophage were compared in **Table 12**. Each crude extract was dissolved with 100% DMSO and were diluted to 5 mg/ml with complete medium with 2.5% DMSO remained. Thus, the toxicity of 2.5% DMSO on the cells was evaluated by MTT assay. The result show that 2.5% DMSO did not have significant effect on cell viability compared to culture medium only (**Appendix 31**).

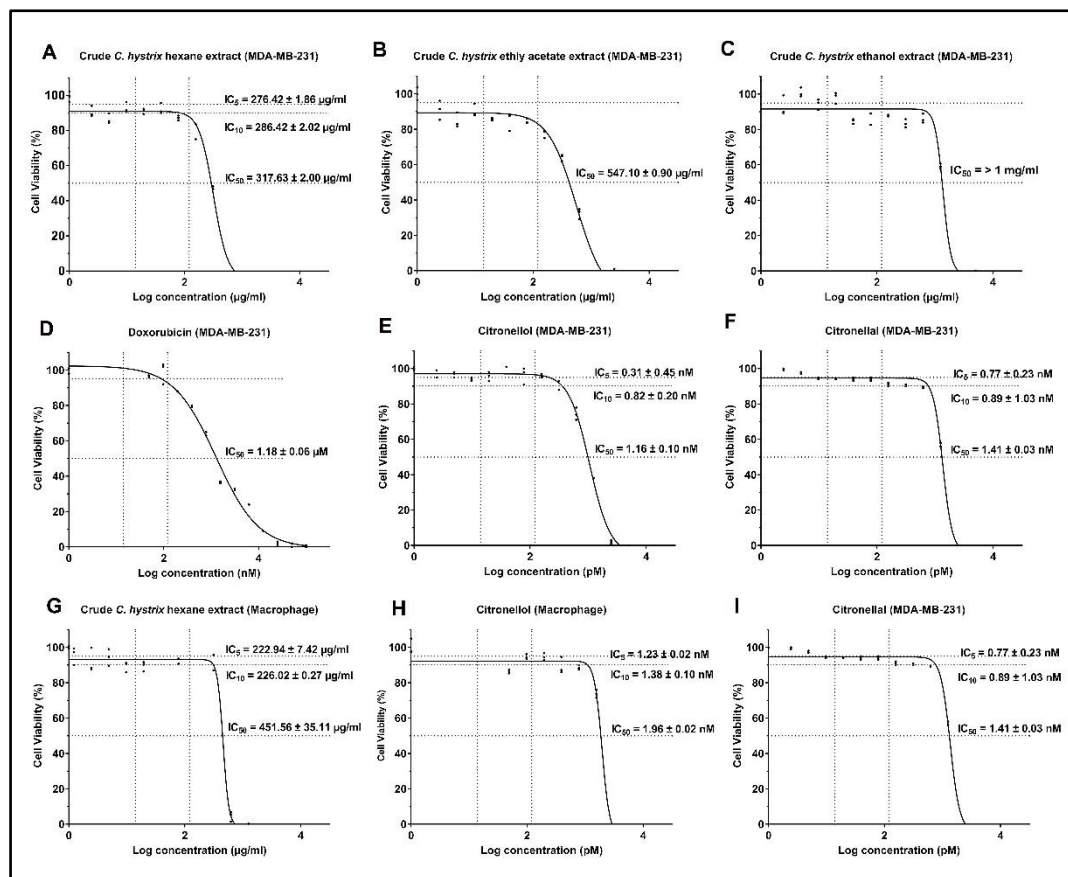


**Figure 29**  $IC_{50}$  value from treatments on MDA-MB-231 cell and primary macrophage

On MDA-MB-231 cells (A) crude hexane, (B) crude ethyl acetate, (C) crude ethanol, (E) citronellol and (F) citronellal and (D) 48 h treatment by doxorubicin, and on primary derived macrophage (G) crude hexane, (H) citronellol and (I) citronellal.

**Table 11 Cytotoxicity of *C. hystrix* crudes extract and its compounds citronellol and citronellal on MDA-MB-231 cell line**

Treatments	MDA-MB-231	Macrophage
	IC <sub>50</sub>	IC <sub>50</sub>
Crude hexane	317.63 ± 2.0 µg/ml	451.56 ± 35.11 µg/ml
Crude ethyl acetate	547.1 ± 0.9 µg/ml	
Crude ethanol	> 1000 µg/ml	
Citronellol	1.16 ± 0.10 nM	1.96 ± 0.02 nM
Citronellal	1.41 ± 0.03 nM	1.81 ± 0.01 nM
Doxorubicin	1.18 ± 0.06 µM	

**Table 12 Comparing IC<sub>50</sub>, IC<sub>10</sub>, IC<sub>5</sub> of crude hexane, citronellol and citronellal on MDA-MB-231 cell and primary macrophage**

Cells		Crude hexane	Citronellol	Citronellal
MDA-MB-231	IC <sub>50</sub>	317.63 ± 2.0 µg/ml	1.16 ± 0.10 nM	1.41 ± 0.03 nM
	IC <sub>10</sub>	286.71 ± 1.55 µg/ml	0.62 ± 0.20 nM	0.95 ± 0.05 nM
	IC <sub>5</sub>	276.89 ± 1.55 µg/ml	0.51 ± 0.20 nM	0.83 ± 0.02 nM
Macrophage	IC <sub>50</sub>	451.56 ± 35.11 µg/ml	1.96 ± 0.02 nM	1.81 ± 0.01 nM
	IC <sub>10</sub>	266.02 ± 0.27 µg/ml	1.38 ± 0.10 nM	1.46 ± 1.13 nM
	IC <sub>5</sub>	222.94 ± 7.42 µg/ml	1.23 ± 0.02 nM	1.36 ± 0.16 nM

### Crude hexane, citronellol and citronellal decreased down MDA-MB-231 cell proliferation rate

The cytotoxicity of crude hexane, citronellol and citronellal on cell proliferation rate of MDA-MB-231 cells were performed by using MTT assay. In non-treated group, cell viability value increased twice at 48 h, which indicated cells significantly increased its proliferation up to 1-fold at 48 h ( $P < 0.05$ ) (**Figure 30**). Contrary, results show all treatments groups (crude hexane, citronellal, citronellol, and doxorubicin) significantly reduced proliferation of MDA-MB-231 cells when compared to non-treated group at each specific incubation time at 24 h and 48 h ( $P < 0.05$ ) in both and time dependent manner (for more detail on statistical comparison value, see **Appendix 23**). Crude *C. hystrix* hexane extract showed much lower  $IC_{50}$  value compared to others.

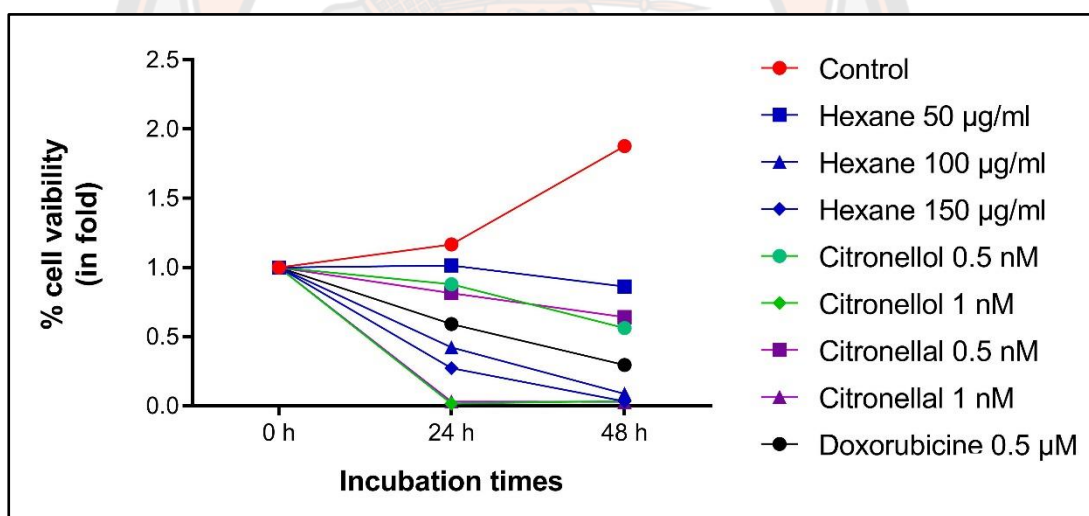
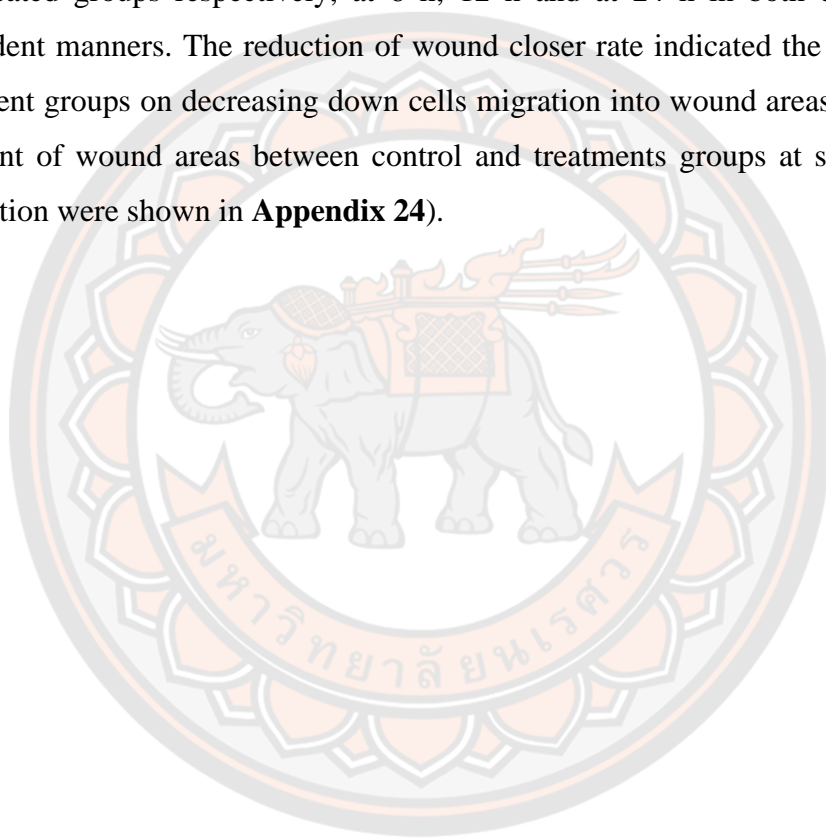


**Figure 30** Inhibition of cell proliferation of crude hexane, citronellol, citronellal on MDA-MB-231 cells.

Doxorubicin was used as positive control. Proliferation of MDA-MB-231 cells was expressed as number of folds. One-way ANOVA with Dunnett's multiple comparisons test was used to analyze the different between control and treatment groups ( $n=3$ ),  $P$  value  $< 0.05$  consider significant.

### ***C. hystrix* hexane extract, citronellol and citronellal inhibited MDA-MB-231 cells migration**

Cells migration is one of the important processes in cancer metastasis. Next, the effect of crude hexane, citronellol and citronellal on cells migration were evaluated by *in vitro* wound scratch migration assay. In the control group, MDA-MB-231 cells migrated to completely close the wound areas at 24 h (**Figure 31 A**). However, wound areas in the treatment groups were much wider when compared to non-treated groups respectively, at 6 h, 12 h and at 24 h in both doses and time dependent manners. The reduction of wound closer rate indicated the efficacy of the treatment groups on decreasing down cells migration into wound areas (the statistical different of wound areas between control and treatments groups at specific time of incubation were shown in **Appendix 24**).



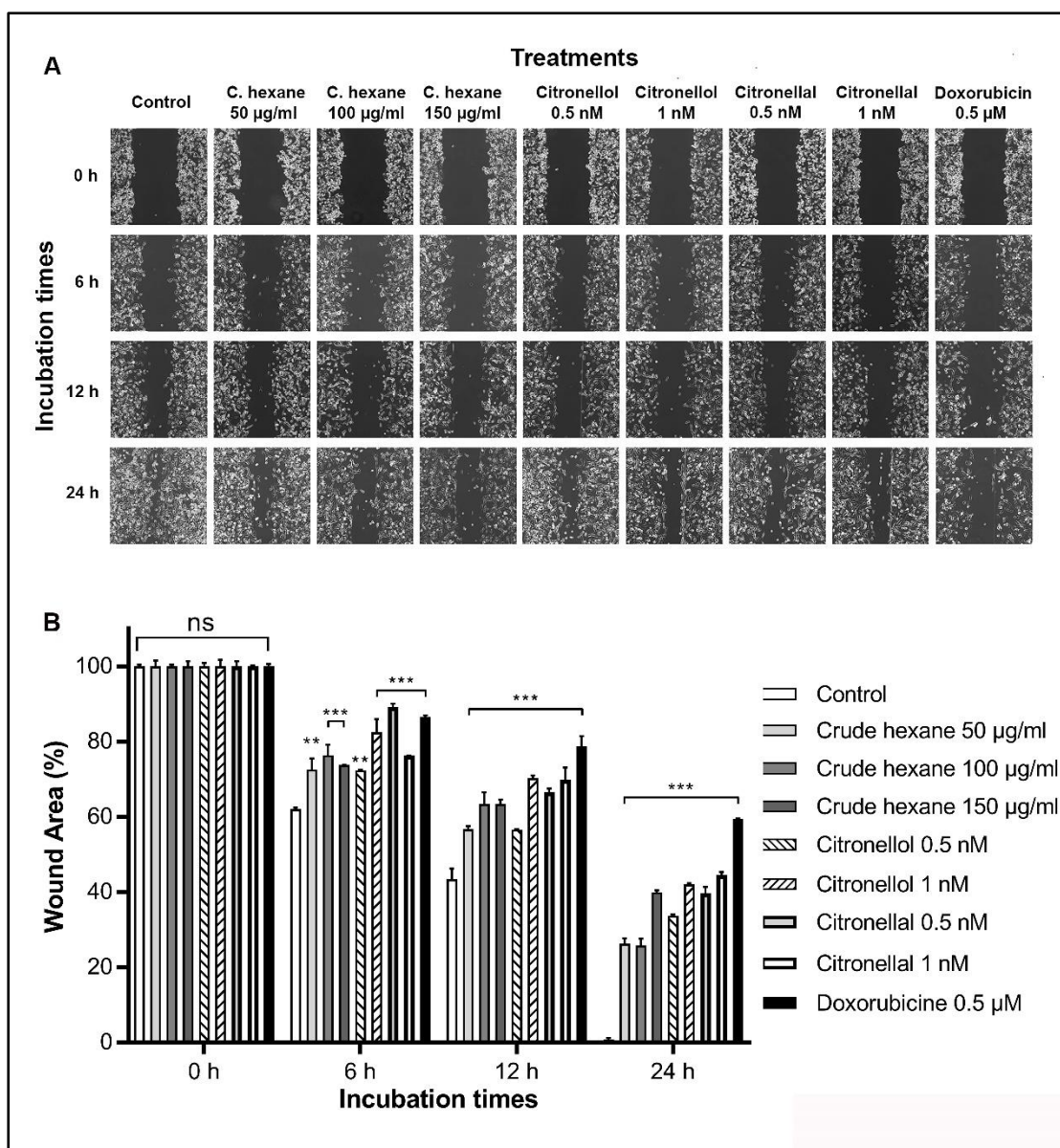
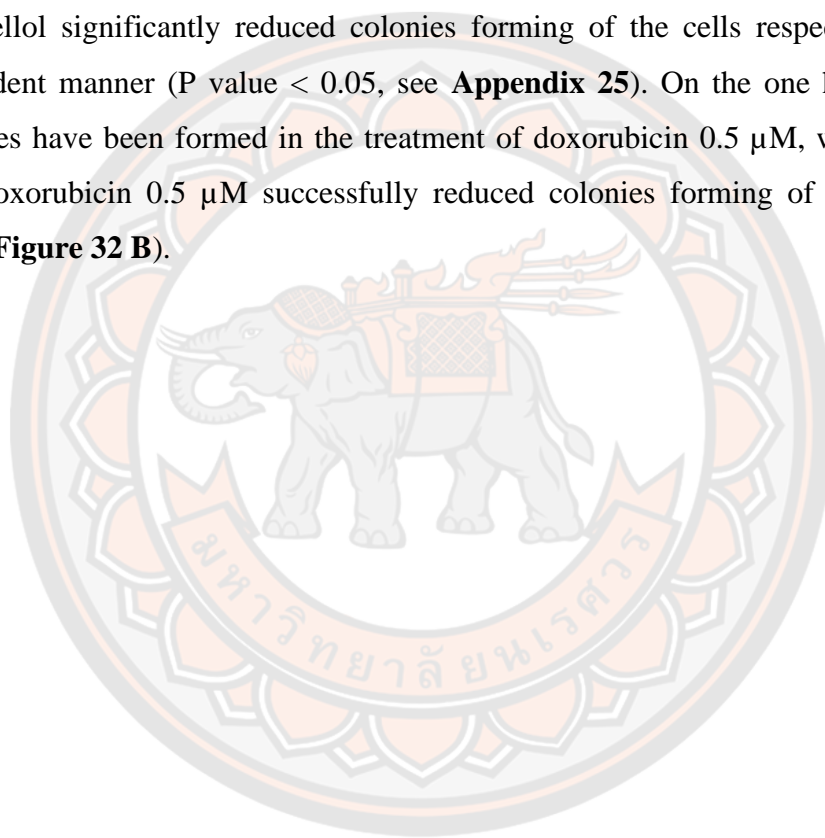


**Figure 31 Wound scratch migration assay.**

MDA-MB-231 cells were scratched at confluence to induce wound areas. Cells were treated by crude hexanes, citronellol, citronellal and doxorubicin, and then were incubated for 24 h. Cells migration into wound areas were observed under microscope at 6 h, 12 h and 24 h. ImageJ 1.52a software was used to analyze cells migration into wound areas. One-way ANOVA with Dunnett's multiple comparisons test was used to analyze the different between control and treatment groups ( $n=3$ ),  $P$  value  $< 0.05$  consider significant (\*\*  $P < 0.01$ , \*\*\*  $P < 0.001$ ).

***C. hystrix* hexane extract, citronellol and citronellal reduced number of colonies forming in MDA-MB-231 cells**

Colony forming assay has been used as a tool to allow us to evaluate cells survival by studying cell grew from a single cell to form colonies in response to toxic substances. Here, the colony forming of MDA-MB-231 cells under treatments by crude hexane, citronellal, citronellol, and doxorubicin as positive control were observed (**Figure 32 A**). In the treatment groups, crude hexane, citronellal and citronellol significantly reduced colonies forming of the cells respectively in dose dependent manner ( $P$  value  $< 0.05$ , see **Appendix 25**). On the one hand, only few colonies have been formed in the treatment of doxorubicin  $0.5 \mu\text{M}$ , which indicated that doxorubicin  $0.5 \mu\text{M}$  successfully reduced colonies forming of MDA-MB-231 cells (**Figure 32 B**).



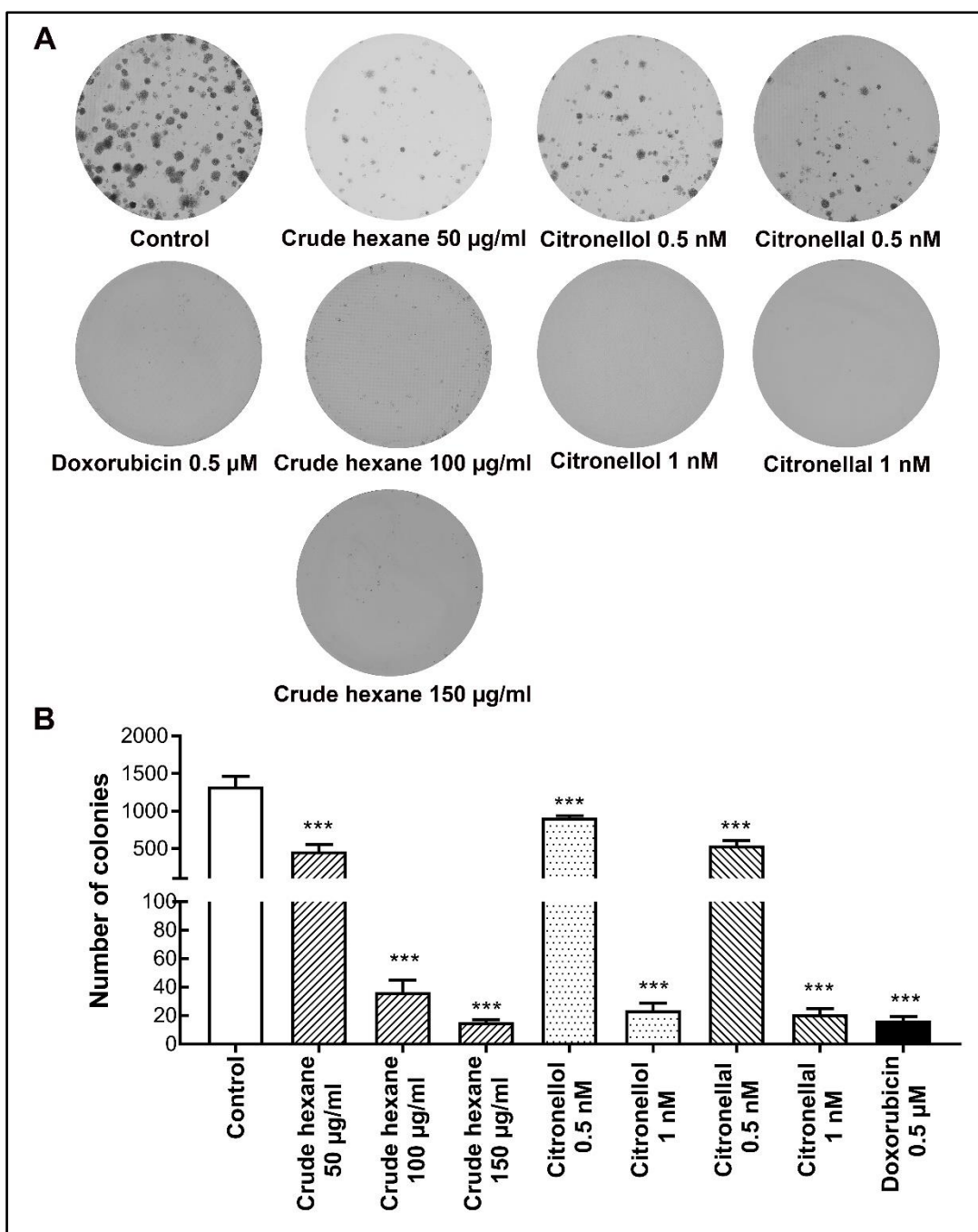


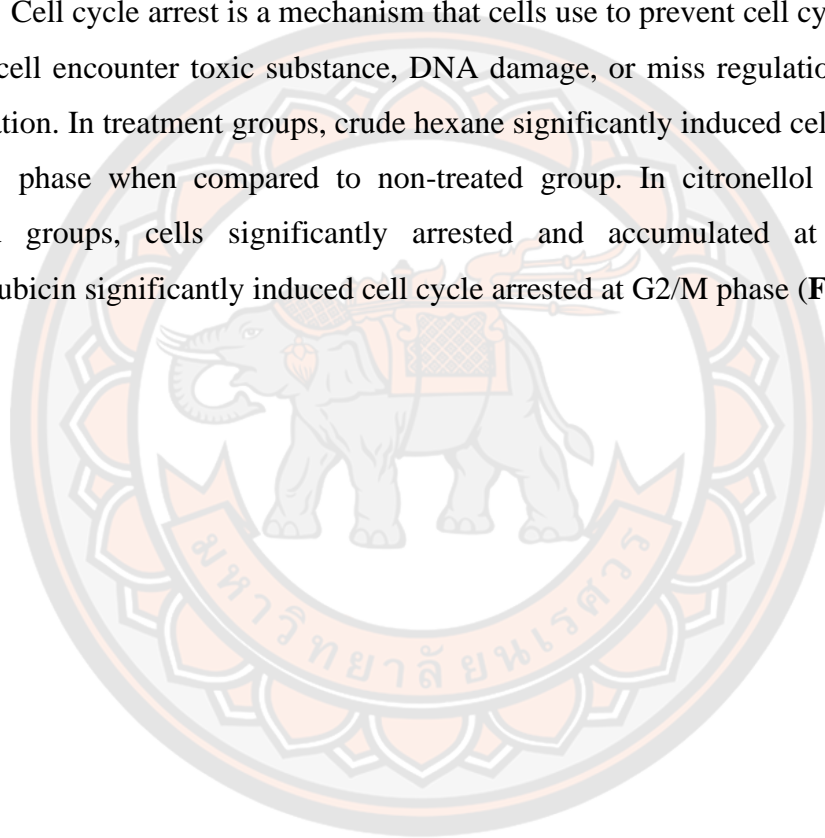
**Figure 32 Clonogenic Assay on MDA-MB-231 cells.**

Colonies forming of MDA-MB-231 cells with 10 days incubation after 24 h treatments with crude hexane, citronellol, citronellal, and doxorubicin. Number of colonies were counted using ImageJ 1.52a software. One-way ANOVA with Dunnett's multiple comparisons test was used to analyze the different between control and treatment groups ( $n=3$ ),  $P$  value  $< 0.05$  consider significant (\*\*\*)  $P < 0.001$ . (A)

colonies picture as 8-bit gray scale images under different treatments, (B) crude hexane (H), citronellol (C.lol), citronellal (C.lal) & doxorubicin (dox).

### **Crude hexane, citronellol and citronellal induced cell cycle arrest in MDA-MB-231 cells**

Cell cycle arrest is a mechanism that cells use to prevent cell cycle progression when cell encounter toxic substance, DNA damage, or miss regulation during DNA replication. In treatment groups, crude hexane significantly induced cell cycle arrest at G0/G1 phase when compared to non-treated group. In citronellol and citronellal treated groups, cells significantly arrested and accumulated at G2/M phase. Doxorubicin significantly induced cell cycle arrested at G2/M phase (**Figure 33**).



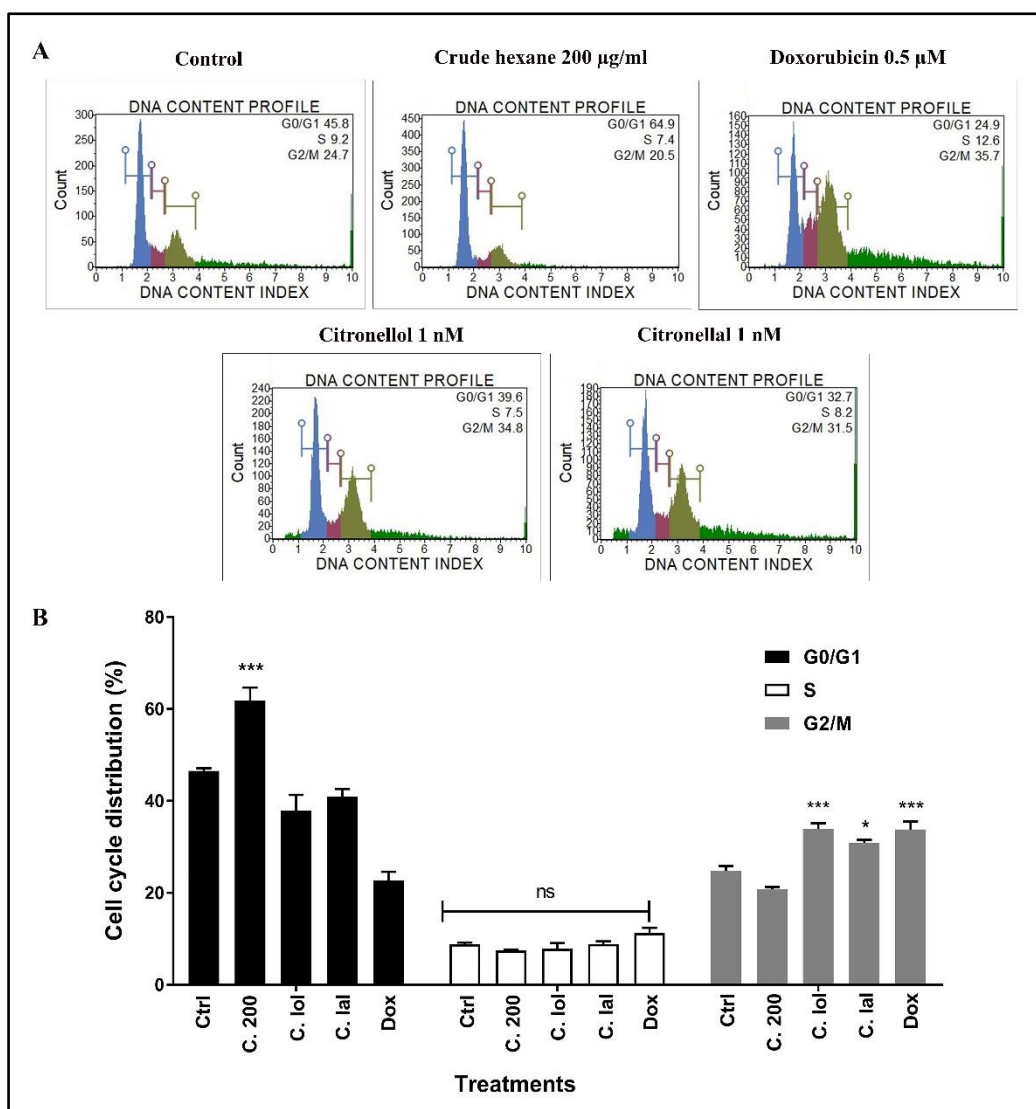


**Figure 33** Comparing effect of crude hexane and crude ethyl acetate by screening on cells apoptosis and cell cycle

(A) Cell cycle arrested induced by treatment groups on MDA-MB-231 cells.  
 (B) One-way ANOVA with Dunnett's multiple comparisons test was used to analyze the different between control and treatment groups ( $n=3$ ),  $P$  value  $< 0.05$  consider significant (\*\*\*)  $P < 0.001$ , \*  $P < 0.05$ ).

### **Crude hexane, citronellol, and citronellal induced apoptosis in MDA-MB-231 cells**

Crude hexane, citronellol, and citronellal slow down cell proliferation rate, reduced cells migration, and reduced number of colonies forming of MDA-MB-231 cells. When cell encounter with toxic substances, they undergone repair mechanism, which reduced their active state. However, when the process cannot be taken, cells undergone cell death program or apoptosis, a phenomenon which appears at the end of cells' life span. Hoechst33342 staining confirmed some morphological change during apoptosis. The non-treated group showed normal nuclear structure of the cells. However, in treatment groups some condense blue fluorescence appeared in the nuclear which indicated chromatin condensation and/or DNA fragmentation in the cells under treatment of crude hexane, citronellol, citronellal, and doxorubicin 0.5  $\mu$ M (**Figure 34 A**). Furthermore, MDA-MB-231 cells undergone apoptosis under treatments of crude hexane, citronellol and citronellal for 24 h were observed by gating on Annexin V and 7-ADD staining (**Figure 34 B**). The results revealed that at dose 200  $\mu$ g/ml crude hexane induced apoptosis in MDA-MB-231 cells to  $11.02 \pm 0.53$  % when compared to control. Similarly, citronellol 1 nM induced apoptosis  $14.30 \pm 0.89$  % in the cells, and  $13.92 \pm 0.31$  % for citronellal at 1 nM. Moreover, doxorubicin 0.5  $\mu$ M induced apoptosis  $19.02 \pm 0.81$  % in the cells.

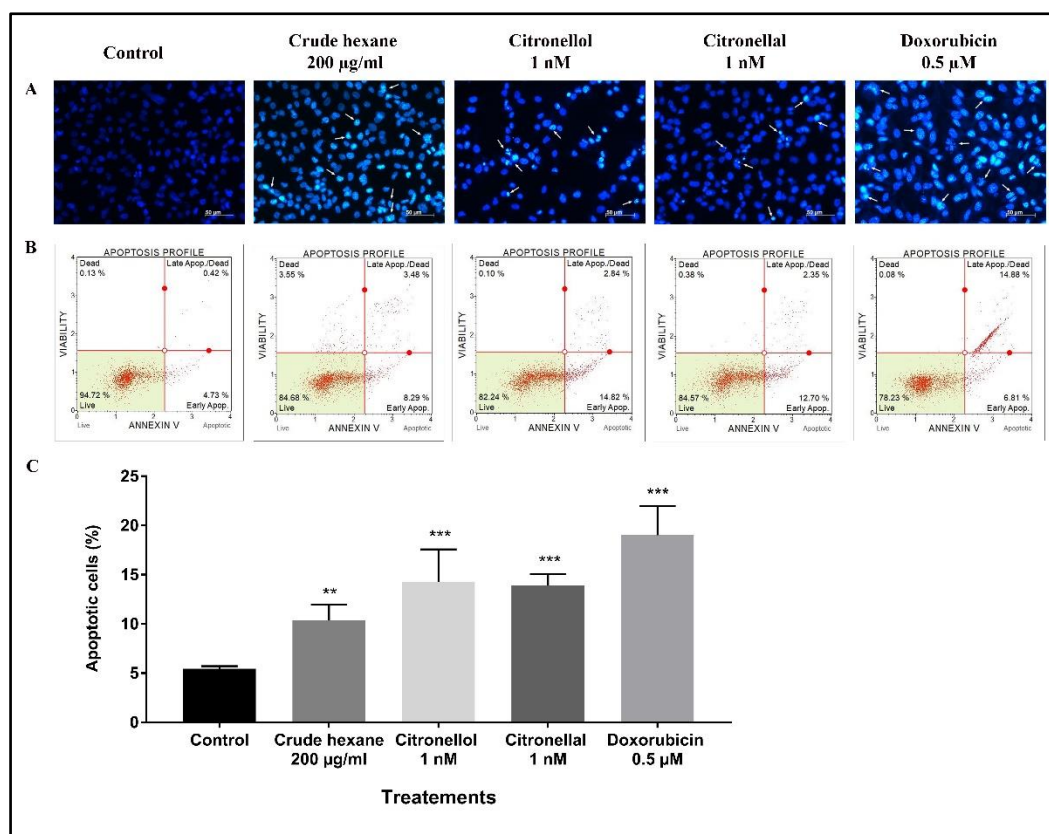


**Figure 34** Flow cytometry and Hoechst33258 staining on MDA-MB-231 cells

(A) Apoptotic cells with Hoechst33258 staining showing chromatin condensation and DNA fragmentation in cells treated with crude hexane 200 µg/ml, citronellol 1 nM, citronellal 1 nM, doxorubicin 0.5 µM. (B) Flow cytometry analysis of apoptotic MDA-MB-231 cells using Annexin-V and P.I staining, 24 h after treating by hexane 200 µg/ml, citronellol 1 nM, citronellal 1 nM, doxorubicin 0.5 µM. (C) One-way ANOVA with Dunnett's multiple comparisons test was used to analyze the different between control and treatment groups (n=3),  $P$  value < 0.05 consider significant (\*\*\*  $P$  < 0.001, \*\*  $P$  < 0.05).

### Crude hexane, citronellol and citronellal modulated apoptosis-related proteins gene expression in MDA-MB-231 cells

To better understand the apoptosis that occur in the cells, level of apoptosis-related proteins genes expression was performed using RT-qPCR. Cells were treated 24 h prior to mRNA extraction. The results showed that expression level of *Bax* gene increased up to 1-fold in the treatment of crude hexane 200  $\mu\text{g/ml}$  ( $P$  value, 0.05), around 1.5-fold in treatment of citronellol or citronellal 1 nM, and around 1.75-fold in doxorubicin 0.5  $\mu\text{M}$  (**Figure 35 A**). On the other hand, the expression level of *Bcl-2* gene was markedly downregulated to almost 0.5-fold in each treated group compared to control ( $P$  value  $< 0.05$ ) (**Figure 35 B**).

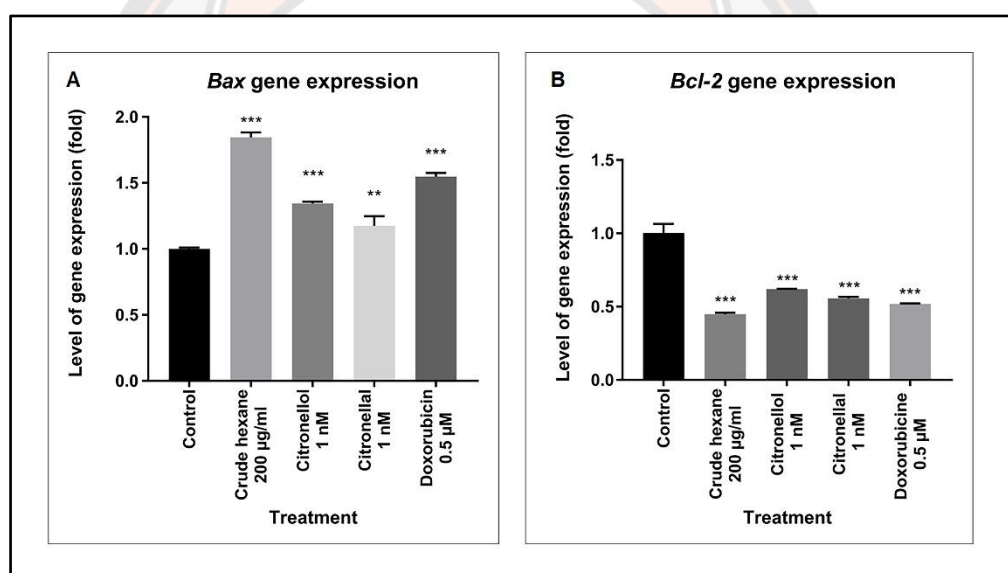


**Figure 35** Alteration apoptosis-related genes expression in treated cells.

(A) *Bax* and (B) *Bcl-2*. Level of protein expression by RT-qPCR after 24h of treatments. One-way ANOVA was used to analyze the different between control group and treatment groups.  $P$  value  $< 0.05$  consider significant (\*\*  $P < 0.01$ , \*\*\*  $P < 0.001$ ).

**Crude hexane, citronellol and citronellal induced apoptosis and DNA fragmentation in the cells by inhibiting the anti-apoptotic Bcl-2 protein and activating caspase dependent apoptotic pathway**

To further confirm the results, another experiment was conducted by measuring protein expression of both Bax and Bcl-2 proteins using Western Blot analysis. Surprisingly, expression of Bcl-2 protein was significantly decreased after treatment of crude hexane 200  $\mu\text{g/ml}$ , citronellol 1 nM, citronellal 1 nM, and doxorubicin 0.5  $\mu\text{M}$  when compared to control group (P value < 0.05) (**Figure 36 A**), while Bax protein expression was upregulated in the same treated groups (**Figure 36 B**). In response to the treatments, cells upregulated of Bax protein expression and downregulated Bcl-2 protein expression. The alteration of Bax/Bcl-2 expression could lead to the activation of Caspase-3 protein, which is an executioner in apoptosis caspase-dependent activation. To confirm this hypothesis, measuring pro-Caspase-3 and cleaved-Caspase-3 protein level was measured by Western blot analysis. The results demonstrated the significantly decrease in intensities of pro-Caspase-3 in treatments groups compared to control (**Figure 36 C**) with the significantly decrease of cleaved-Caspase-3 protein intensity (**Figure 36 D**).

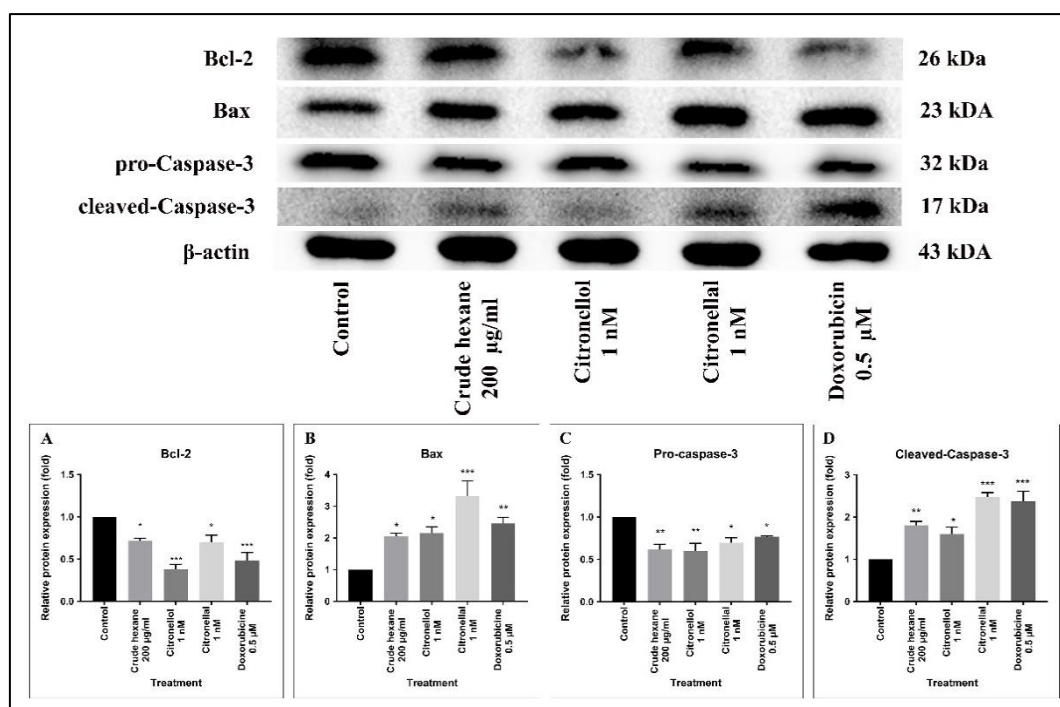


**Figure 36** Crude hexane, citronellol, citronellal induced apoptosis through caspase dependent pathway by inhibiting Bcl-2 protein

(A) Bcl-2 protein, (B) Bax protein, (C) Pro-Caspase-3 protein by Western Blot. One-way ANOVA was used to analyze the different between control group and treatment groups.  $P$  value  $< 0.05$  consider significance (\*  $P < 0.05$ , \*\*  $P < 0.01$ , \*\*\*  $P < 0.001$ ).

## CHAPTER V

### DISCUSSIONS AND CONCLUSIONS

Breast cancer has been reported to have high cancer incident which one of four cancer new cases has been reported with breast cancer in women globally (Cancer, 2018). It was classified into six sub-types reflected by its mRNA expressions and immunohistochemical profiles frequently on hormonal receptors which are progesterone receptor (PR), estrogen receptor (ER), and human epidermal growth factor receptor 2 (Her2) (Eroles et al., 2012). More than that, some of the types like triple-negative breast cancer has been reported with high cancer-relapsing post chemotherapy and poor prognosis due to their highly resistivity and early metastasis in breast cancer patients (Nedeljkovic & Damjanovic, 2019), which has put the treatment for this type of breast cancer into problems (Kim et al., 2018). Furthermore, some of the treatment like hormonal targeted therapy such as anti-PR, anti-ER and anti-Her2 are not applicable to this type of breast cancer due to the lack of these receptors and some of the chemotherapy molecules like cisplatin, taxanes, anthracyclines have been reported resistance with TNBC (Denduluri et al., 2007; Low et al., 2005). Currently, many new compounds that have potential anticancer effect have been identified from medical plants and some like cabazitaxel (a second generation of taxanes derived from *Taxus brevifolia*) and homoharringtonine (an alkaloid derived from *Cephalotaxus harringtonii*) have been approved by FDA (Saklani & Kutty, 2008; Vrignaud et al., 2014). Therefore, the development of anticancer drugs from natural compounds could be the new hope in cancer therapy.

*C. hystrix* is a common tropical plant that have been known for its high aroma and has been used in cuisines, cosmetic, many other fields. Beside these benefits, many researchers have claimed the effect of *C. hystrix* against many cancers in the *in vitro* experiments. It has been reported to exerting cytotoxic effect against four different types of leukemic cell lines (Fah Chueahongthong, 2011), inhibited cell migration in human pancreatic cancer cell line (PANC-1) (S. Sun et al., 2018), and

also has been reported to reduce cell viability of MCF-7 breast cancer cell (Sadasivam et al., 2017). *C. hystrix* has been reported to contain many compounds such as phenolic compounds, flavonoids, terpenoids, alkaloids, coumarins, glycosides, saponins, tanins (Agouillal et al., 2017). Moreover, terpenoids have been reported as the major compound found in *C. hystrix* leaves. Including in that, citronellol and citronellal are two monoterpenoids compounds that found in *C. hystrix* (Warsito et al., 2017). These two compounds have been reported to contain potential effects against many types of cancer such as in liver cancer (Maßberg et al., 2015), in small lung cancer (Song et al., 2015) and in estrogen positive breast cancer (Stone et al., 2013). Then these two molecules were purchased from Sigma Aldrich company to test its effects against the triple negative breast cancer MDA-MB-231 cells. In the experiments, all crude extracts were extracted from *C. hystrix* leaves using the sequential maceration methods by using lower polar solvent to the higher polar solvent (hexane, ethyl acetate and ethanol). Much higher percentage of extraction yield from ethanolic extract was obtained when compared to crude hexane and ethyl acetate. The crude extracts obtained from the extraction and the two standard compounds citronellol and citronellal were then used to test on MDA-MB-231 cells to evaluate their toxicity. The results from MTT assay showing that crude *C. hystrix* hexane extract showed much higher efficiency in reducing MDA-MB-231 cells viability compared to the two other crude extracts, while the two pure compounds showed similar toxicity in reducing MDA-MB-231 cell viability. However on a study, they reported that crude ethyl acetate and crude ethanol showed much higher effect against HeLa cells compared to crude hexane (Wijayanti et al., 2015). Also, the effect of DMSO that would interfere the cytotoxicity of crude extracts was confirmed in which the highest DMSO trace remained in the treatment (2.5%) was not interfered with the results ( $P$  value  $> 0.05$ ). Doxorubicin is an anticancer agent that has been widely used in cancer treatments. It acts as an anti-topoisomerase 2, which prevents DNA from replication. In the experiments,  $IC_{50}$  value of doxorubicin was evaluated by MTT assay and resulted showed the  $IC_{50}$  value around 1  $\mu$ M, which this result was similarly reported in both MDA-MB-231 and MCF-10F cells (Pilco-Ferreto & Calaf, 2016).

After evaluating toxicity of crude extracts, and the two pure compounds against the cancer cells, the screening through chemical profile of crude extracts was performed by first using the thin layer chromatography (TLC). The spots band showed on the silica-based stationary phase indicated much higher chemical compounds traces on the stationary phase when compared to crude ethyl acetate and crude ethanol. Moreover, the RF value of the two standard citronellol and citronellal were similar to those chemical compound traces presented in crude hexane at RF = 0.43 and 0.9 when exposed to anisaldehyde. From these perspective, crude *C. hystrix* hexane extract was selected for further experiment. After that toxicity of crude hexane, citronellol and citronellal against normal cells was tested by using primary macrophage. Then a safer dose below IC<sub>10</sub> on macrophage were selected to further perform experiments on MDA-MB-231 cells (**Appendix 31**). To further analyzed chemical compounds, present in crude hexane GC-MS analysis was conducted. Result indicated that terpenoids were identified as the most abandoned compound that was identified from *C hystrix* leaves, which has been similarly reported in (Dertyasasa & Tunjung, 2017). Also, citronellol and citronellal in crude hexane from the GC-MS spectrum was seen at retention time 10.75 min and 12.85 min.

From the experiments, MDA-MB-231 cells grew in good health that it duplicated its number between around 48 h. By that, the effect of crude hexane, citronellol and citronellal on cells proliferation were testified. The result showed that crude hexane significantly reduced cells growing rate compared to the non-treated group. These anti-proliferative effect of *C. hystrix* was also similarly reported previous studies on leukemic cell lines (Anuchapreeda et al., 2020) and on Hela the cervical cancer cells (Wijayanti et al., 2015). More than that anti-proliferative effect on MDA-MB-231 was also significantly seen under the treatments of both citronellol and citronellal. In previous study, (Maßberg et al., 2015) reported the effect of citronellal in reduce cells proliferation in Huh7 hepatocellular carcinoma, and citronellol inhibited non-small cell lung carcinoma A-549 cells (Song et al., 2015). Then further experiments were performed to help support the result of pre-existing anti-proliferative effect of both crude hexane and the two pure compounds. Clonogenic assay was performed to mimic the actual growth of cancer that grow from

single mutated cells to form cancer cells colonies or tumor mass. In control group, MDA-MB-231 cells grew and formed cells colonies within 15 days of incubation. However, in the treatment groups, crude hexane, citronellol and citronellal significantly reduced number of colonies and even inhibited the colonies forming at the much higher dose. This effect of *C. hystrix* has been mentioned in (S. Sun et al., 2018) that bergamottin, a molecule from *C. hystrix* crude extract has been reported to inhibit colonies forming in PANC-1 human pancreas cancer. In cancer development or metastasis, surviving under tough environment with highly proliferative and migrative abilities are the successful keys in metastasis of the cancer (Marchesi et al., 2004). Therefore, the decrease of these two factors could be a strategy in preventing early metastasis of the cancer. In this regard, wound scratch migration assay was conducted to study the effects of crude hexane, citronellol and citronellal on cells migration. The results indicated that the treatments groups slow down cell migration into wound areas in a dose and time dependent manner. For instance, the anti-migratory effect of *C. hystrix* has also been reported on PANC-1 human pancreas cancer (S. Sun et al., 2018), while the anti-migratory effect of citronellal and citronellol on cancer cells are not likely been reported.

The results above showed the potential anti-cancer effect of *C. hystrix*, citronellol and citronellal by reducing cell proliferation, survival and migration. Many of cancer cells decrease their active state, their proliferation when they encountered with toxic substances or enter apoptosis (Alenzi, 2004). To confirm this hypothesis whether the reduced of cell proliferation, migration and ability to form colonies after treatment were caused by cell apoptosis, the apoptotic cells under treatment of crude hexane, citronellol and citronellal were measured by using flow cytometry. Results from flow cytometry showed significant number of cells arrested at G0/G1 phase. However, *C. hystrix* leaf extract showed different effect on Molt-4 cell line by inducing cell cycle arrested at G2/M phase (Utthawang, 2017). In cells treated with citronellol and citronellal, cells were seen to accumulated at G2/M phase. On the other hand, citronellol was reported to induced the lung cancer NCI-H1299 cell cycle arrested at G0/G1 phase (Yu et al., 2019b). The results from flow cytometry also showed significant number of apoptotic cells under treatments of crude hexane,

citronellol and citronellal. More than that, morphological change like chromatin condensation and swelling were seen under the treatment groups. To help define some support mechanism to cell apoptosis, level of genes and protein that may involve in the apoptosis were analyzed using RT-qPCR and Western Blot analysis. The results proved that level of *Bcl-2* gene and protein expression decreased under the treatment group while *Bax* gene and protein expression increased its intensity. During apoptosis, cleavage of DNA by endonuclease occur after the activation of Caspase-3 (Alenzi, 2004). From Western Blot analysis, the results clearly demonstrated the activation of Caspase-3 through the decreasing density of total Caspase-3 in the treated groups compare to control, and the increasing intensity of cleaved-Caspase-3 protein, which indicated the activation of caspase dependent apoptosis pathway. The induction of apoptosis in MDA-MB-231 by the treated groups was likely activated through the Caspase-dependent apoptosis pathway through the inhibition of anti-apoptotic protein Bcl-2, which led to increase of pro-apoptotic Bax protein activity. Bax mediated the pore formation complex at the outer membrane of mitochondria, and consequentially trigger the release of Cytochrome C, leading to the activation of Caspase 3 protein. The effect of doxorubicin inducing apoptosis through the Caspase-dependent apoptosis pathway has also been similarly reported in previous study by (Pilco-Ferreto & Calaf, 2016). In the previous study, bergamottin which is a compound identified in *C. hystrix*, induced apoptosis in human pancreas cancer cells PANC-1 by inhibiting Akt/mTOR signaling pathway leading to the inhibition on cells survival, proliferation and migration (S. Sun et al., 2018).

In summary, the results demonstrated that crude *C. hystrix* hexane extract and its compounds citronellal and citronellol induced apoptosis in triple negative breast cancer MDA-MB-231 cell line through the inhibition of anti-apoptotic protein Bcl-2, which led to the activation of pro-apoptotic Bax protein, and may induced the downstream caspase dependent apoptosis pathway by activating Caspase-3 protein. The encountered of cells to crude hexane, citronellol, and citronellal downregulated cells active state, which decreased down their proliferation rate, ability to migrate and survive under rough environment. However, more mechanism should be performed to better understand the mechanism behind the cell cycle arrest, reduce of cell migration.

Moreover, animal models should be launched as experiment as the further drug development of these molecules.

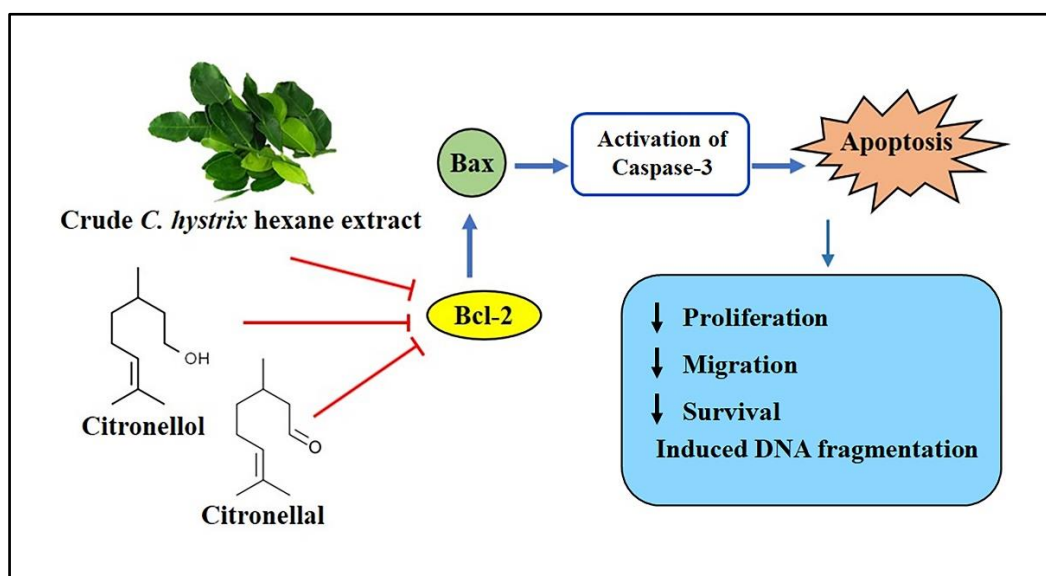


**Figure 37** Inhibition of Bcl-2 protein in MDA-MB-231 cells by *C. hystrix*, citronellal and citronellol leading to the activation of caspase dependent apoptotic pathway.

## REFERENCES

- Abad, A., López-Pérez, J. L., del Olmo, E., García-Fernández, L. F., Francesch, A., Trigili, C., Barasoain, I., Andreu, J. M., Díaz, J. F., & San Feliciano, A. (2012). Synthesis and Antimitotic and Tubulin Interaction Profiles of Novel Pinacol Derivatives of Podophyllotoxins. *Journal of Medicinal Chemistry*, *55*(15), 6724-6737. doi: 10.1021/jm2017573
- Abirami, A., Nagarani, G., & Siddhuraju, P. (2015). Hepatoprotective effect of leaf extracts from *Citrus hystrix* and *C. maxima* against paracetamol induced liver injury in rats. *Food Science and Human Wellness*, *4*(1), 35-41. doi: <https://doi.org/10.1016/j.fshw.2015.02.002>
- Adams, J. M., & Cory, S. (2007). Bcl-2-regulated apoptosis: mechanism and therapeutic potential. *Current opinion in immunology*, *19*(5), 488-496. doi: 10.1016/j.coi.2007.05.004
- Agouillal, F., M. Taher, Z., Moghrani, H., Nasrallah, N., & El Enshasy, H. (2017). A Review of Genetic Taxonomy, Biomolecules Chemistry and Bioactivities of *Citrus hystrix* DC. *Biosciences, Biotechnology Research Asia*, *14*(1), 285-305. doi: 10.13005/bbra/2446
- Ahmad, D., Abulkhair, O., Nemenqani, D., & Tamimi, W. (2012). *Antiproliferative Properties of Methanolic Extract of Nigella sativa against the MDA-MB-231 Cancer Cell Line* (Vol. 13).
- Alberg, A. J., & Singh, S. (2001). Epidemiology of Breast Cancer in Older Women. *Drugs & Aging*, *18*(10), 761-772. doi: 10.2165/00002512-200118100-00005
- Alenzi, F. (2004). Links between apoptosis, proliferation and the cell cycle. *British journal of biomedical science*, *61*, 99-102. doi: 10.1080/09674845.2004.11732652
- Amin, A., Gali-Muhtasib, H., Ocker, M., & Schneider-Stock, R. (2009). Overview of major classes of plant-derived anticancer drugs. *International journal of biomedical science : IJBS*, *5*(1), 1-11.
- Anuchapreeda, S., Chueahongthong, F., Viriyaadhammaa, N., Panyajai, P., Anzawa, R., Tima, S., Ampasavate, C., Saijai, A., Rungrojsakul, M., Usuki, T., & Okonogi, S. (2020). Antileukemic Cell Proliferation of Active Compounds from Kaffir Lime (*Citrus hystrix*) Leaves. *Molecules (Basel, Switzerland)*, *25*(6), 1300. doi: 10.3390/molecules25061300
- Avendaño, C., & Menéndez, J. C. (2015). Chapter 9 - Anticancer Drugs Targeting Tubulin and Microtubules. In C. Avendaño & J. C. Menéndez (Eds.), *Medicinal Chemistry of Anticancer Drugs (Second Edition)* (pp. 359-390). Boston: Elsevier.
- Aysola, K., Desai, A., Welch, C., Xu, J., Qin, Y., Reddy, V., Matthews, R., Owens, C., Okoli, J., Beech, D. J., Piyathilake, C. J., Reddy, S. P., & Rao, V. N. (2013). Triple Negative Breast Cancer - An Overview. *Hereditary genetics : current research*, *2013*(Suppl 2), 001. doi: 10.4172/2161-1041.S2-001
- Babushok, V. I., Linstrom, P. J., Reed, J. J., Zenkevich, I. G., Brown, R. L., Mallard, W. G., & Stein, S. E. (2007). Development of a database of gas chromatographic retention properties of organic compounds. *Journal of Chromatography A*, *1157*(1), 414-421. doi: <https://doi.org/10.1016/j.chroma.2007.05.044>
- Barros, L. A., Yamanaka, A. R., Silva, L. E., Vanzeler, M. L. A., Braum, D. T., &

- Bonaldo, J. (2009). In vitro larvicidal activity of geraniol and citronellal against *Contraecum* sp (Nematoda: Anisakidae). *Brazilian journal of medical and biological research = Revista brasileira de pesquisas médicas e biológicas / Sociedade Brasileira de Biofísica ... [et al.]*, 42, 918-920. doi: 10.1590/S0100-879X2009005000023
- Besson, A., Dowdy, S. F., & Roberts, J. M. (2008). CDK Inhibitors: Cell Cycle Regulators and Beyond. *Developmental Cell*, 14(2), 159-169. doi: <https://doi.org/10.1016/j.devcel.2008.01.013>
- Birjandian, E., Motamed, N., & Yassa, N. (2018). Crude Methanol Extract of *Echinophora Platyloba* Induces Apoptosis and Cell Cycle Arrest at S-Phase in Human Breast Cancer Cells. *Iranian journal of pharmaceutical research : IJPR*, 17(1), 307-316.
- Blajeski, A. L., Phan, V. A., Kottke, T. J., & Kaufmann, S. H. (2002). G(1) and G(2) cell-cycle arrest following microtubule depolymerization in human breast cancer cells. *The Journal of clinical investigation*, 110(1), 91-99. doi: 10.1172/JCI13275
- Bodicoat, D. H., Schoemaker, M. J., Jones, M. E., McFadden, E., Griffin, J., Ashworth, A., & Swerdlow, A. J. (2014). Timing of pubertal stages and breast cancer risk: the Breakthrough Generations Study. *Breast cancer research : BCR*, 16(1), R18-R18. doi: 10.1186/bcr3613
- Borusiewicz, M., Trojanowska, D., Paluchowska, P., Janeczko, Z., W. Petitjean, M., & Budak, A. (2017). Cytostatic, cytotoxic, and antibacterial activities of essential oil isolated from *Citrus hystrix*. *ScienceAsia*, 43(2), 96. doi: 10.2306/scienceasia1513-1874.2017.43.096
- Bracken, A. P., Ciro, M., Cocito, A., & Helin, K. (2004). E2F target genes: unraveling the biology. *Trends in Biochemical Sciences*, 29(8), 409-417. doi: <https://doi.org/10.1016/j.tibs.2004.06.006>
- Brewer, H. R., Jones, M. E., Schoemaker, M. J., Ashworth, A., & Swerdlow, A. J. (2017). Family history and risk of breast cancer: an analysis accounting for family structure. *Breast cancer research and treatment*, 165(1), 193-200. doi: 10.1007/s10549-017-4325-2
- Butryee, C., Sungpuag, P., & Chitchumroonchokchai, C. (2009). Effect of processing on the flavonoid content and antioxidant capacity of *Citrus hystrix* leaf. *International Journal of Food Sciences and Nutrition*, 60(sup2), 162-174. doi: 10.1080/09637480903018816
- Cancer, T. I. A. f. R. o. (2018). *Latest global cancer data: Cancer burden rises to 18.1 million new cases and 9.6 million cancer deaths in 2018* [Press release]
- Chang, D., Xu, N., & Luo, K. (2003). Chang DC, Xu N, Luo KQ.. Degradation of cyclin B is required for the onset of anaphase in Mammalian cells. *J Biol Chem* 278: 37865-37873. *The Journal of biological chemistry*, 278, 37865-37873. doi: 10.1074/jbc.M306376200
- Chen, X., Dang, T.-T. T., & Facchini, P. J. (2015). Noscapine comes of age. *Phytochemistry*, 111, 7-13. doi: <https://doi.org/10.1016/j.phytochem.2014.09.008>
- Chueahongthong, F., Ampasavate, C., Okonogi, S., Tima, S., & Anuchapreeda, S. (2011). Cytotoxic effects of crude kaffir lime (*Citrus Hystrix*, DC.) leaf fractional extracts on leukemic cell lines. *J Med Plants Res*, 5, 3097-3105.

- Collaborative Group on Hormonal Factors in Breast, C. (2012). Menarche, menopause, and breast cancer risk: individual participant meta-analysis, including 118 964 women with breast cancer from 117 epidemiological studies. *The Lancet. Oncology*, 13(11), 1141-1151. doi: 10.1016/S1470-2045(12)70425-4
- Connell-Crowley, L., Harper, J. W., & Goodrich, D. W. (1997). Cyclin D1/Cdk4 regulates retinoblastoma protein-mediated cell cycle arrest by site-specific phosphorylation. *Molecular biology of the cell*, 8(2), 287-301. doi: 10.1091/mbc.8.2.287
- Cooper, G. M., & Hausman, R. E. (2007). Chapter 16: The Cell Cycle In G. M. Cooper & R. E. Hausman. (Eds.), *The Cell: A Molecular Approach* (4th ed., pp. 649-688). U.S.A: Library of Congress Cataloging-in-Publication Data
- Cornblatt, B. S., Ye, L., Dinkova-Kostova, A. T., Erb, M., Fahey, J. W., Singh, N. K., Chen, M.-S. A., Stierer, T., Garrett-Mayer, E., Argani, P., Davidson, N. E., Talalay, P., Kensler, T. W., & Visvanathan, K. (2007). Preclinical and clinical evaluation of sulforaphane for chemoprevention in the breast. *Carcinogenesis*, 28(7), 1485-1490. doi: 10.1093/carcin/bgm049
- Corp, G. H. B.-S. (2011). *Western Blotting Principles and Methods*. Björkgatan 30 751 84 Uppsala Sweden: GE Healthcare Bio-Sciences AB
- Dai, H., Ding, H., Meng, X. W., Lee, S.-H., Schneider, P. A., & Kaufmann, S. H. (2013). Contribution of Bcl-2 Phosphorylation to Bak Binding and Drug Resistance. *Cancer Research*, 73(23), 6998. doi: 10.1158/0008-5472.CAN-13-0940
- Demidenko, Z. N., Kalurupalle, S., Hanko, C., Lim, C. u., Broude, E., & Blagosklonny, M. V. (2008). Mechanism of G1-like arrest by low concentrations of paclitaxel: next cell cycle p53-dependent arrest with sub G1 DNA content mediated by prolonged mitosis. *Oncogene*, 27, 4402. doi: 10.1038/onc.2008.82
- Denduluri, N., Low, J., Lee, J., Berman, A., Walshe, J., Vatas, U., Chow, C., Steinberg, S., Yang, S., & Swain, S. (2007). Phase II Trial of Ixabepilone, an Epothilone B Analog, in Patients With Metastatic Breast Cancer Previously Untreated With Taxanes. *Journal of clinical oncology : official journal of the American Society of Clinical Oncology*, 25, 3421-3427. doi: 10.1200/JCO.2006.10.0784
- Dertyasasa, E., & Tunjung, W. (2017). Volatile Organic Compounds of Kaffir Lime (*Citrus hystrix* DC.) Leaves Fractions and their Potency as Traditional Medicine. *Biosciences, Biotechnology Research Asia*, 14, 1235-1250. doi: 10.13005/bbra/2566
- Dhippayom, T., Kongkaew, C., Chaiyakunapruk, N., Dilokthornsakul, P., Sruamsiri, R., Saokaew, S., & Chuthaputti, A. (2015). Clinical Effects of Thai Herbal Compress: A Systematic Review and Meta-Analysis. *Evidence-Based Complementary and Alternative Medicine*, 2015, 14. doi: 10.1155/2015/942378
- Dilla Dertyasasa, E., & Anindito Sri Tunjung, W. (2017). Volatile Organic Compounds of Kaffir Lime (*Citrus hystrix* DC.) Leaves Fractions and their Potency as Traditional Medicine. *Biosciences, Biotechnology Research Asia*, 14(4), 1235-1250. doi: 10.13005/bbra/2566
- Donzelli, M., & Draetta, G. F. (2003). Regulating mammalian checkpoints through Cdc25 inactivation. *EMBO reports*, 4(7), 671-677. doi: 10.1038/sj.embor.embor887
- Dorr, R. T., Dvorakova, K., Snead, K., Alberts, D. S., Salmon, S. E., & Pettit, G. R.

- (1996). Antitumor activity of combretastatin-A4 phosphate, a natural product tubulin inhibitor. *Investigational New Drugs*, 14(2), 131-137. doi: <https://doi.org/10.1007/BF00210783>
- Du, G.-J., Zhang, Z., Wen, X.-D., Yu, C., Calway, T., Yuan, C.-S., & Wang, C.-Z. (2012). Epigallocatechin Gallate (EGCG) is the most effective cancer chemopreventive polyphenol in green tea. *Nutrients*, 4(11), 1679-1691. doi: 10.3390/nu4111679
- El-Deiry, W. S., Tokino, T., Velculescu, V. E., Levy, D. B., Parsons, R., Trent, J. M., Lin, D., Mercer, W. E., Kinzler, K. W., & Vogelstein, B. (1993). WAF1, a potential mediator of p53 tumor suppression. *Cell*, 75(4), 817-825. doi: [https://doi.org/10.1016/0092-8674\(93\)90500-P](https://doi.org/10.1016/0092-8674(93)90500-P)
- Eroles, P., Bosch, A., Perez-Fidalgo, J. A., & Lluch, A. (2012). Molecular biology in breast cancer: intrinsic subtypes and signaling pathways. *Cancer Treat Rev*, 38(6), 698-707. doi: 10.1016/j.ctrv.2011.11.005
- Fah Chueahongthong, C. A., Siriporn Okonogi, Singkome Tima and Songyot Anuchapreeda. (2011). Cytotoxic effects of crude kaffir lime (*Citrus hystrix*, DC.) leaf fractional extracts on leukemic cell lines. *Journal of Medical Plants Research*, 15, 3097-3105.
- Favaloro, B., Allocati, N., Graziano, V., Di Ilio, C., & De Laurenzi, V. (2012). Role of apoptosis in disease. *Aging*, 4(5), 330-349. doi: 10.18632/aging.100459
- Franken, N. A. P., Rodermond, H. M., Stap, J., Haveman, J., & van Bree, C. (2006). Clonogenic assay of cells in vitro. *Nature Protocols*, 1(5), 2315-2319. doi: 10.1038/nprot.2006.339
- Gabriel N. Hortobagyi, J. L. C., Carl J. D'Orsi, Stephen B. Edge, Elizabeth A. Mittendorf, Hope S. Rugo, Lawrence J. Solin, Donald L. Weaver, David J. Winchester, and Armando Giuliano, & (2017). Breast. In M. Mahul B. Amin, FCAP (Ed.), *AJCC Cancer Staging Manual* (8th ed., pp. 589-613). American College of Surgeons, 633 N Saint Clair St, Chicago, IL 60611-3211 USA Springer International Publishing.
- Golestani Eimani, B., Sanati, M. H., Houshmand, M., Ataei, M., Akbarian, F., & Shakhssalim, N. (2014). Expression and prognostic significance of bcl-2 and bax in the progression and clinical outcome of transitional bladder cell carcinoma. *Cell journal*, 15(4), 356-363.
- Hammond, M. E. H., Hayes, D. F., Dowsett, M., Allred, D. C., Hagerty, K. L., Badve, S., et al. (2010). American Society of Clinical Oncology/College of American Pathologists Guideline Recommendations for Immunohistochemical Testing of Estrogen and Progesterone Receptors in Breast Cancer (Unabridged Version). *Archives of Pathology & Laboratory Medicine*, 134(7), e48-e72. doi: 10.1043/1543-2165-134.7.e48
- Hande, K. R. (2008). Topoisomerase II inhibitors. *Update on Cancer Therapeutics*, 3(1), 13-26. doi: <https://doi.org/10.1016/j.uct.2008.02.001>
- Hollville, E., & Martin, S. J. (2016). Measuring Apoptosis by Microscopy and Flow Cytometry. *Current Protocols in Immunology*, 112(1), 14.38.11-14.38.24. doi: 10.1002/0471142735.im1438s112
- Hutadilok-Towatana, N., Chaiyamutti, P., Panthong, K., Mahabusarakam, W., & Rukachaisirikul, V. (2006). Antioxidative and Free Radical Scavenging Activities of Some Plants Used in Thai Folk Medicine. *Pharmaceutical Biology*,

- 44(3), 221-228. doi: 10.1080/13880200600685592
- Jauhari, S., Singh, S., & Dash, A. K. (2009). Chapter 7 - Paclitaxel. In H. G. Brittain (Ed.), *Profiles of Drug Substances, Excipients and Related Methodology* (Vol. 34, pp. 299-344): Academic Press.
- Jonkman, J. E. N., Cathcart, J. A., Xu, F., Bartolini, M. E., Amon, J. E., Stevens, K. M., & Colarusso, P. (2014). An introduction to the wound healing assay using live-cell microscopy. *Cell adhesion & migration*, 8(5), 440-451. doi: 10.4161/cam.36224
- Karna, P., Sharp, S. M., Yates, C., Prakash, S., & Aneja, R. (2009). EM011 activates a survivin-dependent apoptotic program in human non-small cell lung cancer cells. *Molecular cancer*, 8, 93-93. doi: 10.1186/1476-4598-8-93
- Kaur, M., Mandair, R., Agarwal, R., & Agarwal, C. (2008). Grape seed extract induces cell cycle arrest and apoptosis in human colon carcinoma cells. *Nutrition and cancer*, 60 Suppl 1(Suppl 1), 2-11. doi: 10.1080/01635580802381295
- Khan, S. A., Tyagi, M., Sharma, A. K., Barreto, S. G., Sirohi, B., Ramadwar, M., Shrikhande, S. V., & Gupta, S. (2014). Cell-type specificity of  $\beta$ -actin expression and its clinicopathological correlation in gastric adenocarcinoma. *World journal of gastroenterology*, 20(34), 12202-12211. doi: 10.3748/wjg.v20.i34.12202
- Khor Goot Heah, N. R. B. M. S., Nurul Ain Bt Khoruddin, Syairah Nabila Bt Suhaimi, Yusmiadil Putera B. Mohd Yusof and Tang Thean Hock. (2017). A Review on Di Methyl Thiazoldiphenyl-Tetrazoliumbromide (MTT) Assay in Cell Viability. *Research Journal of Applied Sciences*, 12(7), 372-378. doi: 10.36478/rjasci.2017.372.378
- Kim, C., Gao, R., Sei, E., Brandt, R., Hartman, J., Hatschek, T., Crosetto, N., Foukakis, T., & Navin, N. E. (2018). Chemoresistance Evolution in Triple-Negative Breast Cancer Delineated by Single-Cell Sequencing. *Cell*, 173(4), 879-893.e813. doi: 10.1016/j.cell.2018.03.041
- Kooltheat, N., Kamuthachad, L., Anthapanya, M., Samakchan, N., Sranujit, R. P., Potup, P., Ferrante, A., & Usuwanthim, K. (2016). Kaffir lime leaves extract inhibits biofilm formation by *Streptococcus mutans*. *Nutrition*, 32(4), 486-490. doi: <https://doi.org/10.1016/j.nut.2015.10.010>
- Korsmeyer, S. J., Wei, M. C., Saito, M., Weiler, S., Oh, K. J., & Schlesinger, P. H. (2000). Pro-apoptotic cascade activates BID, which oligomerizes BAK or BAX into pores that result in the release of cytochrome c. *Cell Death & Differentiation*, 7(12), 1166-1173. doi: 10.1038/sj.cdd.4400783
- Krenn, V., & Musacchio, A. (2015). The Aurora B Kinase in Chromosome Bi-Orientation and Spindle Checkpoint Signaling. *Frontiers in oncology*, 5, 225-225. doi: 10.3389/fonc.2015.00225
- Krishna, R., & Mayer, L. D. (2000). Multidrug resistance (MDR) in cancer: Mechanisms, reversal using modulators of MDR and the role of MDR modulators in influencing the pharmacokinetics of anticancer drugs. *European Journal of Pharmaceutical Sciences*, 11(4), 265-283. doi: [https://doi.org/10.1016/S0928-0987\(00\)00114-7](https://doi.org/10.1016/S0928-0987(00)00114-7)
- Kumar, S., Sharma, V. K., Yadav, S., & Dey, S. (2017). Antiproliferative and apoptotic effects of black turtle bean extracts on human breast cancer cell line through extrinsic and intrinsic pathway. *Chemistry Central Journal*, 11(1), 56. doi:

- 10.1186/s13065-017-0281-5
- Lane, D. P. (1992). p53, guardian of the genome. *Nature*, 358(6381), 15-16. doi: 10.1038/358015a0
- Lavrik, I., Golks, A., & Kramer, P. H. (2005). Death receptor signaling. *Journal of Cell Science*, 118(2), 265. doi: 10.1242/jcs.01610
- Lehmann, B. D., Bauer, J. A., Chen, X., Sanders, M. E., Chakravarthy, A. B., Shyr, Y., & Pietenpol, J. A. (2011). Identification of human triple-negative breast cancer subtypes and preclinical models for selection of targeted therapies. *J Clin Invest*, 121(7), 2750-2767. doi: 10.1172/JCI45014
- Linstrom, P., & Mallard, G. (2001). The NIST Chemistry WebBook: A chemical data resource on the Internet. *Journal of Chemical and Engineering Data - J CHEM ENG DATA*, 46. doi: 10.1021/je000236i
- Liu, X., Li, P., Widlak, P., Zou, H., Luo, X., Garrard, W. T., & Wang, X. (1998). The 40-kDa subunit of DNA fragmentation factor induces DNA fragmentation and chromatin condensation during apoptosis. *Proceedings of the National Academy of Sciences*, 95(15), 8461. doi: 10.1073/pnas.95.15.8461
- Liu, X., Zou, H., Slaughter, C., & Wang, X. (1997). DFF, a Heterodimeric Protein That Functions Downstream of Caspase-3 to Trigger DNA Fragmentation during Apoptosis. *Cell*, 89(2), 175-184. doi: https://doi.org/10.1016/S0092-8674(00)80197-X
- Liu, X. S., Zou, H., Widlak, P., Wt, G., & Wang, X. D. (1999). Activation of the apoptotic endonuclease DFF40 (caspase-activated DNase or nuclease). Oligomerization and direct interaction with histone H1. *The Journal of biological chemistry*, 274, 13836-13840. doi: 10.1074/jbc.274.20.13836
- Loane, D. J., Stoica, B. A., & Faden, A. I. (2015). Chapter 22 - Neuroprotection for traumatic brain injury. In J. Grafman & A. M. Salazar (Eds.), *Handbook of Clinical Neurology* (Vol. 127, pp. 343-366): Elsevier.
- Lopez-Romero, J. C., González-Ríos, H., Borges, A., & Simões, M. (2015). Antibacterial Effects and Mode of Action of Selected Essential Oils Components against *Escherichia coli* and *Staphylococcus aureus*. *Evidence-based complementary and alternative medicine : eCAM*, 2015, 795435-795435. doi: 10.1155/2015/795435
- Low, J., Wedam, S., Lee, J., Berman, A., Brufsky, A., Yang, S., Poruchynsky, M., Steinberg, S., Mannan, N., Fojo, T., & Swain, S. (2005). Phase II Clinical Trial of Ixabepilone (BMS-247550), an Epothilone B Analog, in Metastatic and Locally Advanced Breast Cancer. *Journal of clinical oncology : official journal of the American Society of Clinical Oncology*, 23, 2726-2734. doi: 10.1200/JCO.2005.10.024
- Maisonneuve, P. (2017). Epidemiology, Lifestyle, and Environmental Factors. In U. Veronesi & A. Goldhirsch (Eds.), *Breast Cancer* (pp. 62 - 72). Gewerbestrasse 11, 6330 Cham, Switzerland: Springer Nature
- MAMUR, S. (2019). Investigation of Cytotoxic Effect of Monoterpenes Beta-Citronellol and (-)-Menthone in Human Breast Cancer (MCF-7) Cell Line. *Adnan Menderes Üniversitesi Sağlık Bilimleri Fakültesi Dergisi*, 3(2), 111-119.
- Marchesi, F., Monti, P., Leone, B., Zerbi, A., Vecchi, A., Piemonti, L., Mantovani, A., & Allavena, P. (2004). Increased Survival, Proliferation, and Migration in Metastatic Human Pancreatic Tumor Cells Expressing Functional CXCR4.

- Cancer research*, 64, 8420-8427. doi: 10.1158/0008-5472.CAN-04-1343
- Maréchal, A., & Zou, L. (2013). DNA damage sensing by the ATM and ATR kinases. *Cold Spring Harbor perspectives in biology*, 5(9), a012716. doi: 10.1101/cshperspect.a012716
- Maßberg, D., Simon, A., Häussinger, D., Keitel, V., Gisselmann, G., Conrad, H., & Hatt, H. (2015). Monoterpene (-)-citronellal affects hepatocarcinoma cell signaling via an olfactory receptor. *Archives of Biochemistry and Biophysics*, 566, 100-109. doi: https://doi.org/10.1016/j.abb.2014.12.004
- McBride, O. W., Merry, D., & Givol, D. (1986). The gene for human p53 cellular tumor antigen is located on chromosome 17 short arm (17p13). *Proceedings of the National Academy of Sciences of the United States of America*, 83(1), 130-134. doi: 10.1073/pnas.83.1.130
- McIntosh, J. R. (2016). Mitosis. *Cold Spring Harbor perspectives in biology*, 8(9), a023218. doi: 10.1101/cshperspect.a023218
- McMASTER, M. C. (2008). *GC/MS A Practical User's Guide* (Second ed.). Hoboken, New Jersey, United States of America: John Wiley & Sons, Inc.
- Melo, M. S., Guimarães, A. G., Santana, M. F., Siqueira, R. S., De Lima, A. D. C. B., Dias, A. S., Santos, M. R. V., Onofre, A. S. C., Quintans, J. S. S., De Sousa, D. P., Almeida, J. R. G. S., Estevam, C. S., Araujo, B. S., & Quintans-Júnior, L. J. (2011). Anti-inflammatory and redox-protective activities of citronellal. *Biological Research*, 44, 363-368.
- Ministry of Public Health, T. (2017). MAKRUT, BAI *Thai Herbal Pharmacopoeia 2017* (pp. 277-283). Nonthaburi, 11000., Thailand: Department of Medical Sciences, Ministry of Public Health.
- Mitra, J., & Enders, G. H. (2004). Cyclin A/Cdk2 complexes regulate activation of Cdk1 and Cdc25 phosphatases in human cells. *Oncogene*, 23(19), 3361-3367. doi: 10.1038/sj.onc.1207446
- Morris, L., Allen, K. E., & La Thangue, N. B. (2000). Regulation of E2F transcription by cyclin E-Cdk2 kinase mediated through p300/CBP co-activators. *Nature Cell Biology*, 2(4), 232-239. doi: 10.1038/35008660
- Myzak, M. C., Karplus, P. A., Chung, F.-L., & Dashwood, R. H. (2004). A Novel Mechanism of Chemoprotection by Sulforaphane. *Cancer Research*, 64(16), 5767. doi: 10.1158/0008-5472.CAN-04-1326
- Nanasombat, S., & Lohasupthawee, P. (2005). Antibacterial activity of crude ethanolic extracts and essential oils of spices against *Salmonellae* and other Enterobacteria. *KMITL Sci. Technol. J.*, 5.
- Nedeljkovic, M., & Damjanovic, A. (2019). Mechanisms of Chemotherapy Resistance in Triple-Negative Breast Cancer-How We Can Rise to the Challenge. *Cells*, 8(9). doi: 10.3390/cells8090957
- Neidler, S. (2017). *What are the differences between PCR, RT-PCR, qPCR, and RT-qPCR?* Retrieved October 10, 2019, from <http://www.enzolifesciences.com/science-center/technotes/2017/march/what-are-the-differences-between-pcr-rt-pcr-qpcr-and-rt-qpcr/>
- Neimanis, S., Albig, W., Doenecke, D., & Kahle, J. (2008). Sequence Elements in Both Subunits of the DNA Fragmentation Factor Are Essential for Its Nuclear Transport. *The Journal of biological chemistry*, 282, 35821-35830. doi:

10.1074/jbc.M703110200

- Newcomb, P. A., Trentham-Dietz, A., Hampton, J. M., Egan, K. M., Titus-Ernstoff, L., Warren Andersen, S., Greenberg, E. R., & Willett, W. C. (2011). Late age at first full term birth is strongly associated with lobular breast cancer. *Cancer*, *117*(9), 1946-1956. doi: 10.1002/cncr.25728
- Nishan, M., Subramanian, P., Saahatish, R., Antony, V., & Jesudoss, V. A. S. (2017). *Toxicity of Citrus aurantifolia and Citrus hystrix against Aedes albopictus larvae* (Vol. 10).
- Ohtsubo, M., Theodoras, A. M., Schumacher, J., Roberts, J. M., & Pagano, M. (1995). Human cyclin E, a nuclear protein essential for the G1-to-S phase transition. *Molecular and cellular biology*, *15*(5), 2612-2624. doi: 10.1128/mcb.15.5.2612
- Ozretic, P., Alvir, I., Sarcevic, B., Vujaskovic, Z., Rendic-Miocevic, Z., Roguljic, A., & Beketic-Oreskovic, L. (2017). Apoptosis regulator Bcl-2 is an independent prognostic marker for worse overall survival in triple-negative breast cancer patients. *The International Journal of Biological Markers*, *33*(1), 109-115. doi: 10.5301/ijbm.5000291
- Papich, M. G. (2016). Paclitaxel. In M. G. Papich (Ed.), *Saunders Handbook of Veterinary Drugs (Fourth Edition)* (pp. 600-602). St. Louis: W.B. Saunders.
- Pauty, J., Côté, M.-F., Rodrigue, A., Velic, D., Masson, J.-Y., & Fortin, S. (2016). Investigation of the DNA damage response to SFOM-0046, a new small-molecule drug inducing DNA double-strand breaks. *Scientific Reports*, *6*, 23302. doi: 10.1038/srep23302
- <https://www.nature.com/articles/srep23302#supplementary-information>
- Pilco-Ferreto, N., & Calaf, G. (2016). Influence of doxorubicin on apoptosis and oxidative stress in breast cancer cell lines. *International Journal of Oncology*, *49*. doi: 10.3892/ijo.2016.3558
- Pledgie-Tracy, A., Sobolewski, M. D., & Davidson, N. E. (2007). Sulforaphane induces cell type-specific apoptosis in human breast cancer cell lines. *Molecular Cancer Therapeutics*, *6*(3), 1013. doi: 10.1158/1535-7163.MCT-06-0494
- Rao, Y. K., Wu, A. T. H., Geethangili, M., Huang, M.-T., Chao, W.-J., Wu, C.-H., Deng, W.-P., Yeh, C.-T., & Tzeng, Y.-M. (2011). Identification of Antrocin from *Antrodia camphorata* as a Selective and Novel Class of Small Molecule Inhibitor of Akt/mTOR Signaling in Metastatic Breast Cancer MDA-MB-231 Cells. *Chemical Research in Toxicology*, *24*(2), 238-245. doi: 10.1021/tx100318m
- Ravindran, P. N. (2016). Citrus hystrix In P. N. Ravindran (Ed.), *The Encyclopedia of Herbs and Spices* (Vol. 1, pp. 488-491). Bell and Bain Ltd, Glasgow, UK: CABI.
- Raza, H., & John, A. (2005). Green tea polyphenol epigallocatechin-3-gallate differentially modulates oxidative stress in PC12 cell compartments. *Toxicology and Applied Pharmacology*, *207*(3), 212-220. doi: <https://doi.org/10.1016/j.taap.2005.01.004>
- Razak, N. A., Abu, N., Ho, W. Y., Zamberi, N. R., Tan, S. W., Alitheen, N. B., Long, K., & Yeap, S. K. (2019). Cytotoxicity of eupatorin in MCF-7 and MDA-MB-231 human breast cancer cells via cell cycle arrest, anti-angiogenesis and induction of apoptosis. *Scientific Reports*, *9*(1), 1514. doi: 10.1038/s41598-018-37796-w

- Rezaei, P. F., Fouladdel, S., Ghaffari, S. M., Amin, G., & Azizi, E. (2012). Induction of G1 cell cycle arrest and cyclin D1 down-regulation in response to pericarp extract of Baneh in human breast cancer T47D cells. *Daru : journal of Faculty of Pharmacy, Tehran University of Medical Sciences*, 20(1), 101-101. doi: 10.1186/2008-2231-20-101
- Roy, S., & Nicholson, D. W. (2000). Cross-talk in cell death signaling. *The Journal of experimental medicine*, 192(8), F21-F25.
- Russo, J., Wilgus, G., & Russo, I. H. (1979). Susceptibility of the mammary gland to carcinogenesis: I Differentiation of the mammary gland as determinant of tumor incidence and type of lesion. *The American journal of pathology*, 96(3), 721-736.
- Sadasivam, M., Kumarasamy, C., Arasakumar, T., Govindan, M., Kasirajan, G., Vijayan, V., Velmurugan, D., Chia-Her, L., Madhusudhanan, G. R., Thirugnanasampandan, R., & Subramaniam, M. (2017). Phytochemical constituents from dietary plant *Citrus hystrix*. *Natural Product Research*, 32, 1-6. doi: 10.1080/14786419.2017.1399386
- Saibabu, V., Singh, S., Ansari, M., Fatima, Z., & Hameed, S. (2017). Insights into the intracellular mechanisms of citronellal in *Candida Albicans*: Implications for reactive oxygen species-mediated necrosis, mitochondrial dysfunction, and DNA damage. *Revista da Sociedade Brasileira de Medicina Tropical*, 50, 524-529. doi: 10.1590/0037-8682-0114-2017
- Sajadian, S., Vatankhah, M., Majdzadeh, M., Kouhsari, S. M., Ghahremani, M. H., & Ostad, S. N. (2015). Cell cycle arrest and apoptogenic properties of opium alkaloids noscapine and papaverine on breast cancer stem cells. *Toxicology Mechanisms and Methods*, 25(5), 388-395. doi: 10.3109/15376516.2015.1045656
- Sakahira, H., Enari, M., & Nagata, S. (1998). Cleavage of CAD inhibitor in CAD activation and DNA degradation during apoptosis. *Nature*, 391(6662), 96-99. doi: 10.1038/34214
- Saklani, A., & Kutty, S. K. (2008). Plant-derived compounds in clinical trials. *Drug Discovery Today*, 13(3), 161-171. doi: <https://doi.org/10.1016/j.drudis.2007.10.010>
- Sato, A., Asano, K., & Sato, T. (1990). The Chemical Composition of *Citrus Hystrix* DC (Swangi). *Journal of Essential Oil Research*, 2(4), 179-183. doi: 10.1080/10412905.1990.9697857
- Seidel, C., Schnekenburger, M., Dicato, M., & Diederich, M. (2012). Histone deacetylase modulators provided by Mother Nature. *Genes & nutrition*, 7(3), 357-367. doi: 10.1007/s12263-012-0283-9
- Sherr, C., & Roberts, J. (1999). CDK inhibitor: Positive and negative regulators of G1-phase progression. *Genes & development*, 13, 1501-1512. doi: 10.1101/gad.13.12.1501
- Shi, D., & Gu, W. (2012). Dual Roles of MDM2 in the Regulation of p53: Ubiquitination Dependent and Ubiquitination Independent Mechanisms of MDM2 Repression of p53 Activity. *Genes & cancer*, 3(3-4), 240-248. doi: 10.1177/1947601912455199
- Shitashige, M., Toi, M., Yano, T., Shibata, M., Matsuo, Y., & Shibasaki, F. (2001). Dissociation of Bax from a Bcl-2/Bax Heterodimer Triggered by

- Phosphorylation of Serine 70 of Bcl-21. *The Journal of Biochemistry*, 130(6), 741-748. doi: 10.1093/oxfordjournals.jbchem.a003044
- Siew Loh, F., Muhamad, R., Omar, D., & Rahmani, M. (2011). *Insecticidal properties of Citrus hystrix DC leaves essential oil against Spodoptera litura fabricius* (Vol. 5).
- Society, A. C. (2017a). *Breast Cancer*. from <https://www.cancer.org/cancer/breast-cancer/about/what-is-breast-cancer.html>
- Society, A. C. (2017b). *Type of Breast Cancer*. Retrieved July, 2019, from <https://www.cancer.org/cancer/breast-cancer/understanding-a-breast-cancer-diagnosis/types-of-breast-cancer.html>
- Song, W., Liu, X. Y., & Shi, Y. (2015). Citronellol terpenoid inhibits cancer cell proliferation and induces apoptosis in non-small cell lung carcinoma. *34*, 1652-1657.
- Srinivasan, S., & Muruganathan, U. (2016). Antidiabetic efficacy of citronellol, a citrus monoterpene by ameliorating the hepatic key enzymes of carbohydrate metabolism in streptozotocin-induced diabetic rats. *Chemico-Biological Interactions*, 250, 38-46. doi: <https://doi.org/10.1016/j.cbi.2016.02.020>
- Srisukh, V., Tribuddharat, C., Nukoolkarn, V., Bunyaphatsara, N., Chokephaibulkit, K., Phoomniyom, S., Chuanphung, S., & Seifuengfung, S. (2012). Antibacterial activity of essential oils from Citrus hystrix (makrut lime) against respiratory tract pathogens. *ScienceAsia*, 38, 212. doi: 10.2306/scienceasia1513-1874.2012.38.212
- Stegh, A. H. (2012). Targeting the p53 signaling pathway in cancer therapy - the promises, challenges and perils. *Expert opinion on therapeutic targets*, 16(1), 67-83. doi: 10.1517/14728222.2011.643299
- Stone, S., Vasconcellos, F. A., Lenardao, E., Rc, d., Jacob, R., & Leite, F. (2013). Evaluation of potential use of Cymbopogon sp. essential oils, (R)-citronellal and N-citronellylamine in cancer chemotherapy. *International Journal of Applied Research in Natural Products*, 6.
- Su, M., Huang, J., Liu, S., Xiao, Y., Qin, X., Liu, J., Pi, C., Luo, T., Li, J., Chen, X., & Luo, Z. (2016). The anti-angiogenic effect and novel mechanisms of action of Combretastatin A-4. *Scientific Reports*, 6, 28139. doi: 10.1038/srep28139
- Su, Y.-W., Chao, S., Lee, M.-H., Ou, T.-Y., & Ying Chieh, T. (2010). Inhibitory Effects of Citronellol and Geraniol on Nitric Oxide and Prostaglandin E-2 Production in Macrophages. *Planta medica*, 76, 1666-1671. doi: 10.1055/s-0030-1249947
- Sumonrat, C., Suphitchaya, C., & Tipparat, H. (2008). *Antimicrobial activities of essential oils and crude extracts from tropical Citrus spp. Against food-related microorganisms* (Vol. 30).
- Sun, L., Legood, R., Dos-Santos-Silva, I., Gaiha, S. M., & Sadique, Z. (2018). Global treatment costs of breast cancer by stage: A systematic review. *PloS one*, 13(11), e0207993-e0207993. doi: 10.1371/journal.pone.0207993
- Sun, S., Phrutivorapongkul, A., Dibwe, D. F., Balachandran, C., & Awale, S. (2018). Chemical Constituents of Thai Citrus hystrix and Their Antiausterity Activity against the PANC-1 Human Pancreatic Cancer Cell Line. *Journal of Natural Products*, 81(8), 1877-1883. doi: 10.1021/acs.jnatprod.8b00405
- Suwannayod, S., Somboon, P., Junkum, A., Leksomboon, R., Chaiwong, T., Jones, M. K., Sriipa, B., Balthaisong, S., Phuyao, C., Chareonviriyaphap, T., & Sukontason,

- K. (2018). *Activity of kaffir lime (Citrus hystrix) essential oil against blow flies and house fly* (Vol. 49).
- Talarmin, H., Rescan, C., Cariou, S., Glaise, D., Zanninelli, G., Bilodeau, M., Loyer, P., Guguen-Guillouzo, C., & Baffet, G. (1999). The mitogen-activated protein kinase kinase/extracellular signal-regulated kinase cascade activation is a key signalling pathway involved in the regulation of G(1) phase progression in proliferating hepatocytes. *Molecular and cellular biology*, *19*(9), 6003-6011. doi: 10.1128/mcb.19.9.6003
- Taylor, W. R., & Stark, G. R. (2001). Regulation of the G2/M transition by p53. *Oncogene*, *20*(15), 1803-1815. doi: 10.1038/sj.onc.1204252
- Timofeev, O., Cizmecioglu, O., Settele, F., Kempf, T., & Hoffmann, I. (2010). Cdc25 Phosphatases Are Required for Timely Assembly of CDK1-Cyclin B at the G2/M Transition. *The Journal of biological chemistry*, *285*, 16978-16990. doi: 10.1074/jbc.M109.096552
- Toh, S. Y., Wang, X., & Li, P. (1998). Identification of the Nuclear Factor HMG2 as an Activator for DFF Nuclease Activity. *Biochemical and Biophysical Research Communications*, *250*(3), 598-601. doi: <https://doi.org/10.1006/bbrc.1998.9369>
- Tunjung, W., Cinatl, J., Michaelis, M., & Mark Smales, C. (2015). Anti-Cancer Effect of Kaffir Lime (Citrus Hystrix DC) Leaf Extract in Cervical Cancer and Neuroblastoma Cell Lines. *Procedia Chemistry*, *14*, 465-468. doi: 10.1016/j.proche.2015.03.062
- Tunjung, W. A. S., Cinatl, J., Michaelis, M., & Smales, C. M. (2015). Anti-Cancer Effect of Kaffir Lime (Citrus Hystrix DC) Leaf Extract in Cervical Cancer and Neuroblastoma Cell Lines. *Procedia Chemistry*, *14*, 465-468. doi: 10.1016/j.proche.2015.03.062
- Tunjung, W. A. S., & Dertyasasa, E. D. (2017). Volatile Organic Compounds of Kaffir Lime (Citrus hystrix DC.) Leaves Fractions and their Potency as Traditional Medicine. *Biosciences, Biotechnology Research Asia*, *14*, 1235-1250. doi: 10.13005/bbra/2566
- Utthawang, W., Ampasavate, C., Okonogi, S., Rungrojsakul, M., Chiampanichayakul, S., Tima, S., & Anuchapreeda, S. (2017). Low doses of partially purified fraction of kaffir lime (Citrus hystrix DC.) leaf extract induce cell death in Molt4 cells. *Journal of Associated Medical Sciences*, *50*(1), 27-37. doi: 10.14456/jams.2017.3
- van Den Dool, H., & Dec. Kratz, P. (1963). A generalization of the retention index system including linear temperature programmed gas—liquid partition chromatography. *Journal of Chromatography A*, *11*, 463-471. doi: [https://doi.org/10.1016/S0021-9673\(01\)80947-X](https://doi.org/10.1016/S0021-9673(01)80947-X)
- Vousden, K. H. (2000). p53: Death Star. *Cell*, *103*(5), 691-694. doi: [https://doi.org/10.1016/S0092-8674\(00\)00171-9](https://doi.org/10.1016/S0092-8674(00)00171-9)
- Vrignaud, P., Semiond, D., Benning, V., Beys, E., Bouchard, H., & Gupta, S. (2014). Preclinical profile of cabazitaxel. *Drug design, development and therapy*, *8*, 1851-1867. doi: 10.2147/DDDT.S64940
- Wachmann, K., Pop, C., van Raam, B. J., Drag, M., Mace, P. D., Snipas, S. J., Zmasek, C., Schwarzenbacher, R., Salvesen, G. S., & Riedl, S. J. (2010). Activation and Specificity of Human Caspase-10. *Biochemistry*, *49*(38), 8307-8315. doi: 10.1021/bi100968m

- Wahba, H. A., & El-Hadaad, H. A. (2015). Current approaches in treatment of triple-negative breast cancer. *Cancer biology & medicine*, 12(2), 106-116. doi: 10.7497/j.issn.2095-3941.2015.0030
- Wall, P. E. (2005). *Thin-layer Chromatography A Modern Practical Approach*. Thomas Graham House, Science Park, Milton Road, Cambridge CB4 0WF, U: The Royal Society of Chemistry.
- Walsh, T., Casadei, S., Coats, K. H., Swisher, E., Stray, S. M., Higgins, J., Roach, K. C., Mandell, J., Lee, M. K., Ciernikova, S., Foretova, L., Soucek, P., & King, M.-C. (2006). Spectrum of Mutations in BRCA1, BRCA2, CHEK2, and TP53 in Families at High Risk of Breast Cancer. *JAMA*, 295(12), 1379-1388. doi: 10.1001/jama.295.12.1379
- Warsito, W., Palungan, M. H., & Utomo, E. P. (2017). Profiling study of the major and minor components of kaffir lime oil (*Citrus hystrix* DC.) in the fractional distillation process. *The Pan African medical journal*, 27, 282-282. doi: 10.11604/pamj.2017.27.282.9679
- Węsierska-Gądek, J., Gritsch, D., Zulehner, N., Komina, O., & Maurer, M. (2011). Roscovitine, a selective CDK inhibitor, reduces the basal and estrogen-induced phosphorylation of ER- $\alpha$  in human ER-positive breast cancer cells. *Journal of Cellular Biochemistry*, 112(3), 761-772. doi: 10.1002/jcb.23004
- WHO. (2018). *Cancer Fact Sheet, Breast Cancer*. Retrieved 01 Jul, 2019, from <http://gco.iarc.fr/today/data/factsheets/cancers/20-Breast-fact-sheet.pdf>
- Widlak, P. (2000). The DFF40/CAD endonuclease and its role in apoptosis. *Acta biochimica Polonica*, 47, 1037-1044.
- Wijayanti, N., Tunjung, W., & Setyawati, Y. (2015). CYTOTOXICITY AND APOPTOSIS INDUCTION BY KAFFIR LIME LEAVES EXTRACT (*Citrus hystrix* DC.) IN HeLa CELLS CULTURE (HUMAN CERVICAL CANCER CELL LINE). *KnE Life Sciences*, 2, 631. doi: 10.18502/cls.v2i1.233
- Wlodkowic, D., Skommer, J., & Darzynkiewicz, Z. (2009). Flow cytometry-based apoptosis detection. *Methods in molecular biology (Clifton, N.J.)*, 559, 19-32. doi: 10.1007/978-1-60327-017-5\_2
- Wolff, A. C., Hammond, M. E. H., Hicks, D. G., Dowsett, M., McShane, L. M., Allison, K. H., et al. (2013). Recommendations for Human Epidermal Growth Factor Receptor 2 Testing in Breast Cancer: American Society of Clinical Oncology/College of American Pathologists Clinical Practice Guideline Update. *Journal of Clinical Oncology*, 31(31), 3997-4013. doi: 10.1200/JCO.2013.50.9984
- Wongpornchai, S. (2012). Kaffir lime leaf. In K. V. Peter (Ed.), *Handbook of herbs and spices* (2nd ed., Vol. 2, pp. 319-328). , 80 High Street, Sawston, Cambridge CB22 3HJ, UK Woodhead Publishing Limited.
- Xu, B., Kim, S.-T., Lim, D.-S., & Kastan, M. B. (2002). Two molecularly distinct G(2)/M checkpoints are induced by ionizing irradiation. *Molecular and cellular biology*, 22(4), 1049-1059. doi: 10.1128/mcb.22.4.1049-1059.2002
- Yamamoto, T. M., Iwabuchi, M., Ohsumi, K., & Kishimoto, T. (2005). APC/C-Cdc20-mediated degradation of cyclin B participates in CSF arrest in unfertilized *Xenopus* eggs. *Developmental Biology*, 279(2), 345-355. doi: <https://doi.org/10.1016/j.ydbio.2004.12.025>
- Yang, K., Hitomi, M., & Stacey, D. W. (2006). Variations in cyclin D1 levels through

- the cell cycle determine the proliferative fate of a cell. *Cell division*, 1, 32-32. doi: 10.1186/1747-1028-1-32
- Yang, L.-T. J. a. A.-G. (2012). Targeted Apoptosis in Breast Cancer Immunotherapy In R. L. Aft (Ed.), *Targeting New Pathways and Cell Death in Breast Cancer* (pp. 23-27). Janeza Trdine 9, 51000 Rijeka, Croatia Janeza Trdine 9, 51000 Rijeka, Croatia
- Yang, R., Müller, C., Huynh, V., Fung, Y. K., Yee, A. S., & Koeffler, H. P. (1999). Functions of cyclin A1 in the cell cycle and its interactions with transcription factor E2F-1 and the Rb family of proteins. *Molecular and cellular biology*, 19(3), 2400-2407. doi: 10.1128/mcb.19.3.2400
- Yang, V. W. (2018). Chapter 8 - The Cell Cycle. In H. M. Said (Ed.), *Physiology of the Gastrointestinal Tract (Sixth Edition)* (pp. 197-219): Academic Press.
- Yoshida, N., Koizumi, M., Adachi, I., & Kawakami, J. (2006). Inhibition of P-glycoprotein-mediated transport by terpenoids contained in herbal medicines and natural products. *Food and Chemical Toxicology*, 44(12), 2033-2039. doi: <https://doi.org/10.1016/j.fct.2006.07.003>
- Yu, W.-N., Lai, Y.-J., Ma, J.-W., Ho, C.-T., Hung, S.-W., Chen, Y.-H., Chen, C.-T., Kao, J.-Y., & Way, T.-D. (2019a). Citronellol Induces Necroptosis of Human Lung Cancer Cells via TNF- $\alpha$  Pathway and Reactive Oxygen Species Accumulation. *In vivo (Athens, Greece)*, 33, 1193-1201. doi: 10.21873/invivo.11590
- Yu, W.-N., Lai, Y.-J., Ma, J.-W., Ho, C.-T., Hung, S.-W., Chen, Y.-H., Chen, C.-T., Kao, J.-Y., & Way, T.-D. E. R. (2019b). Citronellol Induces Necroptosis of Human Lung Cancer Cells via TNF- $\alpha$  Pathway and Reactive Oxygen Species Accumulation. *In vivo (Athens, Greece)*, 33(4), 1193-1201. doi: 10.21873/invivo.11590

## APPENDIX

### I. CHEMICALS AND REAGENTS

#### 1. Prepare of DMEM medium (1 L)

- DMEM powder to sterile bottle 1 sachet
- NaHCO<sub>3</sub> 3.7 g/L
- D.I water add up to 1 L
- Adjust p.H by HCl or NaOH to p.H 7.4
- Filtered the medium to sterilized and store at 4°C

#### 2. Prepare of complete DMEM medium (1 L)

- FBS 100 ml (final concentration 10%)
- Anti-Anti 10 ml (final concentration 1%)
- Sterile DMEM medium 890 ml
- Store at 4°C

#### 3. Preparation of Freezing medium (10 ml)

- FBS 2 ml (final concentration 20%)
- DMSO 500 µl (final concentration 5%)
- Glycerol 500 µl (final concentration 5%)
- DMEM 7 ml

#### 4. Prepare of complete RPMI medium (1 L)

- FBS 100 ml (final concentration 10%)
- Anti-Anti 10 ml (final concentration 1%)
- Sterile RPMI medium 890 ml
- Store at 4°C

**5. Preparation of 46% Percoll (50 ml)**

- Percoll 23.13 ml
- Complete RPMI 27 ml
- 10X PBS 1.87 ml
- freshly prepare for working

**6. Preparation of phosphate buffer saline (10X) (1L)**

- NaCl 80 g
- $\text{KH}_2\text{PO}_4$  2.4 g
- KCl 2 g
- $\text{Na}_2\text{PO}_4 \cdot 2\text{H}_2\text{O}$  14.4 g
- Dissolve with D.I water and add up to complete 1 L
- Dilute with ration 1:9 with D.I water and adjust to p.H 7.4 for working concentration (1X)
- Autoclave to sterilize the solution
- Store at 4 °C

**7. Preparation of 0.5 M EDTA (100 ml)**

- EDTA 18.61 g
- Add D.I water around 80 ml
- Adjust p.H by NaOH until 8.0 to help dissolve EDTA
- Add D.I up to complete volume 1 L
- Filter the solution and store at room temperature

**8. Preparation of 0.25% Trypsin-EDTA (5X) (100 ml)**

- 10X PBS 10 ml

- 0.5 M EDTA 0.1 ml
- D-glucose 0.1 g
- Penicillin/Streptomycin 0.5 ml
- 2.5% Trypsin 10 ml
- 0.5% Phenol red 0.3 ml
- Adjust p.H with NaOH to 7.35
- Add up D.I to 100 ml
- Filter the solution
- Store at -20°C
- Dilute at ratio 1:5 with 1X PBS for working concentration and store at -20°C

#### 9. Fetal bovine serum inactivation

- Warm D.I water to 56°C then place FBS bottle for 45 mins
- Store in 4°C prior to use

#### 10. Preparation of 10% neutral buffered formalin (100 ml)

- 37% formalin 10 ml
- NaH<sub>2</sub>PO<sub>4</sub> 400 mg
- Na<sub>2</sub>H PO<sub>4</sub> 650 mg
- D.I add up to 100 ml

#### 11. Preparation of 0.5% crystal violet (for 100 ml)

- Crystal violet powder 0.5 g
- Methanol 20 ml
- D.I up to 100 ml

**12. Preparation of master mix for PCR**

- 5x RT buffer 400  $\mu$ l
- dNTP mix 100  $\mu$ l
- Oligo DT 100  $\mu$ l
- Random hexamer 100  $\mu$ l
- Store at -20°C

**13. Preparation cDNA for PCR (10  $\mu$ l)**

- mRNA 6  $\mu$ l
- master mix 4  $\mu$ l
- Store at -20°C

**14. Preparation of Bradford protein staining reagent (1 L)**

- Coomassie brilliant blue G-250 50 mg
- 100% methanol 50 ml
- H<sub>3</sub>PO<sub>4</sub> 100 ml
- D.I add up to 1 L
- Filtered with Whiteman filter paper
- Store at 4°C

**15. Preparation of TBS 10X, p.H 7.6 (1 L)**

- Tris-HCl 24 g
- Tris-base 5.6 g

- NaCl 88 g
- D.I add up to 1 L
- Store at 4°C

**16. Preparation of 1X TBST (1 L)**

- 10X TBS 100 ml
- Tween-20 1 ml
- D.I add up to 1L
- Store at 4°C

**17. Preparation of blocking buffer (100 ml)**

- Skim milk powder 5 g
- 1X TBST add up to 1L
- Store at 4°C

**18. Preparation of antibody diluting buffer (100 ml)**

- BSA powder 1 g
- 1X TBST add up to 1L
- Store at at 4°C

**19. Preparation of loading buffer 2X Laemmli (10 ml)**

- Tris-HCl 0.5 M 2.5 ml (final concentration 0.125 M)
- 10% SDS 4 ml (final concentration 4%)
- Glycerol 2 ml (final concentration 20%)



- 1.5 Tris-HCl, p.H 8.8 3.9 ml
- Resolver A 1.5 ml
- Resolver B 1.5 ml
- 10% SDS 150  $\mu$ l
- 10% APS 150  $\mu$ l
- TEMED 15  $\mu$ l
- **Stacking gel (5 ml)**
- D.I 1.43 ml
- 30% acrylamide 670  $\mu$ l
- 1.5 Tris-HCl, p.H 8.8 1.3 ml
- Resolver A 750  $\mu$ l
- Resolver B 750  $\mu$ l
- 10% SDS 50  $\mu$ l
- 10% APS 50  $\mu$ l
- TEMED 5  $\mu$ l

## II. STATISTICAL ANALYSIS RESULTS

### 23. Statistical analysis of cell proliferation rate assay

**Table 13 Statistical comparison on proliferation rate of MDA-MB-231 cells**

Tukey's test	P value		
	0 h	24 h	48 h
Control vs. Hexane 50 µg/ml	> 0.9999	< 0.0001	< 0.0001
Control vs. Hexane 100 µg/ml	> 0.9999	< 0.0001	< 0.0001
Control vs. Hexane 150 µg/ml	> 0.9999	< 0.0001	< 0.0001
Control vs. Citronellol 0.5 nM	> 0.9999	< 0.0001	< 0.0001
Control vs. Citronellol 1 nM	> 0.9999	< 0.0001	< 0.0001
Control vs. Citronellal 0.5 nM	> 0.9999	< 0.0001	< 0.0001
Control vs. Citronellal 1 nM	> 0.9999	< 0.0001	< 0.0001
Control vs. Doxorubicine 0.5 µM	> 0.9999	< 0.0001	< 0.0001

Statistical different between control group and treatments group of cell proliferation rate using Two-way ANOVA with post-hoc of Turkey's test, *P* value < 0.05 consider significant (n=3).

### 24. Statistical analysis of wound healing migration assay

**Table 14 Statistical comparison on wound migration assay**

Tukey's test	P value			
	0 h	6 h	12 h	24 h
Control vs. Hexane 50 µg/ml	> 0.9999	0.0042	0.0003	< 0.0001
Control vs. Hexane 100 µg/ml	> 0.9999	< 0.0001	< 0.0001	< 0.0001
Control vs. Hexane 150 µg/ml	> 0.9999	0.0007	< 0.0001	< 0.0001
Control vs. Citronellol 0.5 nM	> 0.9999	0.0060	0.0003	< 0.0001
Control vs. Citronellol 1 nM	> 0.9999	< 0.0001	< 0.0001	< 0.0001
Control vs. Citronellal 0.5 nM	> 0.9999	< 0.0001	< 0.0001	< 0.0001
Control vs. Citronellal 1 nM	> 0.9999	< 0.0001	< 0.0001	< 0.0001
Control vs. Doxorubicine 0.5 µM	> 0.9999	< 0.0001	< 0.0001	< 0.0001

Statistical different between control group and treatments group of wound closer areas using Two-way ANOVA with post-hoc of Turkey's test,  $P$  value  $< 0.05$  consider significant ( $n=3$ ).

## 25. Statistical analysis of clonogenic assay

**Table 15 Statistical comparison on colony formation assay**

Dunnett's test	$P$ value
Control vs. Hexane 50 $\mu\text{g/ml}$	$< 0.0001$
Control vs. Hexane 100 $\mu\text{g/ml}$	$< 0.0001$
Control vs. Hexane 150 $\mu\text{g/ml}$	$< 0.0001$
Control vs. Citronellol 0.5 nM	0.0007
Control vs. Citronellol 1 nM	$< 0.0001$
Control vs. Citronellal 0.5 nM	$< 0.0001$
Control vs. Citronellal 1 nM	$< 0.0001$
Control vs. Doxorubicine 0.5 $\mu\text{M}$	$< 0.0001$

Statistical different between control group and treatments group of wound closer areas using One-way ANOVA with Dunnett's multiple comparisons test,  $P$  value  $< 0.05$  consider significant ( $n=3$ ).

## 26. Statistical analysis of apoptotic cell analysis

**Table 15 Statistical comparison on apoptotic cells analysis**

Dunnett's test	$P$ value
Control vs. Hexane 200 $\mu\text{g/ml}$	$< 0.005$
Control vs. Citronellol 1 nM	$< 0.0027$
Control vs. Citronellal 1 nM	$< 0.0108$
Control vs. Doxorubicine 0.5 $\mu\text{M}$	$< 0.0003$

Statistical different between control group and treatments group of wound closer areas using One-way ANOVA with Dunnett's multiple comparisons test,  $P$  value  $< 0.05$  consider significant ( $n=3$ ).

### III. OTHERS

#### 27. Cell viability of 2.5% DMSO compared to culture medium

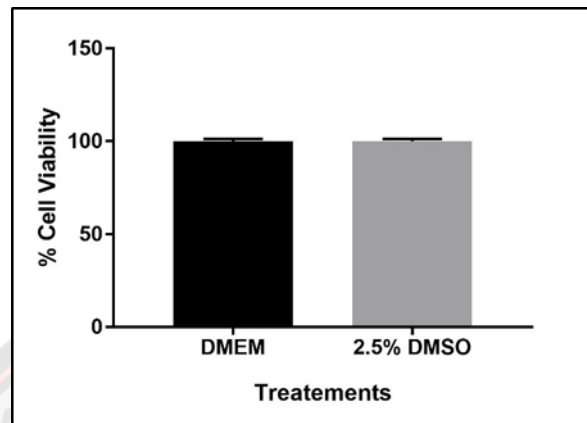


Figure 38 Cell viability of 2.5% DMSO compared to culture medium

#### 28. Free MRI\_Wound\_Healing\_Tool.ijm plugin

at [http://dev.mri.cnrs.fr/attachments/download/1819/MRI\\_Wound\\_Healing\\_Tool.ijm](http://dev.mri.cnrs.fr/attachments/download/1819/MRI_Wound_Healing_Tool.ijm)

#### 29. Calculation of cell proliferation rate

Cell proliferation rate was calculated based on MTT assay between each 24 hours. The proliferation rate was measured as fold following the formula below.

$$\text{Cell proliferation rate (fold)} = \frac{\text{Cell viability of treated cells at } t_i}{\text{Cell viability of control cells at } t_0}$$

$t_i$  cells growth at individual days (24 hours)

$t_0$  cells at seeding density (0 hour)

**30. Calculation of IC<sub>10</sub> and IC<sub>5</sub> from MTT assay using dose-response curve**

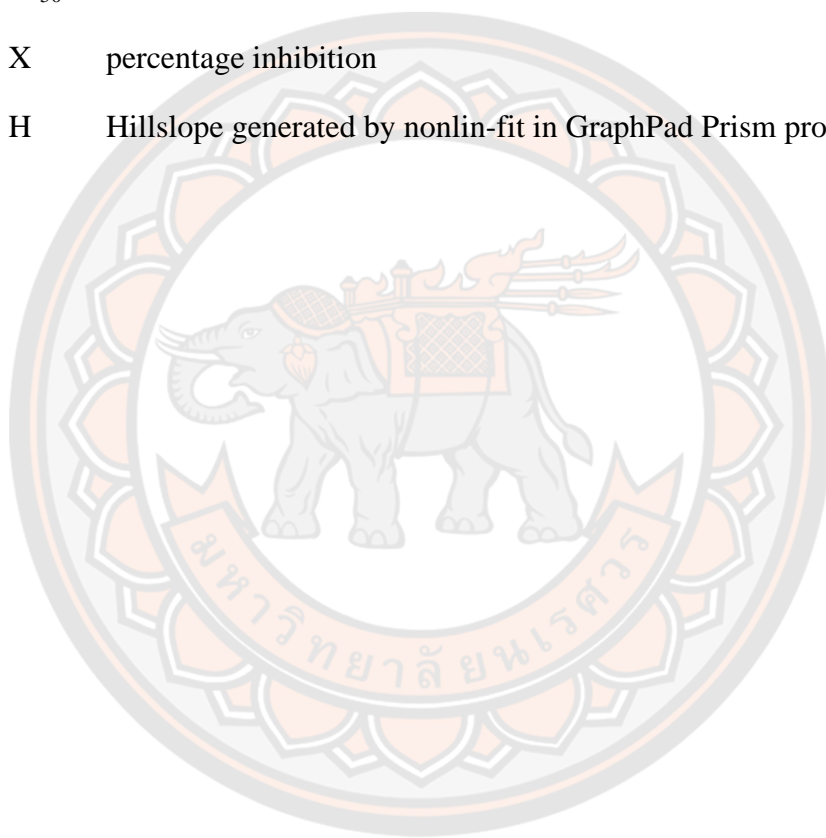
The IC<sub>10</sub> and IC<sub>5</sub> value were calculated using formula from GraphPad Prism.

$$IC_x = \left( \frac{X}{100-X} \right)^{\frac{1}{H}} \times IC_{50}$$

IC<sub>50</sub> inhibition concentration 50%

X percentage inhibition

H Hillslope generated by nonlin-fit in GraphPad Prism program.



### 31. Approval for research conduction

COE No. 215/2019  
IRB No. 0945/62



คณะกรรมการจริยธรรมการวิจัยในมนุษย์ มหาวิทยาลัยนเรศวร  
NARESUAN UNIVERSITY INSTITUTIONAL REVIEW BOARD  
99 หมู่ 9 ตำบลท่าโพธิ์ อำเภอเมือง จังหวัดพิษณุโลก 65000 เบอร์โทรศัพท์ 05596 8642

เอกสารรับรองการยกเว้นพิจารณาจริยธรรมโครงการวิจัย

คณะกรรมการจริยธรรมการวิจัยในมนุษย์ มหาวิทยาลัยนเรศวร ดำเนินการให้การรับรองการยกเว้นพิจารณาจริยธรรมโครงการวิจัย ตามแนวทางหลักจริยธรรมการวิจัยในคนที่เป็นมาตรฐานสากล ได้แก่ Declaration of Helsinki, The Belmont Report, CIOMS Guideline International Conference on Harmonization in Good Clinical Practice หรือ ICH-GCP) และ 45CFR 46.101(b)

ชื่อโครงการ : Anticancer effect of Citrus hystrix leaf extracts on the triple negative breast cancer cell line MDA-MB-231

ผู้วิจัยหลัก : Mr. Yathsoeung Ho

สังกัดหน่วยงาน : คณะสหเวชศาสตร์

เอกสารรับรอง

1. AF 01-10 เวอร์ชัน 1.0 วันที่ 04 พฤศจิกายน 2562
2. AF 02-10 เวอร์ชัน 1.0 วันที่ 04 พฤศจิกายน 2562
3. AF 03-10 เวอร์ชัน 1.0 วันที่ 04 พฤศจิกายน 2562
4. สรุปโครงการเพื่อการพิจารณาทางจริยธรรมการวิจัยในมนุษย์ เวอร์ชัน 1.0 วันที่ 04 พฤศจิกายน 2562
5. โครงการวิจัยฉบับเต็ม เวอร์ชัน 1.0 วันที่ 04 พฤศจิกายน 2562
6. ประวัติผู้วิจัย เวอร์ชัน 1.0 วันที่ 04 พฤศจิกายน 2562
7. รายละเอียดเครื่องมือที่ใช้ในการวิจัย เวอร์ชัน 1.0 วันที่ 04 พฤศจิกายน 2562

ลงนาม

(นายแพทย์สมบูรณ์ ตันสุกสวัสดิกุล)  
ประธานคณะกรรมการจริยธรรมการวิจัยในมนุษย์  
มหาวิทยาลัยนเรศวร

วันที่รับรองการยกเว้นพิจารณาจริยธรรม : 20 พฤศจิกายน 2562

Date of Exemption : November 20, 2019

หมายเหตุ 1. ไม่ต้องส่งส่วนแก้ไขเพิ่มเติมโครงการวิจัย (Amendment) รายงานความก้าวหน้า (Progress Report) และรายงานสรุปผลการวิจัย (Final Report)  
2. หากมีการแก้ไขโครงการวิจัยภายหลังการรับรอง ให้ผู้วิจัยดำเนินการจัดทำเป็นโครงการวิจัยใหม่

## BIOGRAPHY

<b>Name-Surname</b>	YATHSOEUNG HO
<b>Date of Birth</b>	14 November 1993
<b>Address</b>	National road number 5, Ra village, Pteah Prey commune, Pursat city, Pursat Province, Cambodia
<b>Work Experience</b>	Sep 2016 - Dec 2017: Medical Representative, Bayer Pharmaceutical Company, Cambodia Dec 2017 - Present: Hospital pharmacist, Preak Norin Hospital, Cambodia
<b>Current Position</b>	Hospital pharmacist
<b>Education Background</b>	2011 - 2016: Doctor of Pharmacy, University of Health Sciences, Phnom Penh, Cambodia 2018 - Present: Master degree of Biomedical Sciences, Naresuan University, Phisanoulok, Thailand

